International Journal of Modern Physics A
Vol. 34, No. 33 (2019) 1930014 (66 pages)

DOI: 10.1142/S0217751X1930014X

World Scientific
www.worldscientific.com

The Sagnac and Hafele–Keating experiments: Two keys to the understanding of space–time physics in the vicinity of the Earth

J. H. Field

Département de Physique Nucléaire et Corpusculaire Université de Genève, 24, quai Ernest-Ansermet, CH-1211 Genève 4, Switzerland
john.field@cern.ch

Received 22 August 2019
Accepted 25 October 2019
Published 16 December 2019

The role of preferred frames for light propagation and time dilation in the region of a massive, spherical, gravitating bodies, where according to general relativity, space–time curvature is described by the Schwarzschild metric equation, is discussed in the context of the Sagnac effect (for light propagation) and the Hafele–Keating experiment (for time dilation). Predictions for both translational and rotational motion relative to the preferred frame are calculated up to order $(v/c)^3$. Different published theoretical calculations of the Sagnac effect are critically reviewed. The conflation in the literature of measured time differences in Sagnac experiments (a classical order v/c effect) and time dilation (a relativistic order $(v/c)^2$ effect) are also discussed.

Keywords: Sagnac effect; Hafele–Keating experiment; general relativity.

PACS number: 03.30.+p

1. Introduction

Insofar as the conclusions of this paper are likely to be found controversial, as they indicate important limitations on the applicability of textbook special relativity (SR) to space–time experiments performed on the surface of the Earth, or, more generally in the region of any massive body surrounded by a gravitational field, it is important to state, at the outset, that all the lowest order (in v/c) predictions that are discussed below have been experimentally verified. On the theoretical side, it is only assumed that space–time geometry in the region of a spherical massive body is described by the Schwarzschild metric[1,2] as prescribed by general relativity (GR). This has also been verified in the three classical post-Newtonian tests of GR,[a] as well

[a]These are the gravitational redshift of spectral lines, the deflection of light by the Sun and the precession of the perihelion of Mercury (see Chap. 8 of Ref. 2).

as by the Shapiro radar-echo-delay experiments[3] that are crucial in demonstrating the existence of a preferred frame for propagation of light at speeds less than, but close to, the free space vacuum value, c, in the vicinity of the Sun.

The crucial experiments, some consequences of which, for the understanding of space–time physics, are explored in this paper are in chronological order:

(i) The Sagnac interferometer.[4] In this experiment, published in 1913, light beams from a beam splitter followed, in opposite directions, a seven-sided path attached to a rotating turntable.[b] After recombination of the beams the interference pattern was recorded on a photographic plate. A shift in the interference fringes proportional to the angular velocity of rotation and to the area enclosed by the light paths was observed. An English translation of the conclusion of the experiment is:

> "The results of the measurements show that, in the surrounding space, light propagates with the speed c independently of the movement of the light source and the optical system. This property is the experimental characteristic of the luminiferous aether."

As will be discussed in Sec. 3, this conclusion, though essentially correct, and consistent with the prediction of GR, is too strong, since a possible uniform motion with respect to the preferred frame for light propagation is not excluded by the results of the experiment. The analysis of a similar experiment with circular geometry in Sec. 2 shows that conventional velocity transformation formulas of SR are incompatible with the observations of Sagnac.[6] The applicable relativistic formulas for the transformation of relative velocities in the Sagnac experiment were given by Post[7] in 1967, and later, independently, by Klauber.[8] Historical reviews of Sagnac-type experiments are to be found in Refs. 7, 9–12.

(ii) The Michelson–Gale Sagnac experiment.[13] This was published in 1925 and consisted of a rectangular interferometer of dimensions 640 m by 320 m where counter-rotating light beams traveled in evacuated tubes installed in shallow trenches. The rotational motion of the Earth was detected as a consequence of the existence, at the surface of the Earth, of a preferred frame for propagation of light at a speed close to c. This preferred frame is the Earth Centered Inertial (ECI) frame also used for an analysis of the Sagnac effect in the GPS system.[14] It is an instantaneous inertial frame comoving with the centroid of the Earth with axes pointing towards fixed positions on the celestial sphere.

It is clear, from the record[15] of conversations between himself and Shankland late in his life, that Einstein was aware of and admired the Michelson–Gale experiment. However, he did not remark that both this and the earlier experiments using Sagnac interferometers had effectively detected an "ether wind"

[b]At about the same time a similar rotating interferometric experiment was carried out in Germany by Harress.[5]

that the Michelson–Morley experiment had failed to observe (see Refs. 6, 16, 17 and the following). In fact determination of the rotational motion of the Earth by an "internal" measurement as in the Michelson–Gale experiment is forbidden by Poincaré's statement of the special relativity principle.[18] However, the existence of the preferred ECI frame of the Sagnac and Michelson–Gale experiments is a prediction of general relativity.

(iii) The Shapiro radar-echo-delay experiments.[3] In these experiments, microwave signals were bounced off the surfaces of Mercury and Venus and detected in an Earthbound radio telescope. From the measured time delays of the signals, their slowing down, in the gravitational field of the Sun, in accordance with the GR prediction, was observed. Close to superior conjunction for the case of Venus, a delay of 180 μs due to gravitational effects in a round-trip time of 1720s was seen, corresponding to an average microwave signal speed only one part in 10^7 less than c. This demonstrates that the Sun Centered Inertial (SCI) frame, defined similarly to the ECI, is a preferred one for propagation of light at speeds close to c in the region of the Sun.

(iv) The Hafele–Keating experiment (HKE).[19,20] In this experiment, published in 1972, an array of four caesium-beam atomic clocks were flown around the Earth at low latitudes in commercial airliners, once in a west to east and once in an east to west direction. The time intervals recorded by the clocks were compared, in each case, with time intervals recorded during the flights by geostationary precision clocks at the U.S. Naval Laboratory. The analysis of the experiment[21] made direct use of the Schwarzschild metric equation in which the coordinate time was defined as that registered by a clock, in the ECI frame defined above, sufficiently distant from the Earth that the gravitational field of the latter may be neglected. The airborne and geostationary clocks were slowed down relative to a clock registering coordinate time by a time dilation effect, predicted by the Schwarzschild metric equation (but also calculable, at lowest order, by SR) depending on their speed in the ECI frame. The airborne clocks were also speeded-up, relative to the geostationary ones, by the gravitational blue shift of GR resulting from a higher gravitational potential. This experiment demonstrated that the relative rate of two clocks does not depend, as naively expected in SR, only on their relative speed. This is due to the preferred nature of the ECI frame in the calculation of time dilation effects in the experiment.[22]

Because the time intervals recorded by clocks following different space–time trajectories are compared at the same position, the HKE measures the GR effect without requiring an exchange of photons, as in the original Pound–Rebka experiment.[23] Thus, the question of the change (or not) of photon energy, during passage through a gravitational field does not arise in interpreting the results. However, in the HKE, the clock settings are also strongly affected by the time dilation effect of SR due to the motion of the clocks. This effect is minimized in a recently proposed experiment[24] to measure the effect

of gravitational potential on clock rates by comparing high precision active hydrogen masers, situated first at the top and bottom of a high-rise building, before later comparisons of them at the same place. A similar experiment was recently carried out using caesium-beam atomic clocks and a GPS frequency standard by undergraduate students in the USA.[25]

(v) The Fiber Optic Conveyor (FOC) Sagnac experiments.[26,27] These, recently-performed, experiments demonstrate that the Sagnac effect occurs not only for rotational motion, as in Sagnac's original experiment, and in the Michelson–Gale experiment, but also for purely translational motion where both the interferometer proper frame and the preferred light propagation frame are inertial. Thus the lowest order formula for the Sagnac phase shift in a rotating interferometer:

$$\Delta\phi = \frac{8\pi\,\mathbf{\Omega}\cdot\mathbf{A}}{\lambda_0 c}\,, \tag{1.1}$$

(where $\mathbf{\Omega}$ is the angular velocity vector, $\mathbf{A}$ a vector perpendicular to the interferometer plane, A is the area bounded by the light paths, and λ_0 and c are the vacuum wavelength and speed of light) is replaced by the more general formula:

$$\Delta\phi = \frac{4\pi}{\lambda_0 c}\oint \mathbf{v}\cdot d\mathbf{s}\,, \tag{1.2}$$

where $\mathbf{v}$ is the velocity, in the preferred frame (the ECI frame on the surface of the Earth) of the element $d\mathbf{s}$ of the light path, which is valid for both rotational and translational motion relative to the preferred frame.

The preferred nature of the ECI frame for light propagation near the Earth, largely overlooked after the publication of the Michelson–Gale experiment, was rediscovered in an experiment published in 1976 in which clocks in Rosnan (USA) and Koshima (Japan) were synchronized using microwave signals passing via a geostationary satellite transceiver.[28] Due to the rotation of the Earth the signals arrived in Japan $\simeq 328$ ns earlier than if the relative speed of the signals and the receiver had been c.

Properly allowing for light signal speeds different from c in the proper frames of GPS receivers — the GPS "Sagnac effect" — is essential for the accuracy of the system. To first order in the speed v_Ω of the receiver in the ECI frame, the modification of the range, $\mathcal{R}$, of signal transmission due to the Sagnac effect is given by the formula:[29,30]

$$\mathcal{R} = R(t) + \mathbf{R}(t)\cdot[\mathbf{\Omega}\times\mathbf{r}_R(t)]/c = R(t) + 2\mathbf{S}\cdot\mathbf{\Omega}/c = R(t) + 2\Omega A_E/c\,. \tag{1.3}$$

Here, t is the epoch, in the ECI frame, of transmission of the signal, $t+\tau$ its reception epoch, and $\mathcal{R} = c\tau$. The vectors $\mathbf{r}_R(t)$ and $\mathbf{r}_T(t)$ specify the positions of the receiver and transmitter, respectively, relative to the center of the Earth. The vector $\mathbf{R}(t) \equiv \mathbf{r}_R(t) - \mathbf{r}_T(t)$ is directed from transmitter to receiver and $\mathbf{\Omega}$ is the angular velocity of the Earth. $\mathbf{S} \equiv \mathbf{r}_T(t)\times\mathbf{r}_R(t)/2$ is the directed area

of a triangle with vertices at the center of the Earth, the transmitter and the receiver at the epoch of transmission. The area A_E is that of the projection of this triangle on to the equatorial plane of the Earth. A_E is positive (negative) for eastward (westward) signal propagation. The Sagnac effect correction in the GPS is numerically important, it typically amounts to 30 m as compared to a nominal precision of 10 m or better. After correction for the Sagnac effect, an analysis of GPS data showed[31] that the speed of microwave signals in the ECI frame was constant within an uncertainty: $\delta c/c < 5 \times 10^{-9}$.

Due to the gravitational field of the Earth, as in the radar-echo-delay experiments due to the gravitational field of the Sun, the speed of the microwave signals in the ECI frame is slightly less than c. To give an idea of the magnitude of this reduction, consider the time-of-passage of a signal from a GPS satellite at the horizon to a receiver on the surface of the Earth. In this case, the signal path is tangent to the latter. Solving the Schwarzschild metric equation for this case (see Ref. 2 Chap. 8, Eq. 8.7.4) gives for the time-of-passage:

$$T = \frac{\sqrt{R_{\rm S}^2 - R_{\rm E}^2}}{c} + \frac{GM_{\rm E}}{c^2}\left[2\ln\left(\frac{R_{\rm S} + \sqrt{R_{\rm S}^2 - R_{\rm E}^2}}{R_{\rm E}}\right) + \left(\frac{R_{\rm S} - R_{\rm E}}{R_{\rm S} + R_{\rm E}}\right)^{\frac{1}{2}}\right], \qquad (1.4)$$

where $R_{\rm S} = 26.6 \times 10^6$ m is the radius of the (circular) orbit of the GPS satellite,[14] $R_{\rm E} = 6.38 \times 10^6$ m is the radius of the Earth and $M_{\rm E} = 5.97 \times 10^{24}$ kg is the mass of the Earth. The retardation due to the terms proportional to the gravitational constant G amounts to 74 ps in the time-of-passage of 86 ms. For this configuration therefore the signal speed is equal to c at a precision of one part in 10^9.

The existence of preferred frames — the ECI for the Earth, the SCI for the Sun — which constitute effective "local" aethers', in which light propagates at a speed close to c, was previously pointed out by Su.[16] The same author also proposed a "local aether model" of electromagnetic wave propagation[17] which was described as a "new classical model." There is no need for any such new model, however, since the existence of such "local aethers" is, as the calculation just presented shows for the case of the Earth, a straightforward prediction of GR.

Another important remark due to Su[16] concerns the interpretation of the Michelson–Morley experiment[33] and its successors:[35–40]

> "... the propagation mechanism in the Michelson–Morley experiment in no way can be different from that in the GPS and earthbound microwave links from the stand point of any plausible propagation model."[c]

In a Michelson–Morley experiment with arms of equal length L and the longitudinal arm aligned with the direction of the velocity $\mathbf{V}$ of the interferometer relative to the preferred frame in which the speed of light is c, the phase shift given by

[c]This is a good example of an application of the second of Newton's "Rules for the study of natural philosophy:" "... the causes assigned to natural effects of the same kind must be, as far as possible, the same."[34]

exchange of longitudinal and transverse arms is:

$$\Delta\phi_{\rm MM} = \frac{4\pi LV^2}{\lambda_0 c^2} + {\rm O}\left[\left(\frac{V}{c}\right)^4\right]. \tag{1.5}$$

In the conventional interpretation of the experiment, from which both the non-existence of the aether and the existence of relativistic length contraction in SR or, alternatively a Lorentz–Fitzgerald contraction effect in aether theories, have been concluded, V is set equal to the orbital velocity of the Earth around the Sun of $\simeq 30$ km/s. This is tantamount to assuming that the SCI frame is the aether rest frame in the immediate vicinity of the Earth. However the existence of the Sagnac effect, and in particular the result of the Michelson–Gale experiment, as well as GR, require that the "local aether" near the surface of the Earth, where the Michelson–Morley experiment was performed, should instead be assigned to the ECI frame. In this case, $V = v_\Omega = \Omega_{\rm E} R_{\rm E} \cos\lambda \simeq 300$ m/s where λ is the latitude — the speed of the interferometer in the ECI fame due to the rotation of the Earth. The value of $\Delta\phi_{\rm MM}$ is then expected to be a factor 10^{-4} smaller than when V is the Earth's orbital velocity. The Kennedy–Thorndike experiment[35] which had a sensitivity of order 10^{-5} of an interference fringe, set an upper limit of $\simeq 10$ km/s on V, still a factor about 30 times larger than v_Ω. The Michelson–Gale experiment successfully detected the "local aether" due to the gravitational field of the Earth, because the Sagnac phase shift is an order V/c effect as compared to an order $(V/c)^2$ one for the Michelson–Morley experiment and its successors. These experiments were simply not sensitive enough to observe any effect.

This paper presents the relativistic analyses of photonic Sagnac experiments and of the HKE including not only the lowest order predictions, to be found in the previous literature, but also, in a systematic way, $(v/c)^2$ corrections, as well as the case of combined rotational and translational motion for Sagnac interferometers with light-path refractive index $n = 1$ and $n > 1$. Similarly, for the HKE, the effect of an arbitrary choice of inertial frame for the definition of coordinate time in the calculation of the SR contribution is considered.

The plan of this paper is as follows. The following section analyses, following the space–time geometric method of Langevin[41] and Post,[7] a rotating circular Sagnac interferometer. In Sec. 3, a similar analysis of combined rotational and translational motion is presented. Section 4 analyses the FOC with which a purely translational Sagnac effect was demonstrated.[26,27] Both GR and SR analyses of the HKE are found in Sec. 5. Section 6 contains a critical review of some other derivations of the Sagnac effect in the literature. In the final section, the fundamental physical bases of the photonic Sagnac effect and the HKE are compared and contrasted. To add further perspective to the discussion, the lowest order Sagnac effect for massive particles is also briefly discussed and compared with the photonic one in the context of Feynman's space–time formulation of quantum mechanics. Also considered in this section is the erroneous conflation in the literature of the photonic Sagnac effect and the HKE. Some calculational details are relegated to two appendices.

A few words on nomenclature and ontology. In the description of the photonic Sagnac effect the entity which propagates, and the times-of-passage of which are calculated, are generally called "light beams" or "light signals" but, following Feynman's space–time formulation of quantum mechanics, can also be considered, more fundamentally, to be single photons. Indeed in Sagnac interference it is a *single photon* following alternative paths, which, following Dirac's prescription, "interferes with itself."[d] The same is true for an electron in the interferometer discussed in Sec. 7.

2. The Rotational Sagnac Effect

To discuss the physical principles that underlie the Sagnac effect it is convenient, following Post,[7] to consider an idealized interferometer where light beams part back-to-back from a beam splitter (BS) and arrive head-on at opposite sides of the latter having followed circular paths along which they propagate at the vacuum light speed, c, in the laboratory system. The case where beams instead propagate in a transparent medium of refractive index n at rest in the interferometer frame — which may be appropriate when the beams are guided by fiber-optic cables — will be considered later. The Sagnac effect occurs when the interferometer is rotated, as a consequence of different times-of-passage back to the beam splitter (where they are combined) of the clockwise-rotating and counterclockwise-rotating beams. The geometrical configuration, in the laboratory frame, for a clockwise-rotating circular interferometer is shown in Fig. 1(a). At epoch $t = 0$ light signals exit from the beam splitter in opposite directions and follow circular paths of radius R. The positions of the clockwise-rotating signal, counterclockwise-rotating signal and the beam splitter are specified by the angles ϕ^+, ϕ^- and Φ, respectively, relative to a fixed direction in the laboratory frame. At $t = 0$, $\phi^+ = \phi^- = \Phi = 0$. The corresponding configuration in the interferometer frame, that rotates with constant angular velocity Ω in a clockwise direction, is shown in Fig. 1(b). The clockwise-(counterclockwise-)rotating signals have speeds, in the interferometer frame, c'_+ (c'_-) relative to local points of the interferometer, and angular separations ϕ_+ (ϕ_-) from BS where

$$\phi_\pm = \phi^\pm \mp \Phi\,. \tag{2.1}$$

Since the relative velocity of the counterclockwise-rotating signal and BS is greatest, it arrives back before the clockwise-rotating one. As shown in Fig. 2, the beam splitter is at position BS_- when the counterclockwise-rotating signal arrives back and at position BS_+ when the clockwise-rotating signal arrives back. Denoting

[d]Each photon interferes only with itself, Interference between two different photons never occurs.[42] In the photonic Sagnac interferometer there is indeed a single photon with two corresponding probability amplitudes that interfere. Dirac's second assertion is however false, witness the Hanbury–Brown and Twiss experiments.[43,44,46]

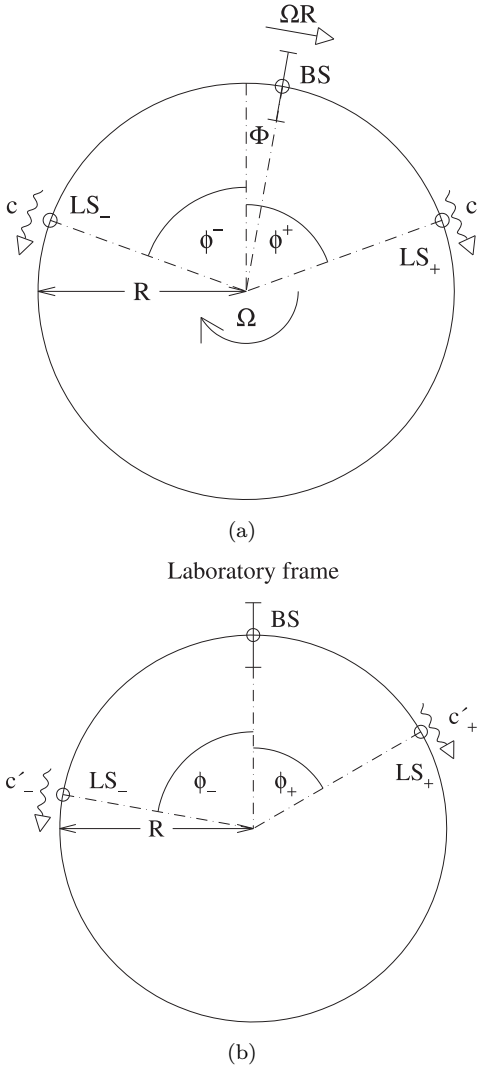

Fig. 1. Angular coordinates and velocities of clockwise-rotating (LS_+) and counterclockwise-rotating (LS_-) light signals in a circular Sagnac interferometer. (a) Relative to a fixed direction in the laboratory frame. (b) Relative to the position of the beam splitter, BS, in the co-rotating frame.

the times-of-passage in the laboratory frame of the clockwise-(counterclockwise-) rotating signals by $T_+(T_-)$ then

$$T_\pm = \frac{2\pi R}{c_\pm}\,, \tag{2.2}$$

where

$$c_\pm = c \mp \Omega R\,. \tag{2.3}$$

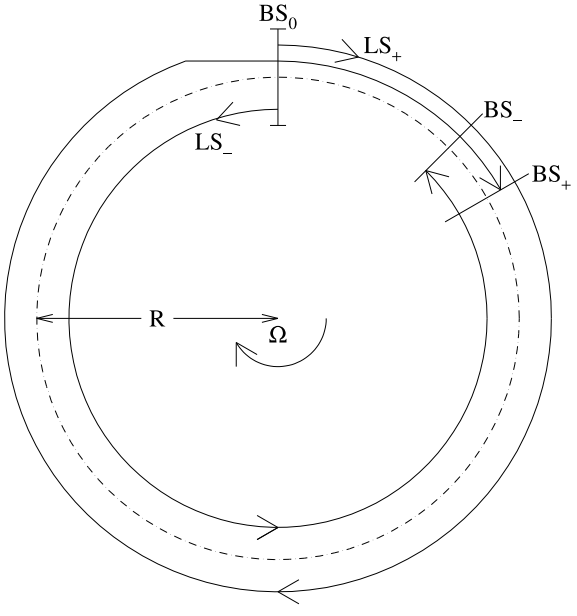

Fig. 2. Laboratory frame configuration of counter-rotating light signals LS_+ and LS_- at the instants of return to the beam splitter (see text for discussion).

Since a clock situated at BS moves with constant speed ΩR relative to the laboratory system it will be subject to a time dilation (TD) effect such that

$$\Delta t = \gamma_\Omega \Delta t' \,, \tag{2.4}$$

where Δt and $\Delta t'$ are time intervals recorded by a clock at rest in the laboratory and one comoving with BS, respectively and $\gamma_\Omega \equiv 1/\sqrt{1-\beta_\Omega^2}$; $\beta_\Omega \equiv \Omega R/c$. The times-of-passage of the signals T'_+, T'_- in the comoving frame of BS are then given as

$$T'_\pm = \frac{2\pi R}{c'_\pm} = \frac{T_\pm c_\pm}{c'_\pm} = \frac{T_\pm}{\gamma_\Omega} \,. \tag{2.5}$$

It follows from (2.3) and (2.5) that

$$c'_\pm = \gamma_\Omega c_\pm = \gamma_\Omega (c \mp \Omega R) \,. \tag{2.6}$$

This is the relativistic transformation formula for *relative velocities* of BS and a local light signal between the laboratory frame and the instantaneous comoving inertial frame of the beam splitter. This formula has been previously derived by Klauber in a relativistic analysis of the Sagnac effect[8] that is discussed in Sec. 6. The corresponding formula for *relative angular velocities*:

$$\omega'_\pm = \gamma_\Omega (\omega \mp \Omega) \,, \tag{2.7}$$

where $\omega'_\pm \equiv d\phi_\pm/dt' = c'_\pm/R$, $\omega \equiv d\phi^\pm/dt = c/R$ was previously derived by Post.[7]

Note the difference between (2.6) and the conventional relativistic parallel velocity addition relation (RPVAR) due to Einstein[47]

$$c'_{\pm,\mathrm{SR}} = \frac{c \mp \Omega R}{1 \mp \frac{c\Omega R}{c^2}} = c\,. \tag{2.8}$$

Since, in a Sagnac interferometer, the interference effect is calculated in the comoving frame of the beam splitter, the RPVAR predicts that in this frame the counter-rotating beams arrive simultaneously, as when $\Omega = 0$, so that no rotation-dependent Sagnac phase shift can occur. That this is the case, i.e. that conventional special relativity theory is incompatible with the observed existence of the Sagnac effect — was already pointed out in 1937 by Dufour and Prunier.[48] Since the Sagnac effect is observed to respect the prediction of Eqs. (2.5) and (2.6) which is, for the phase shift between the two beams

$$\Delta\phi^{\mathrm{CG}} = 2\pi\nu(T'_+ - T'_-) = \frac{8\pi\Omega A\gamma_\Omega}{\lambda_0 c} = \frac{8\pi\Omega A}{\lambda_0 c}\left[1 + \frac{\beta_\Omega^2}{2}\right] + \mathrm{O}\big(\beta_\Omega^5\big)\,, \tag{2.9}$$

(where the suffix "CG" stands for "circular geometry," ν is the frequency, λ_0 the vacuum wavelength of the light and $A = \pi R^2$) it is clear that the RPVAR is *not applicable to the analysis of the Sagnac effect*.[6] For a discussion of the correct physical interpretations of the relativistic relative velocity transformation relation (RRVTR), Eq. (2.6) and the RPVAR, Eq. (2.8), see Refs. 6, 49, 50 and Sec. 5.

The case that light signals propagate in a transparent medium of constant, frequency-independent refractive index n within an interferometer with a circular geometry will now be considered. Taking into account the dragging effect of the moving medium on the speed of light, Eq. (2.3) become, for arbitrary n:

$$c_\pm(n) = \frac{c}{n} \pm f(n)\Omega R \mp \Omega R\,, \tag{2.10}$$

where $f(n)$ is the Fresnel–Fizeau dragging coefficient: $f(n) \equiv 1 - 1/n^2$. Equation (2.5) are then modified, for $n \neq 1$ to

$$T'_\pm(n) = \frac{T_\pm(n)}{\gamma_\Omega} = \frac{2\pi R}{\gamma_\Omega\big(\frac{c}{n} \pm f(n)\Omega R \mp \Omega R\big)} = \frac{2\pi R}{\gamma_\Omega\big(\frac{c}{n} \mp \frac{\Omega R}{n^2}\big)}\,, \tag{2.11}$$

which gives a Sagnac phase shift

$$\begin{aligned}\Delta\phi^{\mathrm{CG}}(n) = 2\pi\nu(T'_+ - T'_-) &= \frac{4\pi^2 R\nu}{\gamma_\Omega}\left[\frac{1}{\frac{c}{n} - \frac{\Omega R}{n^2}} - \frac{1}{\frac{c}{n} + \frac{\Omega R}{n^2}}\right] \\ &= \frac{8\pi A\Omega}{\gamma_\Omega c\lambda_0\Big[1 - \big(\frac{\Omega R}{cn}\big)^2\Big]} = \frac{8\pi A\Omega}{c\lambda_0}\frac{\gamma_\Omega(n)^2}{\gamma_\Omega}\,,\end{aligned} \tag{2.12}$$

where $\gamma_\Omega(n) \equiv 1/\sqrt{1 - (\Omega R/cn)^2}$. Comparison with Eq. (2.9) shows that, except for corrections of order $(\Omega R/cn)^2$ and $(\Omega R/c)^2$, the Sagnac phase shift is the same as the case where $n = 1$ and the light signals propagate in vacuum. The conclusion

that there would be no observable difference in Sagnac phase shifts for $n = 1$ and $n > 1$ is due to Harzer[51,52] and was first experimentally confirmed by Pognay[53,54] (see Ref. 7).

The above calculation, for an interferometer with circular geometry rotating about its symmetry axis gives, at order β_Ω, the lowest order (LO) phase shift of

$$\Delta\phi_{\rm LO}^{\rm CG} = \frac{8\pi\Omega A}{\lambda_0 c} \tag{2.13}$$

regardless of refractive index of the material, at rest in the interferometer frame, traversed by the interfering light beams.

It was pointed out in 1935 by Prunier[55] that the experimentally verified Sagnac phase shift (2.13), for the case $n > 1$ is incompatible with the hypothesis used by von Laue[56] to derive the Fresnel–Fizeau dragging coefficient by the use of the Einstein[47] relativistic velocity transformation formula:

$$c_+(n) = \frac{\frac{c}{n} + \Omega R}{1 + \frac{c\Omega R}{nc^2}} = \frac{c}{n} + \Omega R\left(1 - \frac{1}{n^2}\right) + {\rm O}\left[\left(\frac{\Omega R}{c}\right)^2\right]$$

since this assumes the speed of light in the comoving frame of the interferometer is c/n and not $\gamma_\Omega(c/n - \Omega R/n^2)$ as in Eq. (2.11). If this were the case then the Sagnac effect would vanish.

It will now be demonstrated that for a planar interferometer with light paths consisting of connected line segments, and for an arbitrary axis of rotation of the angular velocity vector $\mathbf{\Omega}$, (2.13) generalizes to

$$\Delta\phi_{\rm LO} = \frac{8\pi\mathbf{\Omega}\cdot\mathbf{A}}{\lambda_0 c}\,, \tag{2.14}$$

where $A = |\mathbf{A}|$ is the area enclosed by the light paths and $\mathbf{A}$ is perpendicular to the interferometer plane. The first step in the calculation is to find the transit time of a light signal along an arbitrary constituent line segment. Since relativistic corrections due to time dilation are neglected, the calculation may be performed either in the laboratory frame or in the co-rotating frame of the interferometer. The geometrical configuration of a particular segment AB of length s is shown, in the laboratory frame, in Fig. 3. The axis of rotation passes through the point O and the angular velocity vector $\mathbf{\Omega}$ is inclined at angle λ relative to the z-axis which is perpendicular to the interferometer plane. The y-axis is chosen so that $\mathbf{\Omega}$ lies in the $y - z$ plane. With this choice of coordinate system the position vector $\mathbf{r}$ of the point P on the segment AB, a unit vector $\hat{s}$ in the direction of the light signal LS, and the angular velocity vector are given, in terms of unit vectors $\hat{\imath}$, $\hat{\jmath}$, and $\hat{k}$, parallel to the x, y and z axes, as:

$$\mathbf{r} = r(\hat{\imath}\sin\alpha + \hat{\jmath}\cos\alpha)\,, \tag{2.15}$$

$$\hat{s} = \hat{\imath}\cos\beta - \hat{\jmath}\sin\beta\,, \tag{2.16}$$

$$\mathbf{\Omega} = \Omega(\hat{\jmath}\sin\lambda + \hat{k}\cos\lambda)\,. \tag{2.17}$$

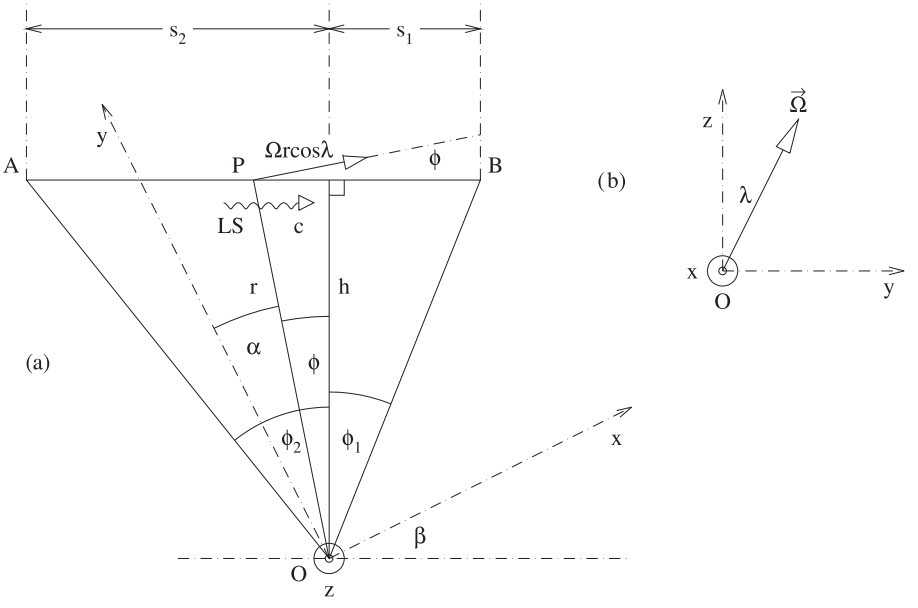

Fig. 3. Geometrical definitions in the laboratory frame for a light signal LS crossing a straight light path AB. AB rotates with angular velocity $\mathbf{\Omega}$ about the point O. (a) xy plane that contains the light path AB. (b) yz plane that contains $\mathbf{\Omega}$ (see text for discussion).

The laboratory frame velocity of the point P, due to the angular velocity Ω, is

$$\mathbf{v} = \mathbf{r} \times \mathbf{\Omega} = \Omega r(\hat{\imath} \cos\alpha \cos\lambda - \hat{\jmath} \sin\alpha \cos\lambda + \hat{k} \sin\alpha \sin\lambda)\,. \tag{2.18}$$

The velocity component of the point P in the direction of the light signal is then

$$\begin{aligned} v_{\parallel} \equiv \hat{s} \cdot \mathbf{v} &= \Omega r(\cos\alpha \cos\beta + \sin\alpha \sin\beta) \cos\lambda \\ &= \Omega r \cos(\beta - \alpha) \cos\lambda = \Omega r \cos\phi \cos\lambda \end{aligned} \tag{2.19}$$

since the geometry of Fig. 3 gives $\pi/2 = (\pi/2 - \beta) + \phi + \alpha$ or $\phi = \beta - \alpha$. Equation (2.19) implies, as shown in Fig. 3, that the projection of $\mathbf{v}$ into the xy plane is of length $\Omega r \cos\lambda$. The time intervals $dt_{\pm}$ for the light signals to cross the interval ds of the segment AB around P are

$$dt_{\pm} = \frac{ds}{c_r^{\pm}} = \frac{h d\phi}{\cos^2\phi(c \mp \Omega h \cos\lambda)}\,, \tag{2.20}$$

where $r d\phi = ds \cos\phi$, $h = r\cos\phi$ and $c_r^{\pm} = c \mp \Omega h \cos\lambda$. The $+(-)$ signs indicate that $\mathbf{v}_{\parallel}$ is parallel (antiparallel) to the direction of the light signal.

Integrating over ϕ in (2.20) and considering the geometry of Fig. 3

$$\int \frac{d\phi}{\cos^2\phi} = \int d(\tan\phi) = \tan\phi_2 + \tan\phi_1 = \frac{s_2}{h} + \frac{s_1}{h} = \frac{s}{h} \tag{2.21}$$

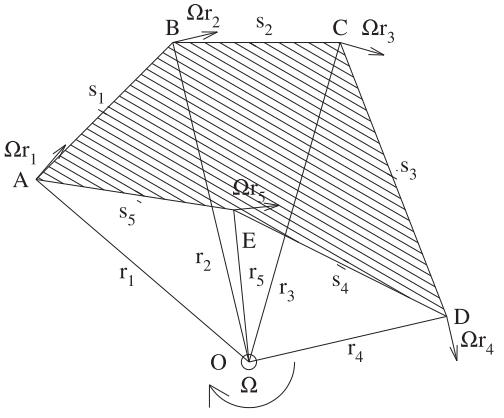

Fig. 4. Geometrical definitions for a rotating plane light circuit ABCDEA. Light propagation in each segment is described as in Fig. 3 (see text for discussion).

so that, neglecting terms of order $\geq (\Omega h/c)^2$, (2.20) and (2.21) give

$$t_{\pm} = \frac{s}{c} \pm \frac{sh\Omega\cos\lambda}{c^2} = \frac{s}{c} \pm 2\Delta(\mathrm{ABO})\frac{\Omega\cos\lambda}{c^2}\,, \tag{2.22}$$

where $\Delta(\mathrm{ABO})$ is the area of the triangle ABO. The above calculation neglects the motion of the points A and B in Fig. 2 during the passage of the light signal between them. As shown in Ref. 6 taking into account this motion gives only order $(\Omega h/c)^2$ corrections to Eq. (2.22).

Consider now, as shown in Fig. 4, the interferometer constituted by five line segments AB, BC, CD, DE and EA. The interferometer and the light signal both rotate in a clockwise direction. For segments AB, BC and CD, $\mathbf{v}_{\parallel}$ is in the same direction as the light signal whereas for DE and EA it is in the opposite direction. The time-of-passage of the clockwise (CW-)rotating signal is therefore

$$\begin{aligned} T_{\mathrm{CW}} &= t_+(1) + t_+(2) + t_+(3) + t_-(4) + t_-(5) \\ &= \sum_{i=1}^{5} \frac{s_i}{c} + \frac{2\Omega\cos\lambda}{c^2}(\Delta(\mathrm{ABO}) + \Delta(\mathrm{BCO}) + \Delta(\mathrm{CDO}) - \Delta(\mathrm{DEO}) - \Delta(\mathrm{EAO})) \\ &= \sum_{i=1}^{5} \frac{s_i}{c} + \frac{2\Omega\cos\lambda}{c^2} A\,. \end{aligned} \tag{2.23}$$

Here, A = Area (ABCDE) is the area enclosed by the light path. In a similar manner the time-of-passage of a counterclockwise (CCW-)rotating signal is

$$\begin{aligned} T_{\mathrm{CCW}} &= t_-(1) + t_-(2) + t_-(3) + t_+(4) + t_+(5) \\ &= \sum_{i=1}^{5} \frac{s_i}{c} - \frac{2\Omega\cos\lambda}{c^2} A\,. \end{aligned} \tag{2.24}$$

The Sagnac phase shift is therefore

$$\Delta\phi_{\rm LO} = 2\pi\nu(T_{\rm CW} - T_{\rm CCW}) = \frac{8\pi\nu\Omega\cos\lambda A}{c^2} = \frac{8\pi\,\mathbf{\Omega}\cdot\mathbf{A}}{c\lambda_0}\,, \tag{2.25}$$

where $\mathbf{A}$ is perpendicular to the plane of the interferometer in the sense of a right-handed screw undergoing counterclockwise rotation around its boundary. The generalization of this calculation to the case where the light path is an arbitrary N-sided plane polygon is evident.

3. The Sagnac Effect with Uniform Rotational and Translational Motion

In this section, the circular interferometer considered in Figs. 1 and 2 is assumed to undergo uniform translational motion at speed V in the laboratory frame. An example of this is the case of a Sagnac interferometer at rest on the surface of the Earth. The "laboratory" frame is then the ECI frame and the velocity $\mathbf{V}$ results from the rotation of the Earth. The latter is sufficiently small that, to a good approximation, the change in the direction of $\mathbf{V}$ may be neglected during the flight time of the light signal in the interferometer. As shown in Figs. 5 and 6(a), the velocity vector $\mathbf{V}$ is inclined at an angle α to a normal to the plane of the interferometer (the x-axis) and lies in the xz plane; $\hat{s}_\pm$ are unit vectors in the plane of the interferometer perpendicular to the radius vectors $\mathbf{r}_\pm$ specifying the instantaneous positions of the light signals $\mathrm{LS}_\pm$ (see Fig. 5). With the above choice

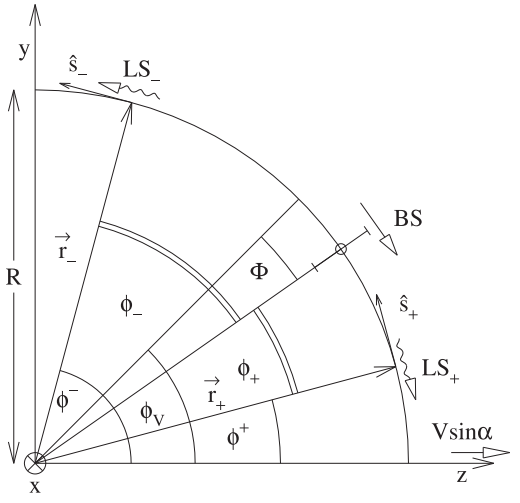

Fig. 5. Geometrical definitions for a circular Sagac interferometer undergoing clockwise rotation and uniform translational motion in the laboratory frame. LS_+ (LS_-) are clockwise-(counterclockwise-)rotating light signals, BS is the clockwise-rotating beam splitter. The projection of the velocity vector $\mathbf{V}$ into the plane of the interferometer is parallel to the z-axis. The x axis is perpendicular to the plane of the interferometer. When the light signals leave the beam splitter the angular separation of the latter with the z-axis is ϕ_V.

of coordinate axes:

$$\mathbf{V} = V(\hat{\imath}\cos\alpha + \hat{k}\sin\alpha)\,, \tag{3.1}$$

$$\mathbf{r}_\pm = R(\hat{\jmath}\sin\phi^\pm + \hat{k}\cos\phi^\pm)\,, \tag{3.2}$$

$$\hat{s}_\pm = \hat{\jmath}\cos\phi^\pm - \hat{k}\sin\phi^\pm\,. \tag{3.3}$$

At epoch $t = 0$ when the light signals leave the beam splitter the radius vector specifying the position of the latter is at an angle ϕ_V to the z-axis. The angles $\phi^+(\phi^-)$ give the positions of the clockwise- (counterclockwise-)rotating signals relative to the z-axis while the angles ϕ_+ (ϕ_-) give the signal positions relative to the radius vector of BS. All geometrical quantities are defined in the laboratory frame. In Figs. 6(c) and 6(b) are shown spatial configurations, in the plane spanned by $\mathbf{V}$ and $\hat{s}_+$ $(\hat{s}_-)$, of clockwise- (counterclockwise-)rotating light signals, separated by small time intervals δt_+ (δt_-). The angles $\chi_\pm$, $\xi_\pm$ in Figs. 6(b) and 6(c) are defined according to the relations

$$V\cos\chi_\pm \equiv -\hat{s}_\pm\cdot\mathbf{V} = V\sin\alpha\sin\phi^\pm\,, \tag{3.4}$$

$$\sin\xi_\pm \equiv \frac{V\delta t_\pm\sin\chi_\pm}{c\delta t_\pm} = \beta_V\sin\chi_\pm\,. \tag{3.5}$$

The circles at $\mathrm{P}_\pm$, $\mathrm{Q}_\pm$ in Figs. 6(b) and 6(c) show successive positions of light signals whereas the squares at $\mathrm{P}_\pm$, $\mathrm{P}'_\pm$ show successive positions of a fixed point on the interferometer. It follows from the geometry of Figs. 6(b) and 6(c) that the relative velocities in the laboratory frame of the light signals and adjacent points of the interferometer are given by the relations

$$c_\pm = \frac{\mathrm{P}'_\pm\mathrm{Q}_\pm}{\delta t_\pm} = \frac{R\delta\phi_\pm}{\delta t_\pm} = c\cos\xi_\pm \mp V\cos\chi_\pm \mp \Omega R\,. \tag{3.6}$$

The geometry of Fig. 5 gives

$$\phi^\pm = \phi_V \mp \phi_\pm - \Phi\,. \tag{3.7}$$

Since $\phi_\pm/\Phi = c_\pm/\Omega R$, combining (3.4), (3.5) and (3.6) gives:

$$\Phi = \frac{\phi_\pm\Omega R}{c_\pm} = \frac{\phi_\pm\Omega R}{c\Big[\sqrt{1-\beta_V^2+\beta_V^2\sin^2\alpha\sin^2\phi^\pm}\mp\beta_V\sin\alpha\sin\phi^\pm\mp\beta_\Omega\Big]} \tag{3.8}$$

$$= \frac{\phi_\pm\beta_\Omega}{1\mp\beta_V\sin\alpha\sin\phi^\pm\mp\beta_\Omega} + \mathrm{O}(\beta^3) \tag{3.9}$$

so that

$$\phi_+ + \Phi = \phi_+\left[1 + \frac{\beta_\Omega}{1-\beta_V\sin\alpha\sin\phi^+ - \beta_\Omega}\right]$$

$$\equiv \phi_+(1+y_+) + \mathrm{O}(\beta^3)\,, \tag{3.10}$$

$$\phi_- - \Phi = \phi_-\left[1 - \frac{\beta_\Omega}{1+\beta_V\sin\alpha\sin\phi^- + \beta_\Omega}\right]$$

$$\equiv \phi_-(1+y_-) + \mathrm{O}(\beta^3)\,. \tag{3.11}$$

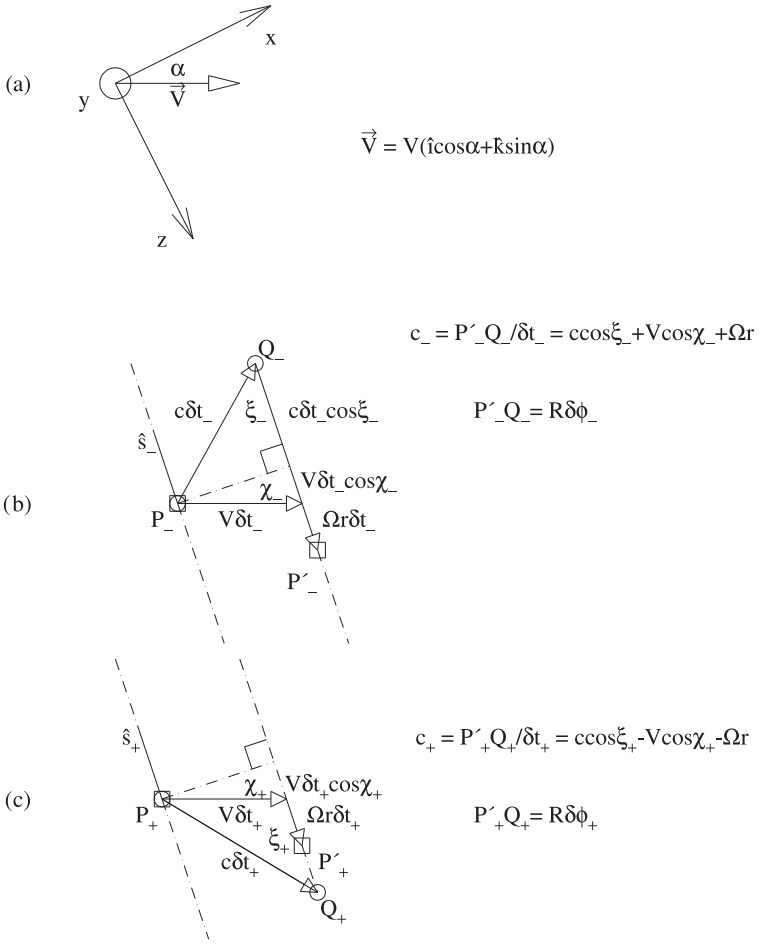

Fig. 6. (a) Definition of the angle α. The velocity $\mathbf{V}$ lies in the xz plane. The x-axis is perpendicular to the plane of the interferometer (cf. Fig. 5). (b) Laboratory frame geometrical definitions in the plane of $\mathbf{V}$ and $\hat{s}_-$ (tangent vector to the circular light path) for a counterclockwise light signal. (c) as (b) but for a clockwise light signal. In (b) and (c), the positions of the light signal (P, Q) and a fixed point on the light path (P, P′) separated by time intervals δt_- and δt_+ are shown. The light signals have speed c in the laboratory frame (see text for discussion).

Combining (3.7) with (3.10) and (3.11) gives

$$\phi^{\pm} = \phi_V \mp \phi_{\pm}(1 + y_{\pm})\,. \tag{3.12}$$

Expanding the denominators in the expressions for $y_{\pm}$ in (3.10) and (3.11) as a series in powers of β_Ω and β_V:

$$y_{\pm} = \pm\beta_\Omega \mp \beta_\Omega\beta_V \sin\alpha \sin(\phi_{\pm} \mp \phi_V) + \beta_\Omega^2 + \mathrm{O}(\beta^3)\,. \tag{3.13}$$

Using Eqs. (3.12) and (3.13) the angles $\phi^{\pm}$, referred to fixed axes in the laboratory frame, can be written, to $\mathrm{O}(\beta^2)$ accuracy, in terms of the angles $\phi_{\pm}$ referred to

a fixed direction (that of the beam splitter) in the interferometer frame. This is convenient for the evaluation of the integrals to obtain the times-of-passage of the light signals in the interferometer.

Combining Eqs. (3.4)–(3.6) gives the following relation between infinitesimal time intervals $dt_\pm$ and angular intervals $d\phi_\pm$:

$$dt_\pm = \frac{R\, d\phi_\pm}{c\Big[\sqrt{1-\beta_V^2+\beta_V^2\sin^2\alpha\sin^2\phi^\pm}\mp\beta_V\sin\alpha\sin\phi^\pm\mp\beta_\Omega\Big]}\,. \tag{3.14}$$

Expressing the angular variables $\phi^\pm$ in terms of $\phi_\pm$ with the aid of Eqs. (3.12) and (3.13) and expanding the right side of (3.14) as a power series in β_V and β_Ω enables the equation to be integrated to obtain the following expressions for the times-of-passage $T'_\pm$ of the light signals from and back to the beam splitter. Details of this calculation are given in App. A

$$\begin{aligned} T_+ &= \int dt_+ \\ &= \frac{2\pi R}{c}\Bigg\{1+\beta_\Omega\Bigg[1+\beta_V\sin\phi_V\sin\alpha+\frac{\beta_V^2}{2}\big[2+(2-\cos 2\phi_V)\sin^2\alpha\big]\Bigg] \\ &\quad +\beta_\Omega^2[1+\beta_V(2\sin\phi_V-\pi\cos\phi_V)\sin\alpha]+\beta_\Omega^3+\frac{\beta_V^2}{2}+\frac{\beta_V^2\sin^2\alpha}{4}\Bigg\}+\mathrm{O}(\beta^4)\,, \end{aligned} \tag{3.15}$$

$$\begin{aligned} T_- &= \int dt_- \\ &= \frac{2\pi R}{c}\Bigg\{1-\beta_\Omega\Bigg[1-\beta_V\sin\phi_V\sin\alpha+\frac{\beta_V^2}{2}\big[2+(2-\cos 2\phi_V)\sin^2\alpha\big]\Bigg] \\ &\quad +\beta_\Omega^2[1-\beta_V(2\sin\phi_V+\pi\cos\phi_V)\sin\alpha]-\beta_\Omega^3+\frac{\beta_V^2}{2}+\frac{\beta_V^2\sin^2\alpha}{4}\Bigg\}+\mathrm{O}(\beta^4)\,. \end{aligned} \tag{3.16}$$

Since the interference between the recombined light signals that constitutes the Sagnac effect is measured in the interferometer rest frame the times of passage of the light signals must also be evaluated in this frame. To do this, the time dilation effect due to the motion, in the laboratory frame, of the beam splitter must be taken into account. The finite time intervals $\Delta t'_\pm$ corresponding to the laboratory frame intervals $\Delta t_\pm$ are given by the relations

$$\Delta t'_\pm = \frac{\Delta t_\pm}{\bar\gamma_\pm^{\mathrm{BS}}}\,. \tag{3.17}$$

Here $\bar\gamma_\pm^{\mathrm{BS}}$ denotes an appropriate time-averaged time dilation factor due to the motion of BS in the laboratory system. Denoting by $\bar\phi_{\mathrm{BS}}$ the average value of the polar angle ϕ_{BS} (see Fig. 5) giving the angular position of BS in the laboratory

frame then

$$\bar{\gamma}_{\pm}^{\rm BS} \simeq \bar{\gamma}_{\rm BS} \equiv \frac{1}{\sqrt{1-\beta_{\bar{U}}^2}}\,; \quad \beta_{\bar{U}} \equiv \frac{\bar{U}}{c}\,,$$

where

$$\bar{U}_x = V\cos\alpha\,, \quad \bar{U}_y = -\Omega R\cos\bar{\phi}_{\rm BS}\,, \quad \bar{U}_z = \Omega R\sin\bar{\phi}_{\rm BS} + V\sin\alpha \tag{3.18}$$

so that

$$\beta_{\bar{U}}^2 = \beta_V^2 + \beta_\Omega^2 + 2\beta_V\beta_\Omega\sin\alpha\sin\bar{\phi}_{\rm BS}\,. \tag{3.19}$$

Since $\phi_{\rm BS} = \phi_V - \Phi$ it follows from (3.7), (3.12) and (3.13) that

$$\bar{\phi}_{\rm BS} = \phi_V - \bar{\phi}_+ y_+ = \phi_V - \pi\beta_\Omega + {\rm O}(\beta^2)\,. \tag{3.20}$$

Since, in the case considered here, $\Omega R \ll c$, the value of ϕ_+ corresponding to the return of the light signal to BS is $\phi_+ \simeq 2\pi$, so that $\bar{\phi}_+ \simeq \pi$. Then (3.17), (3.19) and (3.20) give

$$T'_{\pm} = \frac{T_{\pm}}{\bar{\gamma}_{\pm}^{\rm BS}} = T_{\pm}\left(1 - \frac{\beta_V^2}{2} - \frac{\beta_\Omega^2}{2} - \beta_V\beta_\Omega\sin\alpha\sin\phi_V + \pi\beta_\Omega^2\beta_V\sin\alpha\cos\phi_V\right) + {\rm O}(\beta^4)\,. \tag{3.21}$$

Combining (3.15) and (3.16) with (3.21) gives

$$\begin{aligned} T'_{\pm} = \frac{2\pi R}{c}\Bigg\{1 \pm \beta_\Omega\Bigg[1 \mp \beta_V\cos\phi_V\sin\alpha + \frac{\beta_V^2}{2}\sin^2\alpha(2-\cos 2\phi_V)\Bigg] \\ - \pi\beta_\Omega^2\beta_V\sin\alpha\sin\phi_V - \frac{\beta_V^2}{2} \pm \frac{\beta_\Omega^3}{2} + \frac{\beta_V^2\sin^2\alpha}{4}\Bigg\}\,. \end{aligned} \tag{3.22}$$

The Sagnac phase shift of Eq. (2.9) therefore generalizes for $\beta_V \neq 0$ to

$$\begin{aligned} \Delta\phi^{\rm CG}(\beta_V) &= 2\pi\nu(T'_+ - T'_-) \\ &= \frac{8\pi\Omega A}{\lambda_0 c}\left[1 + \frac{\beta_V^2}{2}\sin^2\alpha[2-\cos 2\phi_V] + \beta_\Omega\beta_V\sin\phi_V\sin\alpha + \frac{\beta_\Omega^2}{2}\right] + {\rm O}(\beta^5)\,. \end{aligned} \tag{3.23}$$

The case in which a homogeneous transparent medium of refractive index n ($n \neq 1$) is traversed by the light signals in the interferometer will now be considered. That is, the generalization of Eq. (2.12) when a circular interferometer undergoes both uniform rotation and uniform translational motion in the laboratory frame. An example of this is the fiber optic gyroscope (FOG) rotating at a fixed point on the surface of the Earth, where the local translational motion is due to the rotation of the Earth.

It can be seen from the geometry of Fig. 6 that, on taking into account the Fresnel light-dragging effect, the vacuum velocity of light, c, in Eq. (3.6) is replaced

by the n-dependent light signal velocities in the laboratory frame

$$c(n)_{\pm} = \frac{c}{n} \pm (V\cos\xi_{\pm}\cos\chi_{\pm} \pm V\sin\xi_{\pm}\sin\chi_{\pm} + \Omega R\cos\xi_{\pm})\left[1 - \frac{1}{n^2}\right], \quad (3.24)$$

which gives, for the velocities of the light signals, relative to the interferometer, in the laboratory frame

$$c(n)^{\rm rel}_{\pm} = \frac{c}{n}\cos\xi_{\pm} \pm \left(V\cos^2\xi_{\pm}\cos\chi_{\pm} \pm V\cos\xi_{\pm}\sin\xi_{\pm}\sin\chi_{\pm} + \Omega R\cos^2\xi_{\pm}\right)$$
$$\times \left[1 - \frac{1}{n^2}\right] \mp V\cos\chi_{\pm} \mp \Omega R\,. \quad (3.25)$$

Making use of Eqs. (3.4) and (3.5) and neglecting terms of $\mathrm{O}(\beta^4)$ and $\mathrm{O}(\beta_V^3)$ Eq. (3.25) may be written as

$$c(n)^{\rm rel}_{\pm} = \frac{c}{n}\left\{1 + \frac{x_{\pm} \mp \beta_{\Omega}}{n} + x_{\pm}^2\left[\frac{1}{2} - \left(n - \frac{1}{n}\right)(1 \mp \beta_{\Omega})\right]\right.$$
$$\left. + \beta_V^2\left[n - \frac{1}{n} - \frac{1}{2} \mp \beta_{\Omega}\left(n - \frac{1}{2n}\right)\right]\right\}, \quad (3.26)$$

where $x_{\pm} \equiv \mp\beta_V\sin\alpha\sin\phi^{\pm}$. Allowing for the time dilation effect given by Eq. (3.17), infinitesimal time intervals $dt'_{\pm}$ in the local comoving frame of the interferometer are related to angular intervals $d\phi_{\pm}$ of the light signal trajectories by the equation

$$dt'_{\pm} = \frac{nR}{c(1 + X_{\pm}(n))}\left\{1 - \frac{\beta_V^2}{2} - \frac{\beta_{\Omega}^2}{2} - \beta_V\beta_{\Omega}\sin\alpha\sin\phi_V\right.$$
$$\left. + \pi\beta_{\Omega}^2\beta_V\sin\alpha\cos\phi_V\right\}d\phi_{\pm} + \mathrm{O}(\beta^4)\,, \quad (3.27)$$

where

$$X_{\pm}(n) \equiv \frac{x_{\pm} \mp \beta_{\Omega}}{n} + x_{\pm}^2\left[\frac{1}{2} - \left(n - \frac{1}{n}\right)(1 \mp \beta_{\Omega})\right]$$
$$+ \beta_V^2\left[n - \frac{1}{n} - \frac{1}{2} \mp \beta_{\Omega}\left(n - \frac{1}{2n}\right)\right].$$

Developing the right side of (3.27) as a power series in β_{Ω} and β_V, retaining only up to $\mathrm{O}(\beta^3)$ terms gives

$$dt'_{\pm} = \frac{R}{c}\left\{n \pm \beta_{\Omega} + \beta_{\Omega}^2\left(\frac{1}{n} - \frac{n}{2}\right) \pm \beta_{\Omega}^3\left(\frac{1}{n^2} - \frac{1}{2}\right)\right.$$
$$- \beta_V^2\left[n^2 - \frac{n}{2} - 1 + \beta_{\Omega}\left(2\left(n - \frac{1}{n}\right) - n^2\right)\right]$$
$$- x_{\pm}\left[1 \pm \beta_{\Omega}\left(\frac{2}{n} - n\right) + 3\beta_{\Omega}^2\left(\frac{1}{n^2} - \frac{1}{2}\right)\right]$$
$$\left. + x_{\pm}^2\left[\frac{1}{n} - \frac{n}{2} + n^2 - 1 \mp \beta_{\Omega}\left\{n - n^2 + 1 - \frac{3}{n^2}\right\}\right]\right\}d\phi_{\pm} + \mathrm{O}(\beta^4)\,. \quad (3.28)$$

Changing variables from $\phi^{\pm}$ to $\phi_{\pm}$ and integrating over $\phi_{\pm}$, making use of Eqs. (A.12) and (A.13) from App. A, gives, for the times-of-passage of the light signals

$$\begin{aligned} T'_{\pm} = \frac{2\pi R}{c}\Bigg\{ & n \pm \beta_\Omega + \beta_\Omega^2\left(\frac{1}{n} - \frac{n}{2}\right) \\ & \pm \beta_\Omega^3\left(\frac{1}{n^2} - \frac{1}{2}\right) + (1-n)\beta_\Omega\beta_V \sin\alpha \sin\phi_V \\ & + \beta_V^2\left[1 - n^2 + \frac{\sin^2\alpha}{2}\left(\frac{1}{n} - \frac{n}{2} + n^2 - 1\right)\right] \pm \beta_\Omega\beta_V^2\left[n^2 - \frac{1}{2}\right. \\ & \left. - 2\left(n - \frac{1}{n}\right) - \frac{\sin^2\alpha}{2}\left\{1 - n^2 + n - \frac{3}{n^2} + \left(\frac{1}{n} - \frac{n}{2} + n^2 - \frac{1}{2}\right)\cos 2\phi_V\right\}\right] \\ & + \beta_\Omega^2\beta_V \sin\alpha\left[(n-1)\pi\cos\phi_V \pm \left(\frac{2}{n} - 1\right)\sin\phi_V\right]\Bigg\} \end{aligned} \tag{3.29}$$

so that Eq. (2.12) generalizes, for $V \neq 0$, to

$$\begin{aligned} \Delta\phi^{\mathrm{CG}}(\beta_V, n) &= 2\pi\nu(T'_+ - T'_-) \\ &= \frac{8\pi A\Omega}{c\lambda_0}\Bigg\{1 + \beta_\Omega^2\left(\frac{1}{n^2} - \frac{1}{2}\right) + \beta_V^2\left[n^2 - \frac{1}{2} - 2\left(n - \frac{1}{n}\right)\right. \\ &\quad \left. - \frac{\sin^2\alpha}{2}\left\{1 - n^2 + n - \frac{3}{n^2} + \left(\frac{1}{n} - \frac{n}{2} + n^2 - \frac{1}{2}\right)\cos 2\phi_V\right\}\right] \\ &\quad + \beta_\Omega\beta_V\left(\frac{2}{n} - 1\right)\sin\alpha\sin\phi_V\Bigg\}. \end{aligned} \tag{3.30}$$

It is seen by comparing Eqs. (2.12), (3.23) and (3.30) that, for all values of the refractive index, the effect of translational motion of the interferometer is only to give correction terms proportional to $\beta_\Omega\beta_V$ and β_V^2. These quadratic correction terms however, unlike the lowest order result, do depend on the value of the refractive index. The Sagnac phase shift $\Delta\phi$ vanishes for purely translational motion. However, for nonvanishing values of Ω sufficiently precise measurements of $\Delta\phi$ with different orientations of the interferometer can in principle, determine the vector $\mathbf{V}$, as well as test the correctness of Fresnel drag coefficient ansatz.

4. The Translational Sagnac Effect: The Fiber Optic Conveyor

The experimental demonstration[26,27] that the Sagnac effect occurs also for purely translational motion (i.e. that rotation is not required for its existence) was done by modification of a fiber optic gyroscope (FOG) employing a single-mode fiber in order to construct a "fiber optic conveyor" (FOC).[26,27] A schematic of a single turn circular FOG is shown in Fig. 7(a). The theory of this device, to order β^3, has been developed in the previous section. The beam-splitter, BS, is a four-way

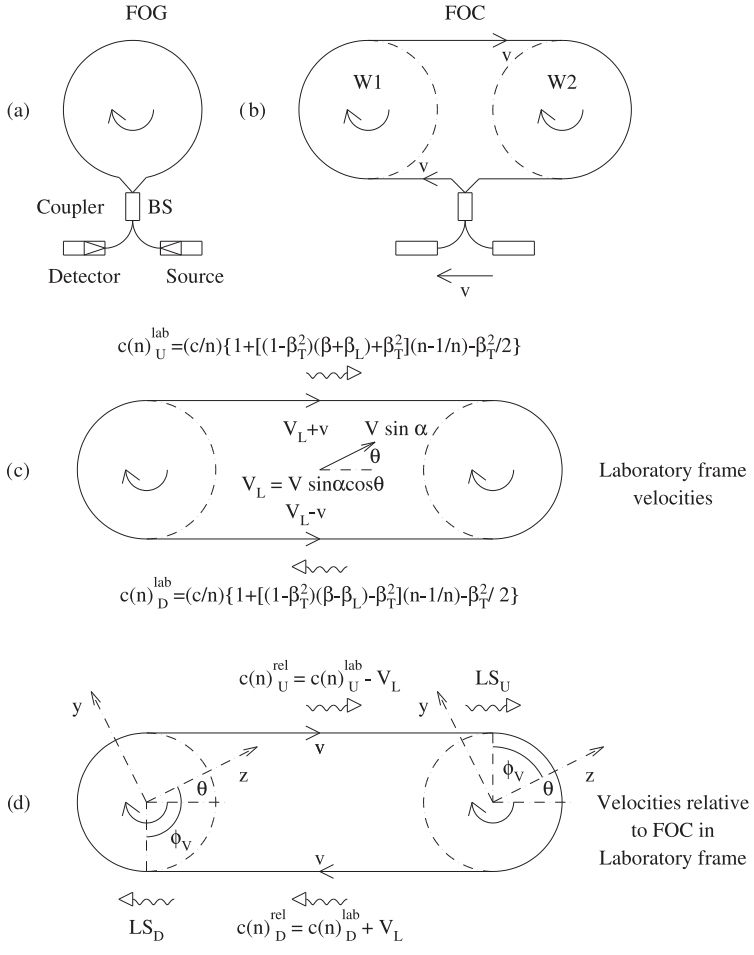

Fig. 7. (a) One-turn fiber optic gyroscope (FOG). (b) One-turn fiber optic conveyor (FOC). The interferometer (Light Source, Coupler and Detector) moves at speed v relative to the centers of the wheels W1 and W2, which rotate due to the motion of the optical fiber. (c) Definitions of velocities of light signals and straight optical fiber segments in the laboratory frame. (d) Relative velocities in the laboratory frame.

fiber-optic light coupler.[57] The light source and detector co-rotate with the optical fiber loop. An FOC (Fig. 7(b)) is constructed by introducing straight sections of optical fiber. The fiber loop passes over freely rotating wheels W1 and W2. The light source, beam splitter and detector undergo translational motion with speed v in the FOC frame. The latter is at rest relative to any fixed, nonmoving, part of the FOC, e.g. the mid-way point between the centers of W1 and W2. The light path has circular portions where the fiber co-rotates with the wheels, intercalated with the straight sections. In the present section, the theory of this device is developed, at order β^3 accuracy, on the assumption that the speed of light is constant in the laboratory frame, taking into account the Fresnel–Fizeau light dragging effect on

the propagation speed of light in the optical fiber, as well as allowing for uniform motion of the FOC frame with speed $\mathbf{V}$ in the laboratory frame.

The speeds of the light signals in the straight sections are shown in the laboratory frame in Fig. 7(c), and relative to the FOC frame in Fig. 1(d):

$$c^{\rm lab}(n)_{\rm U} = \frac{c}{n}\left\{1 + \left[(1-\beta_T^2)(\beta+\beta_L) + \beta_T^2\right]\left(n - \frac{1}{n}\right) - \frac{\beta_T^2}{2}\right\} + {\rm O}(\beta^4)\,, \tag{4.1}$$

$$c^{\rm lab}(n)_{\rm D} = \frac{c}{n}\left\{1 + \left[(1-\beta_T^2)(\beta-\beta_L) + \beta_T^2\right]\left(n - \frac{1}{n}\right) - \frac{\beta_T^2}{2}\right\} + {\rm O}(\beta^4)\,, \tag{4.2}$$

$$c^{\rm rel}(n)_{\rm U} = c^{\rm lab}(n)_{\rm U} - V_L\,, \tag{4.3}$$

$$c^{\rm rel}(n)_{\rm D} = c^{\rm lab}(n)_{\rm D} + V_L\,, \tag{4.4}$$

where the labels U and D indicate the upper and lower straight light paths. The same geometrical definitions are used (see Fig. 5) as in Sec. 3. The component of the velocity of the FOC in the laboratory frame, parallel to the straight light paths in the FOC is: $V_L = V\sin\alpha\cos\theta$. Other definitions used in (4.1) and (4.2) are: $\beta \equiv v/c$, $\beta_V \equiv V/c$, $\beta_L \equiv V_L/c$ and $\beta_T^2 \equiv \beta_V^2 - \beta_L^2$. The expressions (4.1)–(4.4) are obtained from Eqs. (3.24), (3.4) and (3.5) on noting that, from Figs. 5 and 7(d), $c^{\rm lab}(n)_{\rm U}$ corresponds to $\phi^+ = -(3\pi/2+\theta)$ and $c^{\rm lab}(n)_{\rm D}$ to $\phi^+ = -(\pi/2+\theta)$.

The calculation of the times-of-passage of the light signals from and back to the beam splitter is done in three stages:

(i) A global space–time analysis taking into account the light signal velocities relative to the FOC in (4.3) and (4.4), as well as the translational motion of the beam splitter.
(ii) Calculation of the times of passage of the light signals in the semi-circular light paths.
(iii) Calculation of the times of passage of the light signals in the straight light paths.

The global analysis of (i) for a single-turn FOC is shown on Fig. 8 where it is assumed that BS is initially at the mid-point of the lower straight light path of length L. The time intervals in the ECI frame $t_1 - t_5$ for clockwise-rotating signals to arrive at the positions shown are

$$t_1 = \frac{L}{2c^{\rm rel}(n)_{\rm D}}\,, \tag{4.5}$$

$$t_2 = t_1 + \tilde{T}_+(L)\,, \tag{4.6}$$

$$t_3 = t_2 + \frac{L}{c^{\rm rel}(n)_{\rm U}}\,, \tag{4.7}$$

$$t_4 = t_3 + \tilde{T}_+(R)\,, \tag{4.8}$$

$$t_5 \equiv T_+ = \frac{L/2 + c^{\rm rel}(n)_{\rm D} t_4}{c^{\rm rel}(n)_{\rm D} - v}\,, \tag{4.9}$$

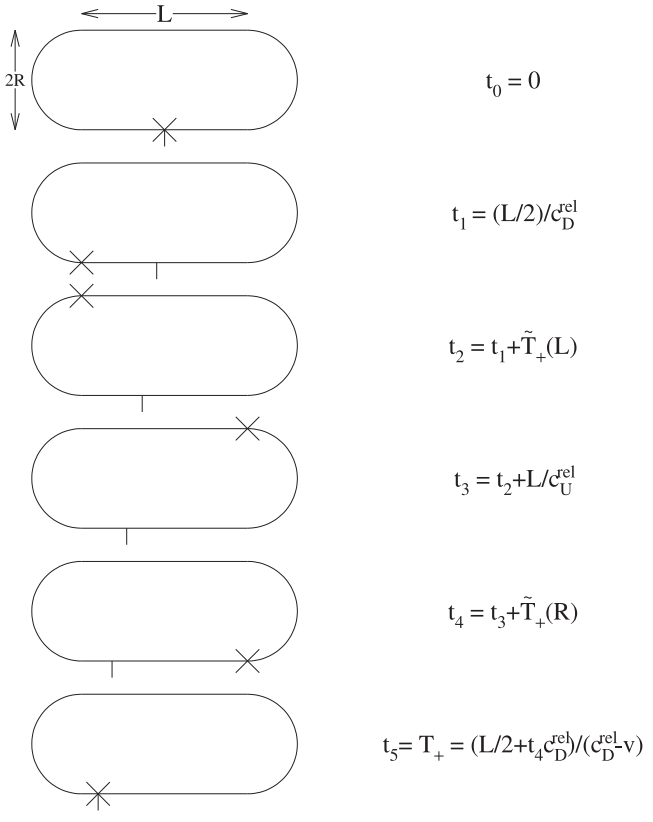

Fig. 8. Laboratory frame configurations and epochs for the passage of a clockwise light signal (indicated by the cross) for the FOC shown in Fig. 7(b).

where $\tilde{T}_+(L)$ and $\tilde{T}_+(R)$ are the times-of-passage of the light signals in the left and right semi-circular paths of radius R. Combining (4.5)–(4.9) gives

$$T_+ \equiv T_+^{\rm rot} + T_+^{\rm trans} = \frac{\tilde{T}_+ c^{\rm rel}(n)_{\rm D}}{c^{\rm rel}(n)_{\rm D} - v} + \frac{L\big(c^{\rm rel}(n)_{\rm U} + c^{\rm rel}(n)_{\rm D}\big)}{c^{\rm rel}(n)_{\rm U}\big(c^{\rm rel}(n)_{\rm D} - v\big)}\,, \qquad (4.10)$$

where $\tilde{T}_+ \equiv \tilde{T}_+(L) + \tilde{T}_+(R)$. The time intervals $\tilde{T}_+(L)$ and $\tilde{T}_+(R)$, required for stage (ii) of the calculation are obtained by adapting the calculation of Sec. 3, where integrals over the angle ϕ_+ — the relative angular separation of the light signal and the beam splitter — were considered. Because of the motion of the optical fiber and the FOC geometry of Fig. 7(d), the time-of-passage of the light signal over the left semi-circular path is given by integrating Eq. (3.28) over the interval zero to $\pi - \delta_+$ of ϕ_+:

$$\delta_+ = \frac{v}{R}\int_0^{\pi-\delta_+} F(\phi_+)d\phi_+ \equiv \frac{v}{R}\tilde{T}_+(L)\,.$$

Noting from Figs. 7(d) and 5 that for the signal $\mathrm{LS_D}$, $\phi_V = -(\pi/2+\theta)$, it is found (for details of the calculation, see App. A) that, neglecting terms of order β^4 and higher

$$\begin{aligned}\tilde{T}_+(L) = \frac{R}{c}\Bigg[&\Bigg\{n+\beta+\frac{\beta^2}{n}+\frac{\beta^3}{n^2}-\beta_V^2\Bigg[n^2-\frac{1}{n}-1+\beta\Bigg[2\bigg(n-\frac{1}{n}\bigg)-n^2\Bigg]\\&-\frac{\sin^2\alpha}{2}\Bigg[\frac{1}{n}-\frac{n}{2}+n^2-1-\beta\bigg(n-n^2+1-\frac{3}{n^2}\bigg)\Bigg]\Bigg]\Bigg\}(\pi-\delta_+)\\&-\beta_V\sin\alpha\Bigg\{\bigg(1+\frac{2\beta}{n}\bigg)[\delta_+\cos\theta-2\sin\theta]+\bigg(\frac{\delta_+^2}{2}-\frac{6\beta^2}{n^2}\bigg)\sin\theta\\&+\frac{\beta^2}{2}[(\pi^2-4)\sin\theta+2\pi\cos\theta]-\bigg[\beta+\beta^2\bigg(1+\frac{2}{n}\bigg)\bigg](\pi\cos\theta-2\sin\theta)\\&-\pi\beta\delta_+\sin\theta-\frac{\beta\beta_V\sin\alpha}{2}\Bigg[\frac{\pi}{2}\cos2\theta+\pi\sin2\theta\Bigg]\Bigg\}\\&-\frac{\beta_V^2\sin^2\alpha}{2}\bigg(\frac{1}{n}-\frac{n}{2}+n^2-1\bigg)[(\beta\pi+\delta_+)\cos2\theta+2\beta\pi\sin2\theta]\Bigg]\end{aligned}\tag{4.11}$$

and that

$$\begin{aligned}\delta_+ = \pi\beta\Bigg\{&n+\beta(1-n^2)+\beta^2\bigg(\frac{1}{n}-2n+n^3\bigg)\\&-\beta_V^2\Bigg[n^2-\frac{n}{2}-1-\frac{\sin^2\alpha}{2}\bigg(\frac{1}{n}-\frac{n}{2}+n^2-1\bigg)\Bigg]\Bigg\}+2\beta\beta_V\sin\alpha\sin\theta\\&+\beta^2\beta_V\sin\alpha\Bigg[\bigg(\frac{4}{n}-2\bigg)\sin\theta+\pi(1-n)\cos\theta\Bigg]+\mathrm{O}(\beta^4)\,.\end{aligned}\tag{4.12}$$

Using (4.12) to eliminate δ_+ from (4.11) it is found that

$$\begin{aligned}\tilde{T}_+(L) = \frac{\pi R}{c}\Bigg\{&n+\beta(1-n^2)+\beta^2\Bigg[\frac{1}{n}-2n+n^3)\Bigg]+\beta^3\bigg(\frac{1}{n^3}-2+3n^2-n^4\bigg)\\&-\beta\beta_V^2\Bigg\{n^2-\frac{n}{2}-1+\beta\bigg(n-\frac{2}{n}-\frac{3n^2}{2}+n^3\bigg)\\&-\frac{\sin^2\alpha}{2}\Bigg[\frac{1}{n}-\frac{n}{2}+n^2-1-\beta\bigg(2-\frac{3n^2}{2}+n^3-\frac{3}{n^2}\bigg)\Bigg]\Bigg\}\\&+\frac{\beta\beta_V\sin\alpha\cos\theta}{\pi}[2(1-n)-\beta(1+n-2n^2)]\\&-\frac{2\beta\beta_V\sin\alpha\sin\theta}{\pi}\Bigg\{1-\frac{2}{n}+\beta\Bigg[3\bigg(1-\frac{1}{n^2}\bigg)+\frac{2}{n}-n-\frac{\pi^2}{4}(1-n^2)\Bigg]\Bigg\}\end{aligned}$$

$$- \frac{\beta\beta_V^2 \sin^2\alpha}{2}\bigg[\bigg(\frac{1}{n} - \frac{3n}{2} + \frac{n^2}{2} + n^3 - \frac{1}{2}\bigg)\cos 2\theta$$
$$+ \bigg(\frac{2}{n} - 3 - n + 2n^2\bigg)\sin 2\theta\bigg]\bigg\} + \mathrm{O}(\beta^4)\,. \tag{4.13}$$

The time interval $\tilde{T}_+(R)$ corresponding to the passage of the light signal LS_U in Fig. 7(d) is also given by integrating Eq. (3.28) over the interval zero to $\pi - \delta_+$ of ϕ_+. In this case $\phi_V = \pi/2 - \theta$.

Hence, for the passage of LS_D:

$$\phi_V = -(\pi/2 + \theta)\,, \quad \sin\phi_V = -\cos\theta\,, \quad \cos\phi_V = -\sin\theta\,,$$
$$\sin 2\phi_V = \sin 2\theta\,, \quad \cos 2\phi_V = -\cos 2\theta\,,$$

while for the passage of LS_U:

$$\phi_V = \pi/2 - \theta\,, \quad \sin\phi_V = \cos\theta\,, \quad \cos\phi_V = \sin\theta\,,$$
$$\sin 2\phi_V = \sin 2\theta\,, \quad \cos 2\phi_V = -\cos 2\theta\,.$$

It follows that $\tilde{T}_+(R)$ is given by (4.12) with the replacements: $\sin\theta \to -\sin\theta$, $\cos\theta \to -\cos\theta$, so that the sum $\tilde{T}_+ = \tilde{T}_+(L) + \tilde{T}_+(R)$ is given by canceling all the terms containing $\sin\theta$ or $\cos\theta$ and multiplying all terms containing $\sin 2\theta$, $\cos^2\theta$ or $\cos 2\theta$, as well as θ-independent terms, by two, i.e.

$$\tilde{T}_+ = \frac{2\pi R}{c}\bigg\{n + \beta(1 - n^2) + \beta^2\bigg[\frac{1}{n} - 2n + n^3)\bigg] + \beta^3\bigg(\frac{1}{n^3} - 2 + 3n^2 - n^4\bigg)$$
$$- \beta_V^2\bigg\{n^2 - \frac{n}{2} - 1 + \beta\bigg(2 - \frac{2}{n} - \frac{3n^2}{2} + n^3\bigg)$$
$$- \frac{\sin^2\alpha}{2}\bigg[\frac{1}{n} - \frac{n}{2} + n^2 - 1 - \beta\bigg(2 - \frac{3n^2}{2} + n^3 - \frac{3}{n^2}\bigg)\bigg]\bigg\}$$
$$- \frac{\beta\beta_V^2}{2}\bigg[\bigg(\frac{1}{n} - \frac{3n}{2} + \frac{n^2}{2} + n^2 - \frac{1}{2}\bigg)\cos 2\theta$$
$$+ \bigg(\frac{2}{n} - 3 - n + 2n^2\bigg)\sin 2\theta\bigg]\bigg\} + \mathrm{O}(\beta^4)\,. \tag{4.14}$$

Substituting this expression for $\tilde{T}_+$ in that for T_+^{rot} in Eq. (4.10) and retaining only up to order β^3 terms gives

$$T_+^{\mathrm{rot}} = \frac{2\pi R}{c}\bigg[n + \beta + \beta^2\bigg(\frac{1}{n} - n + n^2\bigg) + \beta^3\bigg(\frac{1}{n^3} - 1 + n^2 + 3n^3 - 3n^4\bigg)$$
$$- \beta\beta_V \sin\alpha\cos\theta\big[n + \beta(3 - n^2)\big]$$
$$- \beta_V^2\bigg\{n^2 - \frac{n}{2} - 1 + \beta\bigg(\frac{n}{2} - \frac{2}{n} - \frac{5n^2}{2} + \frac{3n^3}{2} + 1\bigg)$$

$$-\frac{\sin^2\alpha}{2}\left[\frac{1}{n}-\frac{n}{2}+n^2-1-\beta\left\{3-\frac{5n^2}{2}+\frac{n^3}{2}-\frac{3}{n^2}-\frac{n}{2}+1\right.\right.$$
$$+\left(\frac{1}{n}-2n+\frac{3n^2}{2}+\frac{n^3}{2}-\frac{3}{2}\right)\cos 2\theta$$
$$\left.\left.+\left(\frac{2}{n}-3-n+2n^2\right)\sin 2\theta\right\}\right]\Bigg\}\Bigg]+\mathrm{O}(\beta^4)\,. \tag{4.15}$$

For the contribution of the straight light paths combining (4.1)–(4.4) with (4.10) gives

$$T_+^{\mathrm{trans}}=\frac{(2nL/c)(1+\alpha_T+\beta_1)}{(1+\alpha_T+\beta_-)(1+\alpha_T+\beta_+)}+\mathrm{O}(\beta^4)\,, \tag{4.16}$$

where

$$\beta_1\equiv\beta(n-1/n)(1-\beta_T^2)\,,\quad \beta_-\equiv(\beta-\beta_L)[(n-1/n)(1-\beta_T^2)-n]\,,$$
$$\beta_+\equiv(\beta+\beta_L)(n-1/n)(1-\beta_T^2)-n\beta_L\,,\quad \alpha_T\equiv\beta_T^2(n-1/n-1/2)\,.$$

As shown in Fig. 9, an FOC configuration with counterclockwise-rotating light signals is the image in a plane mirror of the configuration obtained by making the replacements $v\to -v$, $V_L\to -V_L$ in a configuration with clockwise-rotating light signals. The time intervals T_-^{trans} and T_-^{rot} for counterclockwise-rotating signals are therefore obtained by making the replacements $\beta\to-\beta$ and $\beta_L\to-\beta_L$ in (4.16)

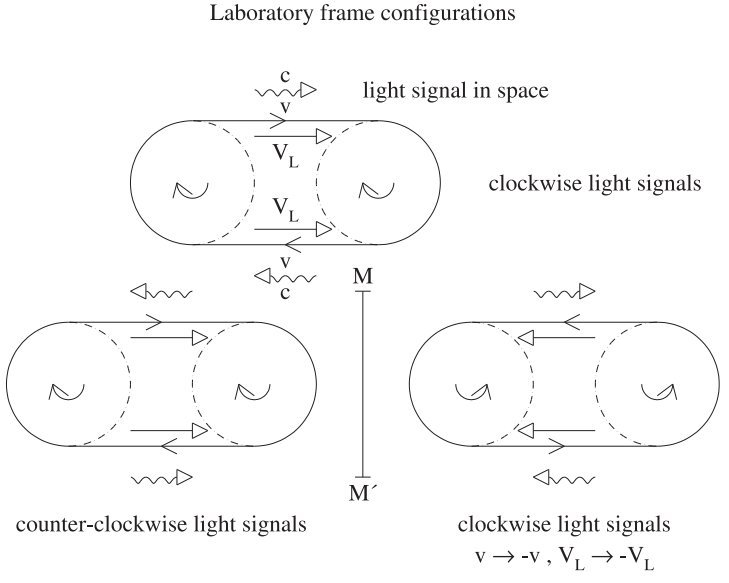

Fig. 9. The physically equivalent image in the plane mirror MM′ with counterclockwise light signals is obtained from the configuration with clockwise light signals, by the operations $v\to -v$, $V_L\to -V_L$. Hence the time of passage of the counterclockwise light signals is obtained from the formula (4.15) for the clockwise light signals on making these replacements.

and the replacements $\beta \to -\beta$ and $\cos\theta \to -\cos\theta$, $\sin 2\theta \to -\sin 2\theta$ in Eq. (4.15) This gives

$$T_-^{\rm trans} = \frac{(2nL/c)(1+\alpha_T-\beta_1)}{(1+\alpha_T-\beta_-)(1+\alpha_T-\beta_+)} + {\rm O}(\beta^4) \tag{4.17}$$

and

$$\begin{aligned} T_-^{\rm rot} = \frac{2\pi R}{c}\Bigg[& n-\beta+\beta^2\left(\frac{1}{n}-n+n^2\right)-\beta^3\left(\frac{1}{n^3}-1+n^2+3n^3-3n^4\right) \\ & -\beta\beta_V \sin\alpha\cos\theta[n-\beta(3-n^2)] \\ & -\beta_V^2\left\{n^2-\frac{n}{2}-1-\beta\left(\frac{n}{2}-\frac{2}{n}-\frac{5n^2}{2}+\frac{3n^3}{2}+1\right)\right. \\ & -\frac{\sin^2\alpha}{2}\left[\frac{1}{n}-\frac{n}{2}+n^2-1+\beta\left\{3-\frac{5n^2}{2}+\frac{n^3}{2}-\frac{3}{n^2}-\frac{n}{2}+1\right.\right. \\ & +\left(\frac{1}{n}-2n+\frac{3n^2}{2}+\frac{n^3}{2}-\frac{3}{2}\right)\cos 2\theta \\ & \left.\left.\left.-\left(\frac{2}{n}-3-n+2n^2\right)\sin 2\theta\right\}\right]\right\}\Bigg] + {\rm O}(\beta^4)\,. \end{aligned} \tag{4.18}$$

Subtracting Eq. (4.17) from (4.16) (for details of the calculation see App. A) gives

$$\begin{aligned} \Delta T^{\rm trans} &\equiv T_+^{\rm trans} - T_-^{\rm trans} \\ &= \frac{4L\beta}{c}\left\{1+\frac{\beta^2}{n^2}+\beta\beta_V\sin\alpha\cos\theta(n^2-3)\right. \\ &\quad \left.+\beta_V^2\left[n^2-2n+\frac{2}{n}-\sin^2\alpha\cos^2\theta\left(\frac{3}{n^2}-\frac{2}{n}-1+2n-n^2\right)\right]\right\}+{\rm O}(\beta^5) \end{aligned} \tag{4.19}$$

while subtracting Eq. (4.18) from (4.15) gives

$$\begin{aligned} \Delta T^{\rm rot} &\equiv T_+^{\rm rot} - T_-^{\rm rot} \\ &= \frac{4\pi R\beta}{c}\left\{1+\beta^2\left(\frac{1}{n^3}-1+n^2+3n^3-3n^4\right)\right. \\ &\quad -\beta_V^2\left[\frac{n}{2}-\frac{2}{n}-\frac{5n^2}{2}+\frac{3n^3}{2}+1+\frac{\sin^2\alpha}{2}\left\{3-\frac{5n^2}{2}+\frac{n^3}{2}-\frac{3}{n^2}-\frac{n}{2}+1\right.\right. \\ &\quad \left.\left.\left.+\left(\frac{1}{n}-2n+\frac{3n^2}{2}+\frac{n^3}{2}-\frac{3}{2}\right)\cos 2\theta\right\}\right]-(3-n^2)\beta\beta_V\sin\alpha\cos\theta\right\}+{\rm O}(\beta^5)\,. \end{aligned} \tag{4.20}$$

All time intervals considered in this section up to this point are those recorded by a clock at rest in the laboratory inertial frame. A fixed point on the nonmoving

part of the FOC moves with speed $\mathbf{V}$ in the laboratory frame, where, (see Figs. 5 and 7(c)):

$$\mathbf{V} = V(\hat{\imath}\cos\alpha + \hat{k}\sin\alpha)\,. \tag{4.21}$$

The interferometer (I) that measures the phase shift between the counter-rotating beams consisting of the light source, the coupler BS, and the photon detector moves with velocity $\mathbf{v}$ relative to a fixed point on the FOC where (see Fig. 7(d)):

$$\mathbf{v} = v(\hat{\jmath}\sin\theta - \hat{k}\cos\theta)\,. \tag{4.22}$$

Taking into account relativistic time dilation the appropriate time interval to calculate the Sagnac interference phase is therefore

$$\Delta T' = \frac{\Delta T}{\gamma_I}\,, \tag{4.23}$$

where $\gamma_I \equiv 1/\sqrt{1-(\mathbf{V}_I/c)^2}$, $\mathbf{V}_I = \mathbf{V} + \mathbf{v}$. According to Eqs. (4.21) and (4.22) then

$$\Delta T' = \Delta T\left(1 - \frac{\beta_V^2}{2} - \frac{\beta^2}{2} + \beta\beta_L\right) + \mathrm{O}(\beta^4)\,. \tag{4.24}$$

Combining (4.19), (4.20) and (4.24) the following Sagnac phase shift is obtained:

$$\Delta\phi_{\mathrm{FOC}}(n) = \Delta\phi_{\mathrm{FOC}}^{\mathrm{trans}}(n) + \Delta\phi_{\mathrm{FOC}}^{\mathrm{rot}}(n)\,, \tag{4.25}$$

$$\begin{aligned}\Delta\phi_{\mathrm{FOC}}^{\mathrm{trans}}(n) = \frac{8\pi L\beta}{\lambda_0}\Bigg\{1 &+ \beta^2\left(\frac{1}{n^2} - \frac{1}{2}\right) + \beta\beta_V\sin\alpha\cos\theta(n^2-2)\\ &+ \beta_V^2\Bigg[n^2 - 2n + \frac{2}{n} - \frac{1}{2}\\ &- \sin^2\alpha\cos^2\theta\left(\frac{3}{n^2} - \frac{2}{n} - 1 + 2n - n^2\right)\Bigg]\Bigg\} + \mathrm{O}(\beta^5)\,,\end{aligned} \tag{4.26}$$

$$\begin{aligned}\Delta\phi_{\mathrm{FOC}}^{\mathrm{rot}}(n) = \frac{8\pi^2 R\beta}{\lambda_0}\Bigg\{1 &+ \beta^2\left(\frac{1}{n^3} - \frac{3}{2} + n^2 + 3n^3 - 3n^4\right)\\ &- \beta_V^2\Bigg[\frac{n}{2} - \frac{2}{n} - \frac{5n^2}{2} + \frac{3n^3}{2} + \frac{3}{2}\\ &+ \frac{\sin^2\alpha}{2}\Bigg\{3 - \frac{5n^2}{2} + \frac{n^3}{2} - \frac{3}{n^2} - \frac{n}{2} + 1\\ &+ \left(\frac{1}{n} - 2n + \frac{3n^2}{2} + \frac{n^3}{2} - \frac{3}{2}\right)\cos 2\theta\Bigg\}\Bigg]\\ &- (2-n^2)\beta\beta_V\sin\alpha\cos\theta\Bigg\} + \mathrm{O}(\beta^5)\,,\end{aligned} \tag{4.27}$$

which simplify, when $n = 1$, to

$$\Delta\phi_{\rm FOC}(n=1) = \Delta\phi^{\rm trans}_{\rm FOC}(n=1) + \Delta\phi^{\rm rot}_{\rm FOC}(n=1)\,, \tag{4.28}$$

$$\Delta\phi^{\rm trans}_{\rm FOC}(n=1)$$
$$= \frac{8\pi L\beta}{\lambda_0}\left[1 + \frac{1}{2}\{\beta^2 + \beta_V^2(1 - 2\sin^2\alpha\cos^2\theta)\} + \beta\beta_V\sin\alpha\cos\theta\right] + {\rm O}(\beta^5)\,, \tag{4.29}$$

$$\Delta\phi^{\rm rot}_{\rm FOC}(n=1)$$
$$= \frac{8\pi^2 R\beta}{\lambda_0}\left[1 + \frac{\beta^2}{2} + \beta_V^2\left(1 + \frac{\sin^2\alpha}{4}[3 + 2\cos^2\theta]\right) - \beta\beta_V\sin\alpha\cos\theta\right] + {\rm O}(\beta^5)\,. \tag{4.30}$$

Neglecting the order β^2 and β_V^2 corrections it is found at lowest order (LO) that

$$\Delta\phi^{\rm LO}_{\rm FOC}(n) = \frac{4\pi}{\lambda_0 c}(2L + 2\pi R)v = \frac{4\pi}{\lambda_0 c}sv = \frac{4\pi}{\lambda_0 c}\oint \mathbf{v}\cdot d\mathbf{s}\,, \tag{4.31}$$

where $s = 2L + 2\pi R$ is the total path length. This is an example of the general Sagnac phase difference formula (1.2). The above calculation is for an FOC with a single turn of optical fiber. For a device with N turns the total path length is Ns so that the phase difference given by Eq. (4.21) is multiplied by a factor N. This may give a large increase in the sensitivity of the device to the value of v. As in the case of the rotational interferometer discussed in Sec. 3, uniform translational motion of the FOC contributes only refractive-index-dependent quadratic terms proportional to $\beta_\Omega\beta_V$ and β_V^2. Also, as for the rotating interferometer, if the value of v is known, sufficiently precise measurement of the interference phase with different orientations enables measurement of the velocity $\mathbf{V}$ relative to the preferred frame and a test of the functional n-dependence of the Fresnel drag coefficient.

5. The Hafele–Keating Experiment

The "airborne clocks" experiment was proposed by Hafele[21] and performed by Hafele and Keating[19,20] in 1971. In the experiment, four caesium beam atomic clocks were flown around the Earth in commercial airliners, once from west to east (W-E) and once from east to west (E-W). After each round trip the clocks were compared with fixed reference clocks at the US Naval Observatory. Rate differences between the airborne and fixed clocks exist both because of different motions of the clocks in the ECI frame, a predominantly special relativistic (SR) effect — time dilation — and because of the GR gravitational blue-shift due to the different higher gravitational potentials experienced by the airborne clocks. Following Hafele[21] a general-relativistic analysis will first be presented here. For later comparison with the Sagnac effect, first-order corrections due to the Earth's gravitational potential and second-order velocity corrections will also be calculated, as well as the lowest-order prediction obtained by Hafele. The contribution of clock motion to the rate change will also be calculated using only special relativity and compared with the

general relativistic prediction. As previously discussed in Ref. 22 the SR analysis will be seen to shed light on the different physical meanings of RPVAR and RRVTR velocity transformation formulas discussed in Sec. 2 as well as the Ehrenfest rotating disc paradox. The calculation is also performed using the SCI instead of the ECI frame to define "coordinate time."

An increment $d\tau$ of the proper time of a clock in the gravitational field of the Earth is related to the "coordinate time" increment dt recorded by a clock at rest in the ECI frame by the Schwarzschild metric equation[1,2] obtained as the solution of the Einstein field equations in the free space around a nonrotating[e] spherically symmetric body with gravitational potential ϕ

$$d\tau = \left[1 + \frac{2\phi}{c^2} - \frac{1}{c^2}\left(\frac{v_r^2}{1 + \frac{2\phi}{c^2}} + v_\theta^2 + v_\phi^2\right)\right]^{\frac{1}{2}} dt\,. \tag{5.1}$$

The spherical polar (r, θ, ϕ) coordinate system has its origin at the center of the body with polar axis parallel to the angular velocity vector of the body. It is assumed in this equation that the conceptual clock recording coordinate time is at a distance from the Earth sufficiently large that all effects due to the gravitational field of the latter may be neglected. A simplified version of the Hafele–Keating experiment will be considered where the ground based clock is at the Equator and the aircraft undergoes an equatorial circumnavigation at fixed altitude h. It is assumed that the Earth is exactly spherical so that the gravitational potentials experienced by the Earth-fixed clock, $\phi_{\rm E}$, and the aircraft, $\phi_{\rm A}$, are

$$\phi_{\rm E} = -\frac{GM_{\rm E}}{R_{\rm E}}\,, \quad \phi_{\rm A} = -\frac{GM_{\rm E}}{R_{\rm E} + h} \simeq -\frac{GM_{\rm E}}{R_{\rm E}}\left(1 - \frac{h}{R_{\rm E}}\right), \tag{5.2}$$

where G is the gravitational constant and $M_{\rm E}$ and $R_{\rm E}$ are the mass and radius of the Earth. To first order in the small quantity h/R, $\phi_{\rm E}$ and $\phi_{\rm A}$ are related as

$$\phi_{\rm A} = \phi_{\rm E}\left(1 - \frac{h}{R_{\rm E}}\right), \quad \frac{h}{R_{\rm E}} \ll 1\,. \tag{5.3}$$

The ECI frame, the comoving inertial frame of the Earth-fixed clock, and the comoving inertial frame of the airborne clock are denoted by S, S′ and S″, respectively, so that the proper times of the Earth-fixed and airborne clocks are τ' and τ'', respectively. For both the Earth-fixed and airborne clocks $v_r = v_\theta = 0$ in Eq. (5.1). The azimuthal velocity, v_ϕ, for the Earth-fixed clock is equal to $v_{\rm E} = R_{\rm E}\Omega_{\rm E}$ where $\Omega_{\rm E}$ is the angular velocity of rotation of the Earth, whereas for the airborne clock

$$v_\phi = v_{\rm A}(\pm) = \frac{v_{\rm E} \pm v'_{\rm A}}{1 \pm \frac{v_{\rm E} v'_{\rm A}}{c^2}}\,, \tag{5.4}$$

[e]The Lense-Thirring[45] "frame dragging" effect due to the Earth's rotation is neglected.

where $v'_{\rm A}$ is the speed of the aircraft relative to the surface of the Earth.[f] The velocities $v_{\rm A}(+)$ ($v_{\rm A}(-)$) correspond to the W-E (E-W) flights. Proper time intervals for the airborne clock for the W-E (E-W) flights are denoted by $d\tau''_{+}$ ($d\tau''_{-}$), and for the Earth-fixed clock by $d\tau'$. The Schwarzschild metric equations for the Earth-fixed and airborne clocks are therefore

$$d\tau' = \left[1 + \frac{2\phi_{\rm E}}{c^2} - \beta_{\rm E}^2\right]^{\frac{1}{2}} dt\,, \tag{5.5}$$

$$d\tau''_{\pm} = \left[1 + \frac{2\phi_{\rm A}}{c^2} - \beta_{\rm A}(\pm)^2\right]^{\frac{1}{2}} dt\,, \tag{5.6}$$

where $\beta_{\rm E} \equiv v_{\rm E}/c$ and $\beta_{\rm A}(\pm) \equiv v_{\rm A}(\pm)/c$. Taking the ratio of (5.6) to (5.5) the coordinate time element dt cancels so that the proper time intervals of the airborne and Earth-fixed clocks are related by the equation

$$\begin{aligned} d\tau''_{\pm} &= \left[\frac{1 + \frac{2\phi_{\rm A}}{c^2} - \beta_{\rm A}(\pm)^2}{1 + \frac{2\phi_{\rm E}}{c^2} - \beta_{\rm E}^2}\right]^{\frac{1}{2}} d\tau' \\ &= \left\{1 - \frac{\phi_{\rm E}}{c^2}\left(\frac{h}{R_{\rm E}}\right) - \frac{\beta'_{\rm A}}{2}(\beta'_{\rm A} \pm 2\beta_{\rm E}) \right. \\ &\quad \left. + \left(\beta'_{\rm A}\right)^2\left[\beta_{\rm E}^2 \pm \frac{\beta_{\rm E}\beta'_{\rm A}}{2} - \frac{(\beta'_{\rm A})^2}{8}\right]\right\} d\tau' + {\rm O}(\phi_{\rm E}\beta^2)\,. \end{aligned} \tag{5.7}$$

Introducing the round-trip time intervals recorded by the airborne and Earth-fixed clocks

$$T''_{\pm} = \int d\tau''_{\pm}\,, \quad T' = \int d\tau' = \frac{2\pi R}{v'_{\rm A}} \tag{5.8}$$

(5.7) gives

$$\begin{aligned} \Delta T'_{\pm} \equiv T''_{\pm} - T' = T'\left\{-\frac{\phi_{\rm E}}{c^2}\left(\frac{h}{R_{\rm E}}\right) - \frac{\beta'_{\rm A}}{2}\left(\beta'_{\rm A} \pm 2\beta_{\rm E}\right)\right. \\ \left. + \left(\beta'_{\rm A}\right)^2\left[\beta_{\rm E}^2 \pm \frac{\beta_{\rm E}\beta'_{\rm A}}{2} - \frac{(\beta'_{\rm A})^2}{8}\right]\right\}. \end{aligned} \tag{5.9}$$

Values of the parameters in Eq. (5.9) comparable to those of the actual HKE are given by choosing $h = 10$ km, $v'_{\rm A} = 300$ m/s. Then with $M_{\rm E} = 5.972 \times 10^{21}$ kg,

[f]Note that v_ϕ occurs at the second order in the Schwarzschild metric equation and determines the size of the time dilation contribution in (5.5) and (5.6). The use of the RPVAR to calculate this kinematical β^2 term, instead of the RRVTR, which must be used to describe order β space–time geometric effects, is further discussed in the following.

$R_{\rm E} = 6.38 \times 10^6$ m, $\Omega_{\rm E} = 7.27 \times 10^{-5}$ rad/s it is found that

$$\frac{\phi_{\rm E}}{c^2} = -6.94 \times 10^{-10}\,,$$
$$\frac{h}{R_{\rm E}} = 1.57 \times 10^{-3}\,,$$
$$\beta_{\rm E} = 1.55 \times 10^{-6}\,,$$
$$\beta'_{\rm A} = 1.00 \times 10^{-6}\,,$$
$$T' = 1.37 \times 10^5 \text{ s}\,.$$

The GR contribution to $\Delta T'_{\pm}$ due to the potential $\phi_{\rm E}$ is then

$$\Delta T'_{\pm}({\rm GR}) = -\frac{T'\phi_{\rm E}}{c^2}\left[\frac{h}{R_{\rm E}}\right] = 145 \text{ ns}\,,$$

while the order β^2 SR time dilation contributions are

$$\Delta T'_{+}({\rm SR}) = T'\left[-\frac{\beta'_{\rm A}}{2}\big(\beta'_{\rm A} + 2\beta_{\rm E}\big)\right] = -274 \text{ ns}\,,$$
$$\Delta T'_{-}({\rm SR}) = T'\left[-\frac{\beta'_{\rm A}}{2}\big(\beta'_{\rm A} - 2\beta_{\rm E}\big)\right] = 140 \text{ ns}\,.$$

For comparison, in the HKE where the predicted time differences were calculated by integration of a generalized version of the differential equation (5.7) over the actual flight paths of the airliners, it was found that[19]

$$\Delta T'_{+}({\rm GR})_{\rm HK} = 144 \pm 14 \text{ ns}\,, \qquad \Delta T'_{-}({\rm GR})_{\rm HK} = 179 \pm 18 \text{ ns}\,,$$
$$\Delta T'_{+}({\rm SR})_{\rm HK} = -184 \pm 18 \text{ ns}\,, \quad \Delta T'_{-}({\rm GR})_{\rm HK} = 96 \pm 10 \text{ ns}$$

and combining the GR and SR contributions:

$$\Delta T'_{+}({\rm GR})_{\rm HK} + \Delta T'_{+}({\rm GR})_{\rm HK} = -40 \pm 23 \text{ ns}\,,$$
$$\Delta T'_{-}({\rm GR})_{\rm HK} + \Delta T'_{-}({\rm GR})_{\rm HK} = 275 \pm 21 \text{ ns}$$

to be compared with the results of the experiment:[20]

$$\Delta T'_{+}({\rm meas})_{\rm HK} = -59 \pm 10 \text{ ns}\,,$$
$$\Delta T'_{-}({\rm meas})_{\rm HK} = 273 \pm 7 \text{ ns}\,.$$

If instead of comparing the airborne clocks to a ground based one, an idealized experiment is considered in which two aircrafts are used to perform simultaneous W-E and E-W round trip flights with the same values of h and $v'_{\rm A}$, then (5.9) gives

$$\Delta T'' \equiv T''_{+} - T''_{-} = -\frac{4\pi R_{\rm E} v_{\rm E}}{c^2}\left[1 - \frac{(\beta'_{\rm A})^2}{2}\right]. \tag{5.10}$$

The difference of the time intervals recorded by the airborne clocks are independent of $v'_{\rm A}$ at lowest order in β but depends linearly on $v_{\rm E}$. Measurement of $\Delta T''$ therefore determines $v_{\rm E}$ and so the rate of rotation of the Earth. Such an experiment would be analogous to the Michelson–Gale experiment[13] which used the Sagnac effect to measure the latter quantity. As will be discussed below, the lowest order Sagnac formula for light propagation time differences is similar to (5.10), which has lead to an unfortunate conflation in the literature of Sagnac and Hafele–Keating-like experiments, which are physically quite distinct. The former measures a nonrelativistic order β effect, the latter an order β^2 relativistic one. Further discussion of the distinction between the Sagnac and Hafele–Keating experiments is found in Sec. 7.

The formula (5.10) for $\Delta T''$ can also be obtained using only special relativity. Time dilation observed from the frame S gives the relations

$$T_{\rm SR} = \gamma(\beta_{\rm E})T' = \gamma(\beta_{\rm A}(\pm))(T''_{\pm})_{\rm SR}\,, \tag{5.11}$$

where $\gamma(\beta) = 1/\sqrt{1-\beta^2}$ and $T_{\rm SR} = \int dt$. The time dilation factor $\gamma(\beta_{\rm A}(\pm))$ between the frames S and S$''$ is related to that $\gamma(\beta'_{\rm A})$ between the frames S$'$ and S$''$ by the Lorentz transformation of the temporal component of the dimensionless four-vector $(V_0;\mathbf{V}) = (\gamma(\beta'_{\rm A});\gamma(\beta'_{\rm A})\beta'_{\rm A},0,0)$

$$\gamma(\beta_{\rm A}(\pm)) = \gamma(\beta_{\rm E})\big[\gamma(\beta'_{\rm A}) \pm \beta_{\rm E}\beta'_{\rm A}\gamma(\beta'_{\rm A})\big] = \gamma(\beta_{\rm E})\gamma(\beta'_{\rm A})\big[1 \pm \beta_{\rm E}\beta'_{\rm A}\big]\,. \tag{5.12}$$

Combining (5.11) and (5.12)

$$(T''_{\pm})_{\rm SR} = \frac{\gamma(\beta_{\rm E})}{\gamma(\beta_{\rm A}(\pm))}T' = \frac{T'}{\gamma(\beta'_{\rm A})\big[1 \pm \beta_{\rm E}\beta'_{\rm A}\big]} \tag{5.13}$$

so that

$$\begin{aligned}\Delta T''_{\rm SR} &\equiv (T''_{+})_{\rm SR} - (T''_{-})_{\rm SR}\\ &= -\frac{2T'\beta_{\rm E}\beta'_{\rm A}}{\gamma(\beta'_{\rm A})\big[1-\big(\beta_{\rm E}\beta'_{\rm A}\big)^2\big]}\\ &= -\frac{4\pi R_{\rm E}v_{\rm E}}{c^2}\left(1-\frac{(\beta'_{\rm A})^2}{2}\right) + {\rm O}(\beta^5)\,,\end{aligned} \tag{5.14}$$

which agrees with (5.10).

Consideration of the space–time geometry of the HKE sheds further light on the physical meanings of the RPVAR and RRVTR velocity transformation formulas discussed in Sec. 2. The conventional RPVAR (5.4) used above to calculate $v_{\rm A}(\pm)$ is algebraically equivalent[g] to the four-vector transformation equation (5.12) used to calculate the time dilation factor $\gamma(\beta_{\rm A}(\pm))$. This kinematical application of the RPVAR is a physically correct one, equivalent to the transformation of the relativistic energy of any ponderable object between two different kinematical configurations. However, as will now be demonstrated, the RPVAR does *not* correctly

[g]That is, if either equation is postulated the other can be derived purely by algebraic manipulation.

describe the space–time geometry of the HKE as observed in these frames. Spatial geometry in the ECI frame S gives, on setting for simplicity $h = 0$, for the path lengths s_+ (s_-) of the W-E (E-W) flights

$$s_+ = v_{\rm E}T + 2\pi R_{\rm E}\,, \tag{5.15}$$

$$s_- = v_{\rm E}T - 2\pi R_{\rm E}\,. \tag{5.16}$$

Because the speed $v'_{\rm A}$ of the aircraft relative to the surface of the Earth is the same in the W-E and E-W flights and the distance traveled relative to the surface of the Earth, $2\pi R_{\rm E}$, is the same, the time T' of the flights, measured in the frame S$'$, is the same for both. Denoting the observed speeds of the aircraft in the frame S by $(v_{\rm A}^{\rm obs})_\pm$, space–time geometry in the frame S gives

$$\big(v_{\rm A}^{\rm obs}\big)_\pm = \frac{s_\pm}{T}\,, \tag{5.17}$$

while time dilation between the frames S and S$'$ gives

$$T' = \frac{2\pi R_{\rm E}}{v'_{\rm A}} = \frac{T}{\gamma(\beta_{\rm E})}\,. \tag{5.18}$$

Combining (5.15)–(5.18) then gives

$$\big(v_{\rm A}^{\rm obs}\big)_\pm = v_{\rm E} \pm \frac{v'_{\rm A}}{\gamma(\beta_{\rm E})}\,, \tag{5.19}$$

which is the analogue of the inverse of the RRVTR (2.6) derived by considerations of the space–time geometry of the Sagnac effect.

Replacing T in (5.15) by T_+, T in (5.16) by T_-, T in (5.17) by $T_\pm$ and $\big(v_{\rm A}^{\rm obs}\big)_\pm$ in (5.19) by $v_{\rm A}(\pm)$, the first member of (5.18) leads, after algebraic manipulation, to

$$T_\pm = \frac{T'v'_{\rm A}}{\pm v_{\rm A}(\pm) \mp v_{\rm E}}\,. \tag{5.20}$$

Substituting $(v_{\rm A}^{\rm obs})_\pm$ from (5.19) for $v_{\rm A}(\pm)$ in this equation gives

$$T_+ = T_- = \gamma(\beta_{\rm E})T' \equiv T \tag{5.21}$$

consistent with (5.15), (5.16) and (5.18). Substituting, instead, $v_{\rm A}(\pm)$ given by the RPVAR (5.4) it is found that

$$T_\pm = T'\gamma(\beta_{\rm E})^2\big(1 \pm \beta_{\rm E}\beta'_{\rm A}\big)\,. \tag{5.22}$$

These relations are inconsistent both with the spatial geometry of the paths in the frame S as described by (5.15) and (5.16), which requires that $T_+ = T_-$ as well as the time dilation relations (5.21). Evidently, the observed space–time geometry of the HKE in the frames S and S$'$ is *not* correctly described by the RPVAR (5.4). At an even more fundamental level, the prediction of (5.22) of different values of T_+ and T_- for the same value of T' is at variance with a general theorem of space–time geometry pointed out by Langevin[58] and recalled by Mermin[59,60] — the frame invariance of a triple worldline intersection. Consider the experiment where the W-E

and E-W flights are performed simultaneously by two aircrafts with the same value of $v'_{\rm A}$. They will arrive back simultaneously at their starting point — a point on the worldlines of both aircraft and of their points of departure.[h] The aircraft will be seen, in any reference frame, to arrive simultaneously at this point. It is impossible that a unique value of T' can correspond to different values of T, as predicted by (5.22).

Consider now the distance $\Delta L'_+ = v'_{\rm A}\Delta\tau'$ of the Eastward flying aircraft from its point of departure after a time interval in the frame S′, $\Delta\tau'$, sufficiently short that the curvature of the surface of the Earth may be neglected. The distance moved by the aircraft in the frame S during the corresponding time interval Δt is

$$\Delta s_+ = (v_{\rm A}^{\rm obs})_+\Delta t = v_{\rm E}\Delta t + \Delta L_+\,, \tag{5.23}$$

where ΔL_+ is the separation of the aircraft from its point of departure in the frame S. Combining (5.19) and (5.23) gives

$$\Delta L_+ = \left[\left(v_{\rm A}^{\rm obs}\right)_+ - v_{\rm E}\right]\Delta t = \frac{v'_{\rm A}\Delta t}{\gamma(\beta_{\rm E})} = v'_{\rm A}\Delta\tau' = \Delta L'_+\,, \tag{5.24}$$

where the time dilation relation $\Delta t = \gamma(\beta_{\rm E})\Delta\tau'$ has been used. This demonstrates the invariance of the length interval between the aircraft and its point of departure at corresponding times in the frames S and S′. Consideration of similar infinitesimal intervals dL'_+, dL_+ for $h = 0$ gives:

$$\int dL'_+ \equiv C' = \int dL_+ \equiv C = 2\pi R_{\rm E}\,, \tag{5.25}$$

which resolves[22] the Ehrenfest paradox concerning the ratio of the circumference, C, to the diameter, $2R$, of a rotating disc. It is neither less than π, as asserted by Ehrenfest[61] nor greater than π, as asserted by Einstein,[62] and no consideration of non-Euclidean geometry is required. The spurious nature of the "length contraction" effect of standard special relativity theory is discussed elsewhere.[49,50,63,64]

The analysis of the HKE will now be redone using coordinate time defined in the SCI frame instead of the ECI frame. The geometrical and kinematical variables employed are shown in Fig. 10. Cartesian coordinates in the equatorial plane of the Earth are defined with y-axis pointing towards the Sun and x-axis in the direction of motion of the centroid of the Earth around the Sun with velocity $\mathbf{V}$. Effects of the change of direction of $\mathbf{V}$ during the flights are neglected as well as the tilt of the axis of rotation of the Earth relative to the normal to its orbital plane. Only special relativistic effects are considered. The ground station containing the Earth-fixed clock is denoted by E, the aircraft by A and the fixed point on the Earth is immediately below the aircraft, at any instant, by G. At the start of the W-E flight

[h]To avoid any collision the aircraft might take off and land from separate runways parallel to the Equator but slightly shifted, by the same distance, to the north or south. On arrival the aircraft and their point of departure will be seen to have the same longitude by an observer in any frame of reference.

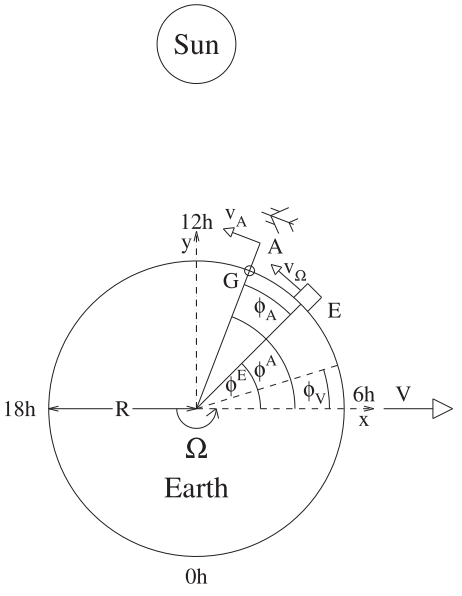

Fig. 10. Definitions of angles and velocities in the comoving frame of the centroid of the Earth (ECI frame). E: ground station, A: aircraft, G: point on the Earth's surface immediately below aircraft which executes equatorial circumnavigation in the W-E direction. The orbital velocity of the Earth around the Sun is V. The initial azimuthal angle of E, A and G is ϕ_V.

shown in Fig. 10. $\phi^{\rm E} = \phi^{\rm A} = \phi^V$, where $\phi^{\rm E}$ and $\phi^{\rm A}$ are azimuthal angles relative to the x-axis. At the end of the flight $\phi_{\rm A} = 2\pi$ where $\phi_{\rm A}$ is the angle between the radius vectors from the center of the Earth to E and A.

In calculating the time dilation effects for the clocks in E and A relative to coordinate time in the SCI frame, contributions to their motions from both the rotational and translational motion of the Earth must be taken into account. For E, since the velocity vectors due to the translational and rotational motion of the Earth are not, in general, parallel, the transformation of the time dilation factor γ between the ECI and SCI frames is given by the four-vector transformation equation

$$\gamma_{\rm E} = \gamma_V \gamma(\beta_\Omega)\big(1 - \beta_V \beta_\Omega \sin\phi^{\rm E}\big)\,, \tag{5.26}$$

where $\gamma_V \equiv 1/\sqrt{1-(V/c)^2}$. Similarly, if $\beta_{\rm A}^{\pm}$ is the scaled speed of the aircraft in the ECI frame, the time dilation factor in the SCI frame is:

$$\gamma_{\rm A}^{\pm} = \gamma_V \gamma\big(\beta_{\rm A}^{\pm}\big)\big(1 - \beta_V \beta_{\rm A}^{\pm} \sin\phi_{\pm}^{\rm A}\big)\,, \tag{5.27}$$

where the time dilation factor $\gamma(\beta_{\rm A}^{\pm})$ between the ECI frame and the comoving frame of the aircraft is given by Eq. (5.12) as

$$\gamma(\beta_{\rm A}^{\pm}) = \gamma(\beta_\Omega)\gamma\big(\beta'_{\rm A}\big)\big(1 \pm \beta_\Omega \beta'_{\rm A}\big)\,. \tag{5.28}$$

The time dilation relations in the SCI frame are

$$dt = \gamma_{\rm E}\, d\tau' = \gamma_{\rm A}^{\pm}\, d\tau''_{\pm}\,, \tag{5.29}$$

which, together with Eqs. (5.26)–(5.28) give[i]

$$d\tau''_{\pm} = \frac{\gamma_{\rm E}}{\gamma^{\pm}_{\rm A}} d\tau' = \frac{(1 - \beta_V \beta_\Omega \sin\phi^{\rm E}) d\tau'}{\gamma(\beta'_{\rm A})\left[1 \pm \beta_\Omega \beta'_{\rm A} - \beta_V(\beta_\Omega \pm \beta'_{\rm A}) \sin\phi^{\rm A}_{\pm}\right]} . \tag{5.30}$$

Developing the right side of this equation in powers of β $\left(\beta = \beta_V, \beta_\Omega, \beta'_{\rm A}\right)$ up to order β^4 gives

$$\begin{aligned} d\tau''_{\pm} = \Bigg\{ & 1 \mp \beta_\Omega \beta'_{\rm A} - \frac{(\beta'_{\rm A})^2}{2} \pm \frac{\beta_\Omega (\beta'_{\rm A})^3}{2} + \beta^2_\Omega (\beta'_{\rm A})^2 - \frac{(\beta'_{\rm A})^4}{8} \\ & + \beta_V \Bigg[(\beta_\Omega \pm \beta'_{\rm A}) \left(1 - \frac{(\beta'_{\rm A})^2}{2} \mp 2\beta_\Omega \beta'_{\rm A}\right) \sin\phi^{\rm A}_{\pm} \\ & - \beta_\Omega \left(1 - \frac{(\beta'_{\rm A})^2}{2} \mp \beta_\Omega \beta'_{\rm A}\right) \sin\phi^{\rm E} \Bigg] \\ & - \beta^2_V \beta_\Omega (\beta_\Omega \pm \beta'_{\rm A}) \sin\phi^{\rm A}_{\pm} \sin\phi^{\rm E} + \beta^2_V (\beta_\Omega \pm \beta'_{\rm A})^2 \sin^2\phi^{\rm A}_{\pm} \Bigg\} d\tau' . \end{aligned} \tag{5.31}$$

The relations obtained from the space–time geometry of Fig. 10:

$$\frac{\phi^{\rm E} - \phi_V}{\phi_{\rm A}} = \frac{\beta_\Omega t}{\beta'_{\rm A} \tau'} = \frac{\gamma_{\rm E} \beta_\Omega}{\beta'_{\rm A}} \equiv r , \quad \pm\phi_{\rm A} = \phi^{\rm A}_{\pm} - \phi^{\rm E}$$

are used to express $\phi^{\rm E}$ and $\phi^{\rm A}$ in terms of $\phi_{\rm A}$:

$$\phi^{\rm E} = r\phi_{\rm A} + \phi_V , \quad \phi^{\rm A}_{\pm} = (r \pm 1)\phi_{\rm A} + \phi_V . \tag{5.32}$$

Integrating the right side of (5.31) over the range[j] $0 < \phi_{\rm A} < 2\pi$ after the change of variable: $d\tau' = R d\phi_{\rm A}/v'_{\rm A}$ and use of Eqs. (5.32) as described in App. B, it is found that

$$\begin{aligned} \Delta T'_{\pm} \equiv & \, T''_{\pm} - T' \\ = & \frac{2\pi R}{c} \Bigg\{ (1 - \beta^2_V) \left(\frac{\beta'_{\rm A}}{2} \pm \beta_\Omega\right) + \beta'_{\rm A} \left(\beta^2_\Omega \pm \frac{\beta_\Omega \beta'_{\rm A}}{2} - \frac{(\beta'_{\rm A})^2}{8}\right) + \frac{\beta^2_V \beta^2_\Omega}{2\beta'_{\rm A}} \\ & \pm \frac{\beta_V \beta'_{\rm A}}{\pi(\beta_\Omega \pm \beta'_{\rm A})} \left[\frac{\beta^2_V}{2} - \frac{\beta^2_\Omega}{2} \mp \beta'_{\rm A} \beta_\Omega - \frac{\beta_V \beta'_{\rm A}}{\pi} F_1(r_0)\right] F_1(r_0) \\ & + \frac{\beta^2_V (\beta_\Omega \pm \beta'_{\rm A})}{4\pi} \left[\frac{\beta_\Omega}{2\beta_\Omega \pm \beta'_{\rm A}} - \frac{1}{2}\right] F_2(r_0) \Bigg\} + {\rm O}(\beta^5) , \end{aligned} \tag{5.33}$$

[i]The algebraic manipulation to obtain (5.30) is shortened by making use of the relation (algebraically equivalent to (5.28)) $\gamma(\beta^{\pm}_{\rm A})\beta^{\pm}_{\rm A} = \gamma(\beta_\Omega)\gamma(\beta'_{\rm A})(\beta_\Omega \pm \beta'_{\rm A})$. This formula is actually the Lorentz transformation, between the Earth-fixed frame in which the velocity $v'_{\rm A}$ is defined and the ECI frame, of the spatial component of the dimensionless four-vector: $(\gamma(\beta'_{\rm A}); \gamma(\beta'_{\rm A})\beta'_{\rm A}, 0, 0)$.
[j]Note that $\phi_{\rm A}$ is a positive quantity proportional to τ'.

where

$$F_1(r_0) \equiv \sin \pi r_0 \sin(\pi r_0 + \phi_V)\,, \quad F_2(r_0) \equiv \sin 2\pi r_0 \sin 2(\pi r_0 + \phi_V)\,.$$

It follows from this equation that

$$\begin{aligned}\Delta T''_{\pm} &\equiv T''_{+} - T''_{-} \\ &= \frac{2\pi R\beta_\Omega}{c}\Bigg\{-2 + (\beta'_{\rm A})^2 + 2\beta_V^2 + \frac{\beta_V \beta'_{\rm A}}{\pi\big[\beta_\Omega^2 - (\beta'_{\rm A})^2\big]} \\ &\quad \times \left[\beta_V^2 - \beta_\Omega^2 - 2\beta'_{\rm A}\left(\beta'_{\rm A} + \frac{F_1(r_0)\beta_V}{\pi}\right)\right] F_1(r_0) + \frac{\beta_V^2 \beta_\Omega \beta'_{\rm A} F_2(r_0)}{2\pi\big[4\beta_\Omega^2 - (\beta'_{\rm A})^2\big]}\Bigg\} \\ &\quad - \frac{R\beta_V^2 \beta'_{\rm A} F_2(r_0)}{c} + {\rm O}(\beta^5)\,. \end{aligned} \tag{5.34}$$

As in the case of the Sagnac effect formulas (3.23), (3.30) including translational motion with uniform velocity $\mathbf{V}$ in addition to uniform rotation gives only order β^2 corrections to the rotation-only prediction. At lowest order the same result is obtained using the ECI or the SCI (or indeed, any other inertial frame) to define coordinate time.

The "Hafele–Keating Paradox" of Nawrot[65] therefore does not exist. This author, remarking that the speed of a clock on the surface of the Earth in the SCI frame due to orbital motion: $\simeq 30$ km/s is much greater than the speed: $\simeq 300$ m/s due to the Earth's rotation, conjectured, without detailed calculation, that the time dilation effects in the HKE should be dominated by orbital motion. Since no such effects were observed in the HKE, it was concluded that[65]

> "The result of the Hafele–Keating experiment proves that the Earth does not rotate about the Sun."

However the explicit calculation above shows that the orbital motion of the Earth contributes only $(V/c)^2$ corrections to the SR contribution, and does not appear at all in the GR calculation where use of the Schwarzschild metric equation makes mandatory the choice of the ECI frame for the definition of coordinate time.

6. Alternative Derivations of the Sagnac Effect

The physical basis of the Sagnac effect is the same as that of any other "two path" quantum mechanical experiment, for example the Young double slit experiment. In a Sagnac-type experiment performed either with photons or massive particles the difference Δs between the lengths of the paths corresponding to the two interfering probability amplitudes is generated by the motion of the beam splitter/combiner in photonic optics, or by the beam combiner, in experiments using neutrons or electrons. The phase shift is $\Delta\phi = 2\pi\Delta s/\lambda$ where $\lambda = h/p$ is the de Broglie wavelength associated with the photons or "matter waves," with free-space momentum

p, employed in the experiment. In the case of photonic experiments the fundamental hypothesis used to calculate Δs is the constancy of the speed of light in the laboratory frame. For experiments performed on the surface of the Earth, where the laboratory frame is the ECI one, then, as discussed in the introduction, the (near) constancy of the speed of light is a prediction of general relativity in which the gravitational field of the Earth, described by the Schwarzschild metric, constitutes an effective "local aether" in the vicinity of the Earth.

The calculation of Δs in the laboratory frame is a simple exercise in Galilean space–time geometry taking into account the relative velocity of the photons or massive particles and the beam splitter/combiner. Since the interference effect actually occurs in the rest frame of the interferometer (which may either be in rotational or uniform translational motion) the time interval for photons $\Delta t = \Delta s/c$ must be replaced by $\Delta t' = \Delta t/\gamma$ where γ is an appropriate time dilation factor, relating laboratory time t to the time t' in the comoving frame of the interferometer. This relativistic correction can be accommodated by a suitable redefinition of the phenomenological de Broglie wavelength $\lambda = \gamma\lambda_0$ where λ_0 is the wavelength in the laboratory frame.

It is clear from the above that the lowest order (in $\beta = v/c$) Sagnac effect follows simply from Galilean space–time geometry (the concept of the relative velocity of two objects in a single frame of reference); special relativity contributes only the time dilation factor γ corresponding, at lowest order, to a β^2 correction. The calculation just sketched, due originally to Post[7] as a relativistic generalization of Langevin's[41] Galilean one, is presented in Sec. 2, leading to Eq. (2.9) for $\Delta\phi$. Sagnac's original calculation[66] is also essentially the same as that of Sec. 2 — based on Galilean space–time geometry in the laboratory frame. The same calculation may be found in the more recent literature.[67,68] In spite of this it has been erroneously claimed by some authors[12,68,70–72,75,76] that the Sagnac effect is a purely relativistic one.

In 1937, Langevin, in response to a communication by Dufour and Prunier[48] pointing out inconsistent predictions, according to special relativity, of the Sagnac effect for observers in the laboratory frame or one co-rotating with the interferometer, gave a "relativistic" derivation of the Sagnac effect[71] different to the one he gave in 1921.[41] The methodology of the analysis of Ref. 71 had been given earlier.[70] In spite of its claimed "relativistic" nature the 1937 calculation was in fact based on a purely Galilean transformation of the invariant interval relation, in cylindrical coordinates with z constant, in an inertial frame

$$(ds)^2 = c^2(dt')^2 - (dr')^2 - (r'\,d\theta')^2 \tag{6.1}$$

into a uniformly rotating one via the Galilean transformation equations:

$$r' = r\,, \quad t' = t\,, \quad \theta' = \theta + \omega t$$

to give

$$(ds)^2 = (c^2 - \omega^2 r^2)(dt)^2 - 2\omega r^2\,d\theta\,dt - (dr)^2 - (r\,d\theta)^2\,. \tag{6.2}$$

By a change of variables the nondiagonal $d\theta\, dt$ term is eliminated to write (6.2) in a "Minkowskian" manner

$$(ds)^2 = c^2(d\tau)^2 - (d\sigma)^2\,, \tag{6.3}$$

where

$$d\tau \equiv \sqrt{1-\omega^2 r^2/c^2}\left(dt - \frac{\omega r^2\, d\theta}{c^2-\omega^2 r^2}\right), \tag{6.4}$$

$$(d\sigma)^2 \equiv (dr)^2 + \frac{(r d\theta)^2}{1-\omega^2 r^2/c^2}\,. \tag{6.5}$$

To first order in $\omega r/c$ (6.4) gives

$$d\tau \simeq dt - \frac{\omega r^2 d\theta}{c^2}\,. \tag{6.6}$$

At the same order, this equation is identical to the Lorentz transformation of time between an inertial frame at rest relative to the axis of rotation of Langevin's "rotating platform" and the comoving frame of a fixed point of the platform, where τ is the time recorded by a clock at rest on the platform, t the time recorded by a clock at rest in the inertial frame, and θ the angle defined in the latter frame — not, as according to Langevin's definition, the angle in the former frame! Langevin next integrates the second term in (6.6) over the range $0 < \theta < 2\pi$ for fixed r

$$\frac{\omega r^2}{c^2}\int_0^{2\pi} d\theta = \frac{\omega 2\pi r^2}{c^2} = \frac{2\omega A}{c^2}\,, \tag{6.7}$$

where $A \equiv \pi r^2$. Integrating (6.6) and using (6.7) the following equations are written without any explanatory comment

$$\tau_1 = t_1 - \frac{2\omega A}{c^2}\,, \tag{6.8}$$

$$\tau_2 = t_2 + \frac{2\omega A}{c^2}\,, \tag{6.9}$$

where t_1 and t_2 are identified with times-of-passage of co-rotating and counter-rotating light signals in the inertial frame. Further identifying τ_1 and τ_2 with the corresponding times-of-passage in the rotating frame (called by Langevin intervals of "local" time) and assuming the constancy of the speed of light so that $\tau_1 = \tau_2$, (6.8) and (6.9) give

$$t_1 - t_2 = \frac{4\omega A}{c^2} \tag{6.10}$$

and a Sagnac phase shift in agreement with the experimentally confirmed value given by Eq. (2.9). This mathematically flawed calculation is the prototype for the widely-known treatment of the Sagnac effect in a textbook by Landau and Lifshitz,[69] to be discussed below, and many other similar "relativistic" derivations to be found in the literature. The calculation is flawed because (r, θ) are by definition *coordinates of a fixed point on the rotating platform*:[70]

> Si r et θ sont les coordonnées polaire autour de ce centre d'un pointe quelconque *lié à la plate-form* ....

The coordinates r and θ are then constant so that $dr = dr' = 0$ and $d\theta = 0$, and (6.2) is correctly written, in special relativity, where $t \neq t'$, as

$$(ds)^2 \equiv c^2(d\tau)^2 = (c^2 - \omega^2 r^2)(dt')^2 \tag{6.11}$$

so that

$$dt' = \frac{1}{\sqrt{1 - \left(\frac{\omega r}{c}\right)^2}} d\tau \,, \tag{6.12}$$

which is the correct time-dilation equation between the inertial frame and the co-moving frame of a fixed point (r, θ) on the rotating interferometer — there is no spurious "relativity of simultaneity" effect as in Eqs. (6.8) and (6.9). Although the calculation is wrong due to the erroneous nature of the primary equation (6.2) other features of it should also give a pause, such as the lack of any consideration of the space–time geometry of light signal propagation, the inconsistent treatment of order $(\omega r/c)^2$ terms (which are neglected in the transformation $t' = t$, but not in the first term on the right side of (6.2)), and finally the "parachuted," unexplained, Eqs. (6.8) and (6.9).

A similar calculation of the Sagnac effect invoking "relativity of simultaneity" is due to Trocheris.[73] Considering an experiment with the geometry of Fig. 2, the following argument is given:

> "Let us suppose that this circuit is a parallel. In the rotating system the light takes the same time to go round the circle in both directions and the two rays which left A at the same time t_0 return to A at the same time $t_1 = t_2$. However, their arrivals back at A are two distinct point events with different coordinates θ
>
> $$\text{Ray 1} \quad r_1 = R \,, \quad \theta_1 = \theta_0 + 2\pi \,, \quad t_1 = t_0 + 2\pi R/c \,,$$
>
> $$\text{Ray 2} \quad r_2 = R \,, \quad \theta_2 = \theta_0 - 2\pi \,, \quad t_2 = t_1 \,.$$
>
> They will therefore have for the fixed observer two different time coordinates t'_1, t'_2 such that
>
> $$t'_1 - t'_2 = \frac{\omega R^2}{c^2}(\theta_1 - \theta_2) = 4\pi \frac{\omega R^2}{c^2} = \frac{4\omega S}{c^2} \,,$$
>
> which is Sagnac's result."

The "relativity of simultaneity" relation employed in the last equation: $t'_1 - t'_2 = [\omega R^2/c^2](\theta_1 - \theta_2)$ relates the angles: θ_1, θ_2 in the co-rotating frame with the times t'_1, t'_2 in the laboratory (inertial) system. Since the rays are assumed to arrive simultaneously at the beam-splitter A in the co-rotating system ($t_1 = t_2$) it is clear that the angular coordinates of rays are also equal, i.e. that $\theta_1 = \theta_0 + 2\pi \Rightarrow \theta_0$, $\theta_2 = \theta_0 - 2\pi \Rightarrow \theta_0$ and so $\theta_1 - \theta_2 = \theta_0 - \theta_0 = 0$, giving $t'_1 = t'_2$. This follows

simply from spatial geometry and the definition of a plane polar angle. There are not "two distinct point events with different coordinates" at A![k] Since there is only one "effective clock" in the problem, situated at A, the time dilation requirement is that always $\Delta t' = \gamma \Delta t$, and $t_1 = t_2$ necessarily implies $t'_1 = t'_2$, and in consequence, as pointed out by Dufour and Prunier,[48] absence of the Sagnac phase difference. The logic of Trocheris' calculation follows that of Langevin in Eqs. (6.7)–(6.10), although Langevin's 1937 paper is not cited.

Another calculation of the Sagnac effect invoking the spurious "relativity of simultaneity" effect manifested in the terms $\pm 2\omega A/c^2$ in Eqs. (6.8) and (6.9) is due to Ashby.[72] Considering an arbitrary signal propagating with speed u_x in an inertial frame S between a source and an observer, separated by a distance dx, both moving parallel to the signal with speed v, the propagation time dt of the signal is

$$dt = \frac{dx}{u_x - v}\,. \tag{6.13}$$

Ashby considers only first-order terms in v/c so that $dx' = dx$ and $dt' = dt$, where x' and t' are space and time coordinates in the comoving frames S′ of the source and the observer. From the definition of velocity the signal speed in the frame S′ is:

$$u'_x \equiv \frac{dx'}{dt'} = \frac{dx}{dt} + \mathrm{O}([v/c]^2) = u_x - v + \mathrm{O}([v/c]^2)\,. \tag{6.14}$$

Ashby however assumes that u'_x is related to u_x not by (6.14) but by the relativistic velocity addition formula

$$u_x = \frac{u'_x + v}{1 + u'_x v/c^2} \tag{6.15}$$

to derive the relation

$$u_x - v = \frac{u'_x[1 - (v/c)^2]}{1 + u'_x v/c^2} = \frac{u'_x}{1 + u'_x v/c^2} + \mathrm{O}([v/c]^2)\,, \tag{6.16}$$

which combined with (6.13) gives:

$$dt = \frac{dx}{u'_x} + \frac{v dx}{c^2} + \mathrm{O}([v/c]^2)\,. \tag{6.17}$$

Ashby then arbitrarily identifies the time difference dt in the Sagnac effect, due to rotation of the interferometer with the "relativity of simultaneity" term $v dx/c^2$ in (6.17), where $v = \Omega R$, which is independent of u'_x, instead of using the correct signal velocity u'_x given by Eq. (6.14). Straightforward application of (6.15) for the case of light signals: $u_x = c$ gives $u'_x = c$ in contradiction with (6.14) and a vanishing Sagnac effect, as pointed out by Dufour and Prunier.[48] A different,

[k]This is particularly transparent on introducing equivalent Cartesian coordinates for the rays and the beam splitter: $x_\mathrm{A} = R\cos\theta_0$, $y_\mathrm{A} = R\sin\theta_0$; $x_1 = R\cos(\theta_0 + 2\pi) = R\cos\theta_0 = x_\mathrm{A}$, $y_1 = R\sin(\theta_0 + 2\pi) = R\sin\theta_0 = y_\mathrm{A}$; $x_2 = R\cos(\theta_0 - 2\pi) = R\cos\theta_0 = x_\mathrm{A} = x_1$, $y_2 = R\sin(\theta_0 - 2\pi) = R\sin\theta_0 = y_\mathrm{A} = y_1$.

correct, derivation of the Sagnac effect by Ashby, consistent with Eq. (6.14), is given below in this section.

The basic hypothesis of the calculation in Refs. 74–76 is that the particle associated with interfering amplitudes has the same speed v (not necessarily equal to c) in both paths in the co-rotating frame of a circular interferometer as shown in Fig. 2. For the case of photonic experiments on the surface of the Earth this hypothesis is both in contradiction with the prediction of general relativity and obviously predicts $\Delta s = 0$ and therefore no Sagnac effect. In any case, in Refs. 74–76 the time Lorentz transformation equation is applied to give (in the notation of this paper)

$$T_{\pm} = \gamma_{\Omega}\left(T'_{\pm} \pm \frac{\Omega R C'}{c^2}\right), \tag{6.18}$$

where C' is the circumference of the path in the co-rotating frame of the interferometer. It is further assumed that

$$T'_{+} = T'_{-} = \frac{C'}{v} = \frac{2\pi R\gamma_{\Omega}}{v}. \tag{6.19}$$

Combining (6.18) and (6.19) gives

$$\Delta T \equiv T_{+} - T_{-} = \frac{4\pi R^2 \Omega \gamma_{\Omega}^2}{c^2}. \tag{6.20}$$

The time dilation effect between the laboratory frame and the comoving frame of the interferometer is then invoked to give

$$\Delta T = \gamma_{\Omega}\Delta T' \equiv \gamma_{\Omega}(T'_{+} - T'_{-}) \tag{6.21}$$

to finally obtain

$$\Delta\phi = 2\pi\nu\Delta T' = \frac{8\pi^2 R^2 \nu \Omega \gamma_{\Omega}}{c^2}, \tag{6.22}$$

which agrees with Eq. (2.9). The authors of Refs. 74–76 correctly assume that what is relevant in the calculation of the Sagnac effect is $\Delta T'$, i.e. the difference in the times-of-passage of the signal in the two paths in the interferometer frame, but according to (6.19) used to derive (6.20) from (6.18), $\Delta T' = 0$! Then (6.21) gives $\Delta T = 0$, in contradiction with (6.20). A "length expansion" effect in the interferometer frame is assumed in the last member of (6.19). This is justified by the statement:[74]

> "It must be kept in mind that Euclidean geometry is not valid on the rotating disc, the circumference of the circle as measured by measuring rods resting on the disc is" $(2\pi R\gamma_{\Omega})$ "on account of the Lorentz contraction."

So the measuring rods are supposed to shrink, whereas elements of the disc in the same comoving frame as corresponding elements of the rod do not! In the calculation, the Sagnac effect arises entirely from the second term on the right side of Eq. (6.18), which also is the source of a spurious "relativity of simultaneity" effect. Indeed it is clear by simple inspection of (6.18) that if $\Delta T' = 0$ as assumed

in (6.19) then $\Delta T \neq 0$ as in (6.20), which is a "relativity of simultaneity" effect, whereas the (physically correct) time dilation relation (6.21) gives $\Delta T = 0$ when $\Delta T' = 0$ — no "relativity of simultaneity." The erroneous conflation of the Sagnac effect with "relativity of simultaneity" is common in the literature.[14,29] Another feature of the calculation of Refs. 74–76 is that the signal speed v does not appear in the final result (6.22), the "c^2" in the denominator of the right side originating from the "relativity of simultaneity" terms just discussed in (6.18). In contrast, the "c" in the denominator of the correctly derived formula (2.9) is the signal speed in the laboratory frame and would be replaced by v if this were the signal speed.

In fact the application of the time interval Lorentz transformation between the laboratory frame and the co-rotating frame of the interferometer to give Eq. (6.18) is erroneous. If t' is the time recorded by a clock at a fixed position in the interferometer, say at the position of the beam splitter, the correct transformation is: $\Delta t = \gamma_\Omega(\Delta t' \pm \Omega R \Delta x'/c^2)$. Since the clock is at a fixed position in the co-rotating frame, $\Delta x' = 0$, which gives the correct time dilation relation $\Delta t = \gamma_\Omega \Delta t'$ used to obtain Eq. (6.21).

In summary the "relativistic" derivation of (6.22) in Refs. 74–76 is based on an incorrect postulate concerning the speed of signals in the interferometer frame, an incorrect application of the temporal Lorentz transformation and contains logically incompatible (self-contradictory) statements in Eqs. (6.19)–(6.21).

Malykin[12] assumes also a constant signal speed, v, in the co-rotating frame of a circular interferometer which is identified as a "phase velocity" of the associated "waves." Again retaining the notation of this paper, Malykin notes the following signal path lengths $s_\pm$ in the laboratory frame, following from the geometry of Fig. 2:

$$s_\pm = 2\pi R \pm \Omega R T_\pm\,, \quad T_\pm = \frac{s_\pm}{v_\pm}\,, \tag{6.23}$$

where $v_\pm$ are the laboratory frame signal velocities assumed to be given by the RPVAR as

$$v_\pm = \frac{v \pm \Omega R}{1 \pm v\Omega R/c^2}\,. \tag{6.24}$$

Combining (6.23) and (6.24) gives

$$T_\pm = \frac{2\pi R[1 \pm (v\Omega R/c^2)]}{v[1 - (\Omega R/c)^2]} \tag{6.25}$$

from which follows

$$\Delta T = T_+ - T_- = \frac{4\pi R^2 \Omega}{c^2[1 - (\Omega R/c)^2]}\,, \tag{6.26}$$

which is the same as Eq. (6.20). Again the signal velocity v cancels from the result. In this case the factor "c^2" in the denominator on the right side of (6.26) originates in the relativistic term in the denominator of the right side of the RPVAR (6.24). Malykin then assumes the time dilation relation (6.21) in order to recover from (6.26) the correct result (6.22). Since the counter-rotating signals have equal

speeds in the co-rotating frame of the interferometer, then, as in (6.19), $T'_+ = T'_-$ so that $\Delta T' = 0$ and from the time dilation relation, also assumed to hold by Malykin, $\Delta T = 0$ in contradiction with (6.26). This calculation of Malykin[12] therefore contains the same internal contradictions as that of Refs. 74–76, and, like them, by a fortuitous cancellation of errors, recovers the formula (2.9).

Reference 12 also contains two calculations of the Sagnac time difference in a circular interferometer in the case that it is filled with a transparent medium of refractive index n. The first calculation in Subsec. 5.1 of Ref. 12 is the same as the above derivation of (2.12) except that the time dilation relation is neglected on transforming into the co-rotating frame. The second calculation in Subsec. 5.2 of Ref. 12 finds for the optical paths $\ell^{\pm}$ in the laboratory system, in the geometry of Fig. 2, the relation

$$\ell^{\pm} = 2\pi R \pm \frac{2\pi R^2 \Omega n}{c}$$

to be compared with the corresponding result that would be found in the calculation of Sec. 2

$$\ell^{\pm} = 2\pi R \pm \frac{2\pi R^2 \Omega}{c/n \mp \Omega R/n^2}\,.$$

Both formulas give a Sagnac time difference, at the lowest order in $\Omega R/c$, that is independent of n. The mistake in the derivation of Ref. 12 is to neglect the effect of the motion of the interferometer in the calculation of the optical path lengths.

The paper of Logunov and Chugreev,[68] although demonstrating the contrary by direct calculation, also claims a purely special relativistic nature for the Sagnac effect:

> "We therefore think that it is pertinent at this point *on the basis of methodological considerations and also to avoid any possible misconception, to emphasize one more time that the Sagnac effect is of a purely special relativistic nature.*" (Italics in the orignal)
>
> "In the present paper we will show that an explanation of the Sagnac effect is completely within the capability of the special theory of relativity and that none of the following need to be invoked: the general theory of relativity, velocities higher than the speed of light, or any other postulates."

After a quotation from Sommerfeld[77] that asserts that the Sagnac effect is of order v/c and classically calculable, and showing explicitly by calculation that this is indeed the case, the authors of Ref. 68 reproduce the laboratory frame calculation of Sec. 2[l] to obtain Eq. (2.9) for the Sagnac phase difference, stating correctly, that in this case it was not necessary to consider any light signals with velocity greater than c.

[l]i.e. one in which the time dilation effect, leading to $\gamma_\Omega \neq 1$ in Eq. (2.9), is neglected.

There follows an abstract mathematical discussion of the relation between a pseudo-Euclidean Minkowski space with a nondiagonal metric and a conventional diagonal-metric Minkowski space. It is asserted that the metric of the latter space, which is related to the former by transformation formulas that are given, is specified by a single parameter "c" with the dimensions of velocity that is a universal physical constant. The connection of this mathematical exercise, to the Sagnac effect, in the context of the other arguments given, is not clear to the present author. Then, there is a discussion of transformation formulas between an inertial and a uniformly rotating frame similar to that to be found in a textbook by Landau and Lifshitz (see Ref. 69, Chap. 10, Sec. 82, p. 227). The flaws in this treatment of the metric of a rotating frame are discussed below. Finally, the calculation in the laboratory frame in Eqs. (4)–(8) of Ref. 68 is repeated, verbatim, from Eq. (14) to the end of the paper, but it is claimed that the calculation is now being performed in the rotating frame! It is clear that when the calculation is actually performed in the rotating frame, i.e. in terms of the proper time recorded by a clock comoving with the beam splitter/combiner, as in Sec. 2 or in Eqs. (4)–(12) of Post's review article,[7] that light signal relative velocities both greater than and lesser than c must be taken into account, and that use of the RPVAR to transform velocities between the laboratory and interferometer frames leads to the prediction of a vanishing Sagnac effect, refuting the claim of Ref. 68 that the existence of the Sagnac effect is completely consistent with conventional special relativity and that no light velocities greater than c need to be considered.

Reference 68 contains the statement, after the second calculation of the Sagnac effect mentioned above:

> "We also note that in the rotating frame of reference the coordinate velocity of light is anisotropic $d\phi/dt = -\omega \pm c/R$."

Since time dilation gives $t = \gamma t'$ where t' is the proper time of a clock at rest in the rotating frame, the equation just mentioned gives

$$\frac{d\phi}{dt'} \equiv \omega' = \gamma(-\omega \pm c/R)\,, \tag{6.27}$$

which is equivalent to the relation (2.7) above as derived by Post.[7] In conclusion, the results of two correct calculations to be found in Ref. 68, the first Galilean, the second equivalent to (6.27), are in direct contradiction with the written conclusions of the paper, as summarized in the above quotations. In fact the Sagnac effect is classical (Galilean) at lowest order, and does imply the existence of signal velocities greater or less than c in the rotating frame.

A number of authors[78–80] following the treatment in "The Classical Theory of Fields" by Landau and Lifshitz (see Ref. 69, Chap. 10, Sec. 82, p. 227), which is similar to Langevin's work of 1937, discussed above, have given a general-relativistic interpretation of the Sagnac effect. This approach assumes that the speed of light is equal to c in both the laboratory and rotating frames (i.e. validity of the RPVAR)

and claims that the spatial geometry in the rotating frame is non-Euclidean and that no spatially-separated clocks in the rotating frame can be synchronized. The following statement concerning the space–time geometry of rotating frames can be found:[69]

> "In an inertial reference system, in Cartesian coordinates, the interval ds is given by the relation:
>
> $$ds^2 = c^2\,dt^2 - dx^2 - dy^2 - dz^2\,.$$
>
> Upon transforming to any other inertial reference system (i.e. under Lorentz transformation) the interval, as we know, retains the same form. However, if we transform to a noninertial system of reference, ds^2 will no longer be a sum of squares of the four coordinate differentials.
>
> So, for example, when we transform to a uniformly rotating system of coordinates,
>
> $$x = x'\cos\Omega t - y'\sin\Omega t\,, \quad y = x'\sin\Omega t + y'\cos\Omega t\,, \quad z = z'$$
>
> (Ω is the angular velocity of rotation, directed along the z-axis), the interval takes on the form
>
> $$ds^2 = \big[c^2 - \Omega^2\big((x')^2 + (y')^2\big)\big]\,dt^2 - (dx')^2 - (dy')^2 - (dz')^2 + 2\Omega y'\,dx'\,dt - 2\Omega x'\,dy'\,dt\,.$$
>
> No matter what the law of transformation of time coordinates, this expression cannot be represented as a sum of squares of the coordinate differentials."

The contrary of the last assertion will now be demonstrated by applying the temporal Lorentz transformation. Since this transformation depends only on the instantaneous magnitude of the velocity, and not on the acceleration, it applies equally to transformations between inertial frames or, as in the present case between an inertial and an accelerated frame. It is convenient to use polar coordinates in both the inertial frame: (r, ϕ) and in the rotating frame: (r', ϕ') and to set $z = z' = 0$. The interval equation in the inertial frame is then

$$ds^2 = c^2\,dt^2 - r^2\,d\phi^2\,. \tag{6.28}$$

Consider a clock at the fixed position (R, ϕ'_0) in the rotating frame. Introduce local Cartesian coordinate systems with origin at the clock, and x, x' axes in the azimuthal direction. Infinitesimal intervals dx, dt on the worldline of the clock then transforms into the rotating frame as

$$dx' = R\,d\phi' = 0 = \gamma_\Omega(dx - \Omega R\,dt) = \gamma_\Omega(R\,d\phi - \Omega R\,dt)\,, \tag{6.29}$$

$$dt' = \gamma_\Omega\big(dt - \Omega R\,dx/c^2\big) = \gamma_\Omega\big(dt - \Omega R^2\,d\phi/c^2\big)\,. \tag{6.30}$$

Using the equation of motion of the clock in the inertial frame $d\phi = \Omega\, dt$ to eliminate $d\phi$ from (6.30) gives

$$dt = \gamma_\Omega\, dt' \,. \tag{6.31}$$

Substituting $dt = \gamma_\Omega\, dt'$, $d\phi = \Omega\gamma_\Omega\, dt'$ in (6.28) gives

$$ds^2 = c^2\gamma_\Omega^2\left[1 - \left(\frac{\Omega R}{c}\right)^2\right](dt')^2 = c^2(dt')^2 \,. \tag{6.32}$$

The same result is obtained by substituting $dx' = dy' = dz' = 0$, $(x')^2 + (y')^2 = R^2$ and $dt = \gamma_\Omega\, dt'$ in the formula for ds^2 in the text from Ref. 69 quoted above. Contrary to the above statement, ds^2, evaluated in the rotating frame, is expressed as a sum (with only one term) of "squares of the coordinate differentials." Also, since no spatial coordinate appears in the time dilation relation (6.31), there is no difficulty to synchronize clocks at different positions in the rotating frame, provided they all have the same value of r', a condition that is evidently satisfied for a Sagnac experiment with circular geometry. However it is not possible to synchronize, at more than one instant, clocks at different r' values, due to the dependence of γ_Ω on this quantity.

The main flaw in the discussion of rotating frames (see Ref. 69, Chap. 10, Sec. 82, p. 227) is the inconsistent use of the Galilean transformation $t' = t$. On application of the Lorentz transformations the "β^2" term $-\Omega^2R^2$ in g_{00} is exactly canceled by a similar term arising from the time transformation. The "non-Euclidean metric" with g_{00} different from c^2 is a consequence of an inconsistent approximation where some $(v/c)^2$ terms are neglected and others are retained. Another similar example occurs in "nonrelativistic," or "Galilean," treatments of quantum-mechanical phases which appear to be frame dependent.[74–76,81–83] Again $(v/c)^2$ terms originating in the Lorentz transformation of time are neglected. Also, when the transformation equations concern events at a fixed position in the rotating frame, as is the case when questions of clock synchronization are considered, the intervals dx', dy' vanish so that there are no off-diagonal terms in the metric of the rotating frame.

In the subsequent calculation of the Sagnac effect in Ref. 69, time differences for light signals, based on the non-Euclidean metric in the rotating frame, originate in similar spurious "relativity of simultaneity" terms as in the calculation of Malykin discussed above. In spite of this it is finally correctly stated that, at lowest order in v/c the speed of the light signals in the rotating frame are $c \pm \Omega R$,[m] in agreement with Eq. (2.6), and that this also follows from an alternative classical (i.e. nonrelativistic) calculation. For further discussion of the treatment of the Sagnac effect by Ref. 69, see also Ref. 6.

Malykin has also appealed to general relativity in an attempt to resolve the incompatibility of the existence of the Sagnac phase difference with the velocity

[m]The formula is (89.4) of Ref. 69, Chap. 10, Sec. 82, p. 227: $c' = c \pm 2\Omega S/L$, where $S = \pi R^2$ and $L = 2\pi R$.

transformation formula of SR, by invoking a "Relativistic Zeno Paradox."[84] This involves conjecturing a fundamental difference in the space–time geometry between the accelerated reference system $K'_{\rm nonin}$ of the beam splitter in a rotating Sagnac interferometer, and the corresponding comoving inertial frame: $K'_{\rm in}$. It is supposed that the speed of light is different in these two frames in such a way so as to generate a nonvanishing time difference in $K'_{\rm nonin}$. Thus, it makes the existence of acceleration essential in the explanation of the Sagnac effect, whereas it is known experimentally[26,27] that it occurs also for uniform translational motion. Also precise measurement of time dilation in the decay of muons trapped in a circular storage ring has shown[85] that no observed difference between $K'_{\rm nonin}$ and $K'_{\rm in}$ is detected in the presence of a transverse acceleration of 10^{19} m/s^2.

The transformation between an inertial frame and a rotating ring can be considered to be a series of instantaneous Lorentz transformations with the same velocity parameters but in different directions; there is no need to invoke non-Euclidean geometry. This has previously been pointed out in the literature by Anandan:[67]

> "Many authors have concluded ... that (measuring rods) determine a non-Euclidean geometry with respect to the disc. However the "circumference" measured by these rods is really the length of the helical curve in space–time consisting of events which are locally simultaneous with respect to the instantaneous inertial frames attached to the periphery of the disc .... Thus there is no violation of Euclidean geometry as a result of the rotation if the gravitational field due to the disc is neglected."

This conclusion is consistent with the resolution of the "Ehrenfest paradox" presented in Sec. 5 and in Ref. 22.

Including the time dilation relation (6.31) the invariant interval equation for events on a circle of fixed radius R in a rotating frame is

$$ds^2 = c^2(dt')^2 - 2\Omega R^2\gamma_\Omega\, dt'\, d\phi' - R^2(d\phi')^2\,. \tag{6.33}$$

As shown by Klauber[8] this relation provides an elegant way to derive the prediction for the Sagnac phase shift and the related kinematical formulas obtained in Sec. 2. Making the hypothesis that a light signal following the circular path has speed c in the laboratory frame gives the equation of motion $R\,d\phi = c\,dt$ in this frame so that the invariant interval between neighboring events on the worldline of the light signal is

$$ds^2 = c^2\,dt^2 - R^2\,d\phi^2 = 0\,. \tag{6.34}$$

Setting $ds^2 = 0$ in (6.33) and solving the resulting quadratic equation for $c\,dt'$ gives

$$c\,dt' = \gamma_\Omega(1+\beta_\Omega)R\,d\phi'\,. \tag{6.35}$$

So that

$$R\frac{d\phi'}{dt'} \equiv c'_+ = \frac{c}{\gamma_\Omega(1+\beta_\Omega)} = c\sqrt{\frac{1-\beta_\Omega}{1+\beta_\Omega}} = c\gamma_\Omega(1-\beta_\Omega)\,. \tag{6.36}$$

In this way the RRVTR (2.6) and the prediction (2.9) for the Sagnac phase shift are recovered. Setting $\gamma_\Omega = 1$ in (6.31) and so retaining only order β_Ω terms the above calculation simplifies to that of Langevin in 1921.[41]

Ashby,[80] also following Langevin[41] used this method to obtain the Sagnac effect time difference in a single path due to rotation, by neglecting time dilation: $t' = t$ — equivalent to setting $\gamma_\Omega = 1$ in (6.31) — to obtain, instead of Eq. (6.35)

$$c\,dt' = R\,d\phi' + \frac{\Omega R^2\,d\phi'}{c} + \mathrm{O}\big(\beta_\Omega^2\big)\,, \tag{6.37}$$

which gives

$$R\frac{d\phi'}{dt'} \equiv c'_+ = \frac{c}{1+\beta_\Omega} = c(1-\beta_\Omega) + \mathrm{O}\big(\beta_\Omega^2\big)\,. \tag{6.38}$$

The above calculation in the rotating frame also demonstrates the Euclidean spatial geometry of this frame and the absence of any "length contraction" effect or "Ehrenfest paradox" related to a putative non-Euclidean spatial geometry. Denoting by C (C') the circumference of the light path in the laboratory (rotating) frame, the space–time geometry in the laboratory frame gives for the path length

$$s_+ = C + \Omega R T_+\,, \quad T_+ = \frac{s_+}{c} \tag{6.39}$$

so that

$$T_+ = \frac{C}{c(1-\beta_\Omega)}\,. \tag{6.40}$$

Using (6.36), (6.39), (6.40) and the time dilation relation $T_+ = \gamma_\Omega T'_+$ gives

$$T'_+ = \frac{C'}{c'_+} = \frac{C'}{c\gamma_\Omega(1-\beta_\Omega)} = \frac{T_+}{\gamma_\Omega} = \frac{C}{c\gamma_\Omega(1-\beta_\Omega)} \tag{6.41}$$

from which follows $C' = C$ — there is no "length contraction" non-Euclidean spatial geometry or "Ehrenfest paradox."

7. Comparison of the "Sagnac Effect," Sagnac Interferometers and the Hafele–Keating Experiment

This concluding section considers the fundamental physics underlying (i) the "Sagnac effect," (ii) the *modus operandi* of Sagnac interferometers, and (iii) the Hafele–Keating experiment, which have sometimes been erroneously conflated in the literature.[14,29,80,91] The first important distinction to be made is that between the "Sagnac effect" (i) relating to signal propagation in the vicinity of the Earth, which is a space–time geometric effect described by the RRVTR (2.7), and the quantum mechanical phenomenon, (ii) occurring in interferometers with counter-rotating

beams of photons or massive particles when they are in rotational or translational motion. The geometrical Sagnac effect for microwave signals was discovered[28] while using a geostationary satellite for distant clock synchronization, and constitutes an important correction that must be taken into account in the operation of the GPS.[14,29,30,80] In this latter application, only the Galilean limit of the RRVTR (2.7) (given by setting $\gamma_\Omega = 1$ in this equation) is required by the accuracy of the GPS, so despite statements to the contrary[12,68,74] neither special nor general relativity theory is needed to calculate the Sagnac effect correction for the GPS.

At the lowest nontrivial order in v/c, both photonic and massive-particle Sagnac interferometers (ii) are most economically described by purely spatial "classical" wave theories with appropriate phenomenological de Broglie wavelengths. In the language of Feynman's space–time formulation of quantum mechanics[86–89] all Sagnac interferometers are two path experiments like a Young two-slit experiment, a Michelson interferometer or a Mach–Zehnder interferometer. The lowest order Sagnac phase shift is, in all cases, given by the difference in length of the spatial paths, generated by rotation or translational motion, divided by the de Broglie wavelength and multiplied by 2π. For this calculation, no consideration of time differences or any other temporal effect is required. However, as discussed in detail in Refs. 88 and 89, at the fundamental quantum-mechanical level, according to Feynman's formulation, the space–time structure of the probability amplitudes that are in one-to-one correspondence with the space–time paths are completely different for photons and massive particles, in spite of the fact that the theory does predict the existence of identical effective, purely spatial, "classical" wave theories.

Since the invariant, free-space, propagator of a particle of mass m has the phase $\exp[-imc^2\Delta\tau/\hbar]$ where τ is the proper time on the worldline of the particle[88,90] its contribution to the phase of the probability amplitude vanishes for a photon. Then the phase of the probability amplitude resides entirely in the decay amplitude of the photon source,[88] being proportional to the difference of production times of the photon in the two paths and to the energy of the photon. The difference of production times is equal to the difference of flight times of a photon in the two paths since the time of the detection event must be the same in both paths if interference of the probability amplitudes is to occur. The time difference can either be calculated in the co-rotating or, more generally, comoving, frame of the interferometer, using the RRVTR (2.7), or alternatively, in the laboratory frame, using Galilean kinematics, subsequently transforming the time intervals found in this case into the comoving frame of the interferometer by use of an appropriate time dilation relation.

In contrast, for the case of massive particles (typically neutrons or electrons) the phase of the probability amplitude is given entirely by the space–time propagator of the particle, and the size of the observed interference effect requires that the particle has a (slightly) different velocity in the two paths but that it is produced at the same time in both paths. In this case there is no time difference and therefore no "Sagnac effect" (i). The rationale for this conclusion is explained in detail in Refs. 88 and 89, but will be briefly illustrated here by analyzing, in the notation of

this paper, a simplified version of the electron Sagnac interferometer experiment of Hasselbach and Nicklaus.[91]

A circular interferometer as shown in Fig. 1 is considered but with a source of electrons and an electron detector at the extremities of a diameter so that when the interferometer is at rest there are equal path lengths $s_\pm = \pi R$. Under clockwise-rotation of the interferometer

$$s_+ = \pi R + \Phi R\,, \quad s_- = \pi R - \Phi R\,. \tag{7.1}$$

It is now assumed that the electron has the same production time in each path but a different velocity:

$$s_+ = v_+ t\,, \quad s_- = v_- t\,, \quad \Phi = \Omega t\,. \tag{7.2}$$

It follows from (7.1) and (7.2) that

$$s_+ - s_- = 2\Phi R = 2\Omega t R \tag{7.3}$$

and

$$t = \frac{2\pi R}{v_+ + v_-} \equiv \frac{\pi R}{\bar{v}}\,, \quad v_+ - v_- = 2\Omega R \equiv 2v_\Omega\,. \tag{7.4}$$

The lowest order Sagnac phase shift is then given by (7.3) and (7.4) as

$$\Delta\phi_{\rm e} = 2\pi\frac{(s_+ - s_-)}{\bar{\lambda}} = 4\pi\frac{\Omega(\pi R^2)\bar{p}}{h\bar{v}} = \frac{2\Omega A\bar{E}}{\hbar c^2}\,, \tag{7.5}$$

where $\bar{E}$ is the mean total energy of the electrons, the de Broglie relation $\bar{\lambda} = h/\bar{p}$ and the relativistic kinematical relation $\bar{v} = \bar{p}c^2/\bar{E}$ have been used. This prediction is the same as the formula derived in Ref. 91 by use of the WKB approximation.

If it is instead assumed that the electron has the same velocity in the laboratory system for each path (as must be the case for a photon) a different effective de Broglie wavelength is obtained. Denoting equal production time paths by ET and equal velocities by EV it is found that[88,89]

$$\bar{\lambda}_{\rm ET} = \frac{h}{\bar{p}}\,, \quad \bar{\lambda}_{\rm EV} = \frac{h\bar{p}}{m^2c^2} \tag{7.6}$$

then

$$\frac{\bar{\lambda}_{\rm EV}}{\bar{\lambda}_{\rm ET}} = \frac{\bar{p}^2}{m^2c^2} = \frac{\bar{v}^2}{c^2} = \frac{2\bar{T}}{mc^2}\,, \tag{7.7}$$

where $\bar{T}$ is the mean kinetic energy of the electron. With $\bar{\lambda}_{\rm ET} = 0.3$ Å found to be in good agreement with the phase shifts measured in the experiment of Ref. 91 and a typical value of $\bar{T}$ of 1000 eV in the same experiment then (7.7) gives $\bar{\lambda}_{\rm EV} = 5.8 \times 10^{-4}$ Å. Evidently the prediction of the equal velocity hypothesis is incompatible with the results of the experiment.

In the experiment of Ref. 91 the maximum separation, $2d$ of the electron beams was of order 40 μm and the angular velocity $\Omega = \pi$ rad s^{-1} so that $v_\Omega \simeq \Omega d = 6.3 \times 10^{-5}$ m s^{-1} so that

$$\Delta v = v_+ - v_- = 2v_\Omega = 1.26 \times 10^{-4} \text{ m s}^{-1} .$$

From the last member of (7.7) the typical kinetic energy of 1000 eV corresponds to a velocity of $\bar{v} = 1.88 \times 10^7$ m s^{-1} (0.063 c). Then,

$$\frac{\Delta v}{\bar{v}} = 6.7 \times 10^{-12}$$

to be compared with a typical spread of electron velocities:

$$\frac{\sigma_v}{\bar{v}} = \frac{1}{2}\frac{\sigma_T}{\bar{T}} = \frac{1}{2}\frac{0.35 \text{ eV}}{1000 \text{ eV}} = 1.75 \times 10^{-4} .$$

Thus, the velocity spread in the beams are some seven orders of magnitude larger than the velocity difference needed to satisfy the "equal time" condition of Eq. (7.2).

For comparison the lowest order result for the circular photon interferometer in Fig. 2 may be written as

$$\Delta\phi_\gamma = \frac{4\Omega A E_\gamma}{\hbar c^2} . \tag{7.8}$$

The factor two difference on the right sides of (7.5) and (7.8) results from the two times longer path lengths in the photon experiment. In spite of an entirely different underlying microphysics the two formulas are the same.

Since $p/\hbar = 2\pi/\lambda \equiv k$, where k is the wave number, Eq. (7.5) may also be written, for an arbitrary particle, in a Sagnac interferometer of arbitrary shape, (see Sec. 2):

$$\Delta\phi = \frac{2k}{\bar{v}} \boldsymbol{\Omega} \cdot \mathbf{A} . \tag{7.9}$$

An alternative derivation of this formula was proposed in Ref. 92. For the case of semi-circular paths considered above, a Doppler effect due to the motion of the source in the laboratory system was used to calculate modified de Broglie wavelengths for clockwise (+) or counterclockwise (−) propagation

$$\lambda_\pm = \frac{v\lambda}{v \pm R\Omega} . \tag{7.10}$$

The Sagnac phase difference was then calculated as

$$\Delta\phi = 2\pi\left[\pi R\left(\frac{1}{\lambda_+} - \frac{1}{\lambda_-}\right)\right] = \frac{2}{v}\left(\frac{2\pi}{\lambda}\right)\pi R^2\Omega = \frac{2k}{v}A\Omega \tag{7.11}$$

in agreement with Eq. (7.9). The flaws in this derivation are as follows:

(i) The Doppler-modified wavelength of Eq. (7.10) assumes constant velocity of the associated "matter wave" in the laboratory frame. Since, however the de Broglie wavelength is given by $\lambda = h/p = h/(\gamma m v)$ for a particle of mass m (specifically, neutrons were considered in Ref. 92), it is impossible for λ to change if v is constant.

(ii) In Eq. (7.11), equal path lengths πR were assumed, thus neglecting the motion of the particle detector, which necessarily results in different path lengths for different propagation directions. Thus, the path-length difference which is the fundamental physical characteristic of any Sagnac interferometer is not taken into account in the calculation of Ref. 92.

In summary, the calculation of Ref. 92 is a physically nonsensical one which, fortuitously, gives the correct result.

Another "derivation" of Eq. (7.5) may be found in Ref. 93. In this case, the nonrelativistic limit $\bar{E} \to mc^2$ of (7.5) was considered

$$\Delta\phi_{\mathrm{S}} = \frac{2m}{\hbar} \int \boldsymbol{\Omega} \cdot d\mathbf{A} \,. \tag{7.12}$$

The similarity between the Sagnac phase difference in Eq. (7.12) and the Aharonov–Bohm (AB) phase shift[94,95] produced by an enclosed flux of magnetic field between two alternative paths for the passage of a particle of charge e

$$\Delta\phi_{\mathrm{AB}} = \frac{e}{\hbar c} \int \mathbf{B} \cdot d\mathbf{A} \tag{7.13}$$

was noted, as well as that, via the substitution $(e/c)\mathbf{B} \to 2m\boldsymbol{\Omega}$ (7.12) is obtained from (7.13). This is a (perhaps interesting) remark, but certainly not (as claimed in Ref. 93) a *derivation* of $\Delta\phi_{\mathrm{S}}$. In fact the microphysical physical bases of the Sagnac and AB effects are quite different. In the Sagnac effect, the paths in the laboratory frame corresponding to the interfering probability amplitudes have a different length. In the AB effect, the paths may be of equal length or different lengths, with or without, the presence of the magnetic field and the probability amplitudes are modified by the dynamical effect of the magnetic vector potential, which occurs in the Lagrangian, L that specifies the phase of the probability amplitude:[86,96]

$$\phi = \frac{iS}{\hbar} = i \int \frac{L dt}{\hbar} \,. \tag{7.14}$$

Since the magnetic field is given by spatial derivatives of the magnetic vector potential it may well vanish along the paths of the interferometer. The dynamical effects responsible for the interference phase are due only to the magnetic vector potential itself, which does not vanish in the region of the paths. In contrast in the Sagnac effect the probability amplitudes correspond to free-space particle propagation and the changes in the interference phase result from path length differences that are proportional to the angular velocity of the interferometer. The Sagnac and AB experiments are both "two-path" experiments where single particles "interfere with themselves" but, in view of the very different underlying microphysics of the two types of experiments, there is no deeper analogy as claimed in Ref. 93.

In spite of the fact that the lowest order (in v_Ω/c) Sagnac effect is a simple consequence of Galilean space–time geometry and that the physical bases of the HKE are purely relativistic: general relativistic gravitational blue-shift and special-relativistic time-dilation, the Sagnac effect and the HKE are often conflated in the

literature. This is particularly the case for the difference of the times $(T''_{\pm})_{\rm SR}$ as given in Eq. (5.14):

$$\Delta T_{\rm HK} \equiv (T''_{+})_{\rm SR} - (T''_{-})_{\rm SR} = -\frac{4\pi R v_{\rm E}}{c^2}$$

$$= -\frac{4\pi R^2 \Omega}{c^2} = -\frac{4A\Omega}{c^2} \quad \text{(HK Expt)} \tag{7.15}$$

and the time difference between counter-rotating light signals in a circular Sagnac interferometer (cf. Eq. (2.9):

$$\Delta T_{\rm S} \equiv T_{+} - T_{-} = \frac{4A\Omega}{c^2} + {\rm O}\big(\beta_{\Omega}^2\big) \quad \text{(Sagnac Expt)}\,. \tag{7.16}$$

The fortuitous equality $\Delta T_{\rm HK} = -\Delta T_{\rm S}$ has lead many authors to conflate the two experiments and in particular to claim that $\Delta T_{\rm HK}$ is a "Sagnac effect." The most extreme example of this, to be considered now, is to be found in the work reported in Ref. 80 where an equation equivalent to (7.15) for the HKE is obtained by a purely classical derivation without any consideration of relativistic time dilation!

Considering a uniformly rotating frame, but neglecting time dilation, the relation (6.37) obtained in Ref. 80 may be integrated to obtain the time for a light signal to follow a circular path in the rotating frame

$$T'_{\rm S} = R\int_{\rm path} \frac{d\phi'}{c} + \frac{2\Omega}{c^2}\int_{\rm path} dA \quad \text{(light signal)}\,, \tag{7.17}$$

where $dA = R^2\, d\phi'/2$ is the area swept out by the radius vector of the light signal when the azimuthal angle changes by $d\phi'$. Making use of Eq. (5.9) a relation similar to (7.17) may be derived by replacing the light signal by the airborne clock of the HKE, Considering, as in Eq. (7.17), motion of the clock in the same direction as the rotational motion of the Earth it is found that

$$T'_{\rm HK} = \int_{\rm path} d\tau + \left[\frac{\beta'_{\rm A}}{cR} + \frac{2\Omega}{c^2}\right]\int_{\rm path} dA \quad \text{(clock)}\,, \tag{7.18}$$

where $d\tau = d\tau''_{+}$, a proper time interval of the airborne clock, and the notation of Sec. 5 has been used. In Ref. 80 a relation similar to (7.18) was obtained (but without the $\beta'_{\rm A}/(cR)$ term), which was claimed by the author to show the exact correspondence of the proper time interval $\int d\tau$ and the time of passage (at speed c in the rotating frame) $R\int d\phi'/c$ of a light signal. In order to derive this equation the Galilean version ($t = t'$, $\gamma_{\Omega} = 1$) of Eq. (6.16), as given in the quotation (see Ref. 69, Chap. 10, Sec. 82, p. 227) of the Minkowski invariant interval relation in a rotating frame was invoked

$$ds^2 = \left(1 - \frac{\Omega^2 R^2}{c^2}\right)c^2(dt')^2 - 2\Omega R^2\, d\phi'\, dt' - R^2(d\phi')^2\,. \tag{7.19}$$

In the notation of Sec. 5, $\Omega R/c = \beta_{\rm E}$, $R\, d\phi'/dt' = \beta'_{\rm A}$, (7.19) gives

$$\frac{ds}{c} = dt'\left[1 - \frac{\beta_{\rm E}^2}{2} - \frac{\big(\beta'_{\rm A}\big)^2}{2} - \beta_{\rm E}\beta'_{\rm A}\right] + {\rm O}(\beta^4)\,. \tag{7.20}$$

In the HKE $\beta_{\rm E} \simeq 1.6 \times 10^{-6}$, $\beta'_{\rm A} \simeq 1.0 \times 10^{-6}$. The velocity-dependent terms in the square brackets of (7.20) are therefore of comparable magnitude. In Ref. 80, however, it was assumed that: $\beta_{\rm E}^2$, $\left(\beta'_{\rm A}\right)^2 \ll \beta_{\rm E}\beta'_{\rm A}$ so as to neglect the terms $\beta_{\rm E}^2/2$ and $\left(\beta'_{\rm A}\right)^2/2$ in (7.20), as well as that $ds/c = d\tau''_+ = d\tau$ so as to obtain from Eq. (7.20)

$$T'_{\rm HK} = \int_{\rm path} d\tau + \frac{2\Omega}{c^2} \int_{\rm path} dA \quad \text{(clock Ref. 80)}\,, \tag{7.21}$$

which has exactly the same form as (7.17). The identification of ds/c with $d\tau''_+$ is erroneous. From the definition of ds^2 in terms of temporal and spatial intervals, it can only be identified with a proper time interval in a frame in which all spatial intervals vanish. This occurs for a clock at rest in the nonrotating inertial frame — the ECI frame in the HKE — corresponding to an interval dt of coordinate time not the proper time interval $d\tau''_+$ of the airborne clock. These two time intervals are related by the time dilation relation (5.6). In summary, Eq. (7.21), which is claimed to demonstrate the equivalence of the HKE with the Sagnac effect is flawed by an erroneous assignment of proper time intervals and illegitimate approximations. In it a formula for $T'_{\rm HK}$ in which the term $\beta_{\rm E}\beta'_{\rm A}$, which originates from relativistic time dilation is claimed to be derived on the assumption of the Galilean relation $t' = t$ — a logical impossibility.

In conclusion, in order to understand better the erroneous conflation, on the basis of Eqs. (7.16) and (7.15) of the Sagnac effect (light signals) and the HKE (moving clocks), respectively. It is instructive to consider in some detail their space–time-geometrical aspects, so as to better appreciate their similarities and differences.

In both experiments the ECI frame is a preferred one. In the HKE the time dilation effects of the Earth-bound and airborne clocks are calculated relative to coordinate time as registered by a hypothetical clock at rest in this frame. In the Sagnac effect, in accordance with general relativity, light propagation is almost isotropic with a speed less than, but very close to, c in this frame. In both experiments the observed "effects" are due to the rotation, with angular velocity, $\mathbf{\Omega}$ of the ECEF[n] frame relative to the ECI frame. In the experiments circumnavigation of light signals or clocks through angles of 2π in the ECEF frame are considered. The definitions of $\Delta T_{\rm HK}$ in (7.15) and $\Delta T_{\rm S}$ in (7.16) are however, very different. In (7.15) $(T''_{\pm})_{\rm SR}$ are proper time intervals recorded by the airborne clocks during one rotation in the ECEF frame. The speed of the aircraft relative to the surface of the Earth is constant in both directions. In (7.16) $T_{\pm}$ are the times of passage in the ECI frame of the light signals, which move at constant speed in this frame but, due to the rotation of the Earth have different path lengths. In contrast, in the ECEF frame the paths have the same lengths but the light signals have different velocities, which is in contradiction at first order in β_Ω with the standard velocity transformation formula of SR. The time interval $(T''_+)_{\rm SR}$ is different from $(T''_-)_{\rm SR}$

[n]The Earth-Centered Earth-Fixed frame.

due to the time dilation effect relative to coordinate time. The clocks moving in different directions at the same speed in the ECEF frame have, due to the rotation of the Earth, different speeds in the ECI frame, which results in different time dilation factors γ. This implies that the "c^2" in the denominator on the right side of (7.15) has its origin in the $(v/c)^2$ term in the purely relativistic time dilation factor (see the derivation of Eq. (5.14)):

$$\gamma = \frac{1}{\sqrt{1-(v/c)^2}} \simeq 1 + \frac{v^2}{2c^2} + \mathrm{O}[(v/c)^4]\,.$$

In contrast, the "c^2" in Eq. (7.16) originates in a nonrelativistic $(v/c)^2$ term due to different path lengths at constant speed in the ECI frame or different light signal speeds over the same distance $2\pi R$ in the rotating ECEF frame, giving, in Galilean space–time geometry

$$\begin{aligned}\Delta T_{\mathrm{S}} \equiv T_+ - T_- &= 2\pi R\left[\frac{1}{c-\Omega R} - \frac{1}{c+\Omega R}\right] \\ &= \frac{4\pi\Omega R^2}{c^2[1-(\Omega R/c)^2]} \simeq \frac{4A\Omega}{c^2}\,.\end{aligned}$$

In the case of the Sagnac effect for massive particles where the phase is given by Eq. (7.5) there is no difference in the times of passage in opposite directions: $T_+ = T_-$. The origin of the "c^2" in the denominator is also special relativity; not time dilation, as in Eq. (7.15), but the mass energy equivalence equation: $E_0 = mc^2$! Even so, the Sagnac phase difference for massive particles remains, at the lowest order, calculable using Galilean space–time geometry, as in the derivation of Eq. (7.5).

8. Conclusions

The predictions of general relativity for the behavior of light signals and clocks in a static gravitational field as embodied in the Schwarzschild metric equation have been verified in the respective experiments of Sagnac and Hafele and Keating. Order β^2 relativistic corrections for both rotational and translational Sagnac interferometers are given as well as corrections at order $(V/c)^2$ due to translational motion at speed V of both Sagnac interferometers and Hafele–Keating-type experiments. The shortcomings of some different interpretations in the literature of Sagnac interferometers are pointed out. The essentially quantum-mechanical nature of the Sagnac phase difference and the very different space–time physics underlying the operation of Sagnac interferometers employing photons or massive particles are described.

The erroneous conflation in the literature of time interval differences in a Hafele–Keating-type experiment (an order β^2 relativistic effect) and in a photonic Sagnac interferometer (a classical order β effect due to different relative velocities of light signals) is clarified: the lowest order Sagnac effect is correctly described in Galilean relativity; special relativity (time dilation) is adequate to describe velocity dependence in the Hafele–Keating experiment, whereas position-dependence is given by the general-relativistic variability of clock rate in a changing gravitational potential.

Appendix A

Introducing the notation

$$x_\pm \equiv \mp\beta_V \sin\alpha \sin\phi^\pm \tag{A.1}$$

enables Eq. (3.14) to be written

$$dt_\pm = \frac{Rd\phi_\pm}{c\Big[\sqrt{1-\beta_V^2+x_\pm^2}+x_\pm \mp \beta_\Omega\Big]}\,. \tag{A.2}$$

Neglecting some terms of order β^4 or higher in (A.2) gives

$$\begin{aligned} dt_+ &= \frac{Rd\phi_\pm}{c[1+X_+]}d\phi_\pm + \mathrm{O}(\beta^4) \\ &= \frac{R}{c}\big[1 - X_+ + X_+^2 - X_+^3 + \cdots\big]d\phi_+ + \mathrm{O}(\beta^4)\,, \end{aligned} \tag{A.3}$$

where

$$X_+ \equiv \frac{x_\pm^2}{2} + x_+ - \beta_\Omega - \frac{\beta_V^2}{2}\,. \tag{A.4}$$

Equations (A.3) and (A.4) give, on expanding the right side of (A.3) in powers of β_Ω and β_V

$$\begin{aligned} dt_+ = \frac{R}{c}\Bigg[&1 + \beta_\Omega + \beta_\Omega^2 + \beta_\Omega^3 + \frac{\beta_V^2}{2} + \beta_V^2\beta_\Omega \\ &- x_+\left(1 + 2\beta_\Omega + 3\beta_\Omega^2 + \frac{\beta_V^2}{2}\right) + x_+^2\left(\frac{1}{2} + 2\beta_\Omega\right)\Bigg]d\phi_+\,. \end{aligned} \tag{A.5}$$

Inspection of (A.2) shows that dt_- at the same level of approximation as dt_+ in Eq. (A.5) is given by the replacements: $x_+ \to x_-$, $d\phi_+ \to d\phi_-$, $\beta_\Omega \to -\beta_\Omega$ in the latter equation

$$\begin{aligned} dt_- = \frac{R}{c}\Bigg[&1 - \beta_\Omega + \beta_\Omega^2 - \beta_\Omega^3 + \frac{\beta_V^2}{2} - \beta_V^2\beta_\Omega \\ &- x_-\left(1 - 2\beta_\Omega + 3\beta_\Omega^2 + \frac{\beta_V^2}{2}\right) + x_-^2\left(\frac{1}{2} - 2\beta_\Omega\right)\Bigg]d\phi_-\,. \end{aligned} \tag{A.6}$$

Using Eqs. (3.12) and (3.13) to write x_+ in terms of ϕ_+ gives

$$\begin{aligned} x_+ &= \beta_V \sin\alpha \sin(\phi_+(1+y_+) - \phi_V) \\ &= \beta_V \sin\alpha[\sin\phi_+(1+y_+)\cos\phi_V - \cos\phi_+(1+y_+)\sin\phi_V]\,. \end{aligned} \tag{A.7}$$

Also

$$\begin{aligned} \sin\phi_+(1+y_+) &= \sin\phi_+\cos\phi_+ y_+ + \cos\phi_+\sin\phi_+ y_+ \\ &\simeq \sin\phi_+\left(1 - \frac{(\phi_+ y_+)^2}{2}\right) + \phi_+ y_+\cos\phi_+ \end{aligned}$$

$$= \sin\phi_+\left(1-\frac{\beta_\Omega^2}{2}\phi_+^2\right)+\phi_+\cos\phi_+\big(\beta_\Omega-\beta_\Omega\beta_V\sin\alpha\sin(\phi_+-\phi_V)+\beta_\Omega^2\big)$$

$$= \sin\phi_+-\frac{\beta_\Omega^2}{2}\phi_+^2\sin\phi_+ +\big(\beta_\Omega+\beta_\Omega^2\big)\phi_+\cos\phi_+$$

$$-\beta_\Omega\beta_V\sin\alpha\big[\phi_+\cos\phi_+\sin\phi_+\cos\phi_V-\phi_+\cos^2\phi_+\sin\phi_V\big] \tag{A.8}$$

and

$$\cos\phi_+(1+y_+)$$

$$= \cos\phi_+\cos\phi_+ y_+ - \sin\phi_+\sin\phi_+ y_+$$

$$\simeq \cos\phi_+\left(1-\frac{(\phi_+ y_+)^2}{2}\right)-\phi_+ y_+\sin\phi_+$$

$$= \cos\phi_+\left(1-\frac{\beta_\Omega^2}{2}\phi_+^2\right)-\phi_+\sin\phi_+\big(\beta_\Omega-\beta_\Omega\beta_V\sin\alpha\sin(\phi_+-\phi_V)+\beta_\Omega^2\big)$$

$$= \cos\phi_+-\frac{\beta_\Omega^2}{2}\phi_+^2\cos\phi_+-\big(\beta_\Omega+\beta_\Omega^2\big)\phi_+\sin\phi_+$$

$$+\beta_\Omega\beta_V\sin\alpha\big[\phi_+\sin^2\phi_+\cos\phi_V-\phi_+\sin\phi_+\cos\phi_+\sin\phi_V\big]. \tag{A.9}$$

In these equations terms of order β_Ω^3 are neglected.

Combining (A.7)–(A.9)

$$x_+ = \beta_V\sin\alpha\Big\{\cos\phi_V\sin\phi_+-\sin\phi_V\cos\phi_+$$

$$+\frac{\beta_\Omega^2}{2}\big(\phi_+^2\cos\phi_+\sin\phi_V-\phi_+^2\sin\phi_+\cos\phi_V\big)$$

$$+\big(\beta_\Omega+\beta_\Omega^2\big)[\phi_+\cos\phi_+\cos\phi_V+\phi_+\sin\phi_+\sin\phi_V]$$

$$-\frac{\beta_\Omega\beta_V\sin\alpha}{2}(\phi_+\sin 2\phi_+\cos 2\phi_V-\phi_+\cos 2\phi_+\sin 2\phi_V)\Big\}. \tag{A.10}$$

Retaining terms of order β_V^2 and $\beta_V^2\beta_\Omega$ in x_+^2, (A.10) gives

$$x_+^2 = \frac{\beta_V^2\sin^2\alpha}{2}\big[1-\cos 2\phi_V\cos 2\phi_+-\sin 2\phi_V\sin 2\phi_+\big]$$

$$+\beta_V^2\beta_\Omega\sin^2\alpha\big[\phi_+\sin 2\phi_+\cos 2\phi_V-\phi_+\cos 2\phi_+\sin 2\phi_V\big]. \tag{A.11}$$

Integrating over ϕ_+, making use of the relations

$$\int_0^{2\pi}\sin\phi\,d\phi=\int_0^{2\pi}\cos\phi\,d\phi=\int_0^{2\pi}\phi\cos\phi\,d\phi=\int_0^{2\pi}\phi\cos 2\phi\,d\phi=0\,,$$

$$\int_0^{2\pi}\phi\sin\phi\,d\phi=-2\pi\,,$$

$$\int_0^{2\pi} \phi \sin 2\phi \, d\phi = -\pi \,,$$

$$\int_0^{2\pi} \phi^2 \sin\phi \, d\phi = -4\pi^2 \,,$$

$$\int_0^{2\pi} \phi^2 \cos\phi \, d\phi = 4\pi$$

gives

$$\int_0^{2\pi} x_+ \, d\phi_+ = 2\pi\beta_V\beta_\Omega \sin\alpha \left[\pi\beta_\Omega \cos\phi_V - \sin\phi_V + \frac{\beta_V \sin\alpha \cos 2\phi_V}{4}\right], \quad \text{(A.12)}$$

$$\int_0^{2\pi} x_+^2 \, d\phi_+ = \pi\beta_V^2 \sin^2\alpha(1 - \beta_\Omega \cos 2\phi_V) \,. \quad \text{(A.13)}$$

On integrating over ϕ_+ and making use of (A.12) and (A.13), Eq. (A.5) gives

$$T_+ = \int dt_+ = \frac{2\pi R}{c}\Big\{1 + \beta_\Omega\Big[1 + \beta_V \sin\phi_V \sin\alpha + \frac{\beta_V^2}{2}\big[2 + (2 - \cos 2\phi_V)\sin^2\alpha\big]\Big] + \beta_\Omega^2\big[1 + \beta_V(2\sin\phi_V - \pi\cos\phi_V)\sin\alpha\big] + \beta_\Omega^3 + \frac{\beta_V^2}{2} + \frac{\beta_V^2 \sin^2\alpha}{4}\Big\}. \quad \text{(A.14)}$$

It follows from (A.1) and (3.12) that

$$x_- = \beta_V \sin\alpha \sin[\phi_-(1 + y_-) + \phi_V] \,. \quad \text{(A.15)}$$

Since it also follows from Eq. (3.13) that

$$y_- = y_+\big(\phi_+ \to \phi_-, \beta_\Omega \to -\beta_\Omega, \phi_V \to -\phi_V\big)$$

then, comparing the first member of (A.7) with (A.15)

$$x_- = x_+(\phi_+ \to \phi_-, \beta_\Omega \to -\beta_\Omega, \phi_V \to -\phi_V) \,.$$

In consequence, T_- is given by making the replacements: $\beta_\Omega \to -\beta_\Omega$ and $\phi_V \to -\phi_V$ in (A.14) to give

$$T_- = \int dt_- = \frac{2\pi R}{c}\Big\{1 - \beta_\Omega\Big[1 - \beta_V \sin\phi_V \sin\alpha + \frac{\beta_V^2}{2}\big[2 + (2 - \cos 2\phi_V)\sin^2\alpha\big]\Big] + \beta_\Omega^2[1 - \beta_V(2\sin\phi_V + \pi\cos\phi_V)\sin\alpha] - \beta_\Omega^3 + \frac{\beta_V^2}{2} + \frac{\beta_V^2 \sin^2\alpha}{4}\Big\}, \quad \text{(A.16)}$$

Eqs. (A.14) and (A.16) are Eqs. (3.18) and (3.19) of the main text.

The motion of the light signal LS_D over the left-hand semi-circular path in the FOC shown in Fig. 1(d) is given by integration of Eq. (3.28) over the interval

$0 < \phi_+ < \pi - \delta_+$ with $\phi_V = -(\pi/2 + \theta)$. The corresponding values of x_+ and x_+^2 are given by (A.10) and (A.11) as

$$\begin{aligned} x_+ = \beta_V \sin\alpha \Big\{ & \cos\phi_+ \cos\theta - \sin\phi_+ \sin\theta \\ & + \frac{\beta^2}{2}(\phi_+^2 \sin\phi_+ \sin\theta - \phi_+^2 \cos\phi_+ \cos\theta) \\ & - (\beta + \beta^2)[\phi_+ \cos\phi_+ \sin\theta + \phi_+ \sin\phi_+ \cos\theta] \\ & + \frac{\beta\beta_V \sin\alpha}{2}(\phi_+ \sin 2\phi_+ \cos 2\theta + \phi_+ \cos 2\phi_+ \sin 2\theta) \Big\}, \end{aligned} \tag{A.17}$$

$$\begin{aligned} x_+^2 = {} & \frac{\beta_V^2 \sin^2\alpha}{2}\big[1 + \cos 2\theta \cos 2\phi_+ - \sin 2\theta \sin 2\phi_+\big] \\ & - \beta_V^2 \beta \sin^2\alpha \big[\phi_+ \sin 2\phi_+ \cos 2\theta + \phi_+ \cos 2\phi_+ \sin 2\theta\big]. \end{aligned} \tag{A.18}$$

Retaining only first- and second-order terms in the small quantity δ, the angular integrals needed to evaluate the quantity $\tilde{T}_+(L)$ occurring in Eq. (4.6) are

$$\int_0^{\pi-\delta} \sin\phi \, d\phi = 2 - \frac{\delta^2}{2},$$

$$\int_0^{\pi-\delta} \cos\phi \, d\phi = \delta,$$

$$\int_0^{\pi-\delta} \sin 2\phi \, d\phi = \delta^2,$$

$$\int_0^{\pi-\delta} \cos 2\phi \, d\phi = -\delta,$$

$$\int_0^{\pi-\delta} \phi \sin\phi \, d\phi = \pi\left(1 - \frac{\delta^2}{2}\right),$$

$$\int_0^{\pi-\delta} \phi \cos\phi \, d\phi = -2 + \pi\delta + \frac{\delta^2}{2},$$

$$\int_0^{\pi-\delta} \phi \sin 2\phi \, d\phi = -\frac{\pi}{2}(1 - 2\delta^2) - \frac{\delta}{2},$$

$$\int_0^{\pi-\delta} \phi \cos 2\phi \, d\phi = -\pi(1 + \delta) + \frac{\delta^2}{2},$$

$$\int_0^{\pi-\delta} \phi^2 \sin\phi \, d\phi = \pi^2 - 4 + \frac{\delta}{2}(3 - \pi^2),$$

$$\int_0^{\pi-\delta} \phi^2 \cos\phi \, d\phi = -2\pi + \pi^2\delta - \pi\delta^2.$$

Substituting Eqs. (A.16) and (A.17) into Eq. (3.28), performing the integral over ϕ_+ and retaining only first- and second-order terms in δ_+ yields Eq. (4.12) of the main text.

Subtracting Eq. (4.17) from (4.16) and introducing the quantity: $\tilde{\alpha} \equiv 1 + \alpha_T$ gives

$$\begin{aligned}
\Delta T^{\rm trans} &\equiv T_+^{\rm trans} - T_-^{\rm trans} \\
&= \frac{2nL}{c}\left[\frac{\tilde{\alpha}+\beta_1}{(\tilde{\alpha}+\beta_-)(\tilde{\alpha}+\beta_+)} - \frac{\tilde{\alpha}-\beta_1}{(\tilde{\alpha}-\beta_-)(\tilde{\alpha}-\beta_+)}\right] \\
&= \frac{2nL}{c}\left[\frac{(\tilde{\alpha}+\beta_1)(\tilde{\alpha}-\beta_-)(\tilde{\alpha}-\beta_+) - (\tilde{\alpha}-\beta_1)(\tilde{\alpha}+\beta_-)(\tilde{\alpha}+\beta_+)}{(\tilde{\alpha}^2-\beta_-^2)(\tilde{\alpha}^2-\beta_+^2)}\right] \\
&= \frac{4nL}{c}\left[\frac{\tilde{\alpha}^2(\beta_1-\beta_--\beta_+)+\beta_1\beta_-\beta_+}{(\tilde{\alpha}^2-\beta_-^2)(\tilde{\alpha}^2-\beta_+^2)}\right] \\
&= \frac{4nL}{c}\{(\beta_1-\beta_--\beta_+)[1-2\alpha_T+\beta_-^2+\beta_+^2]+\beta_1\beta_-\beta_+\}+{\rm O}(\beta^5)\,. \qquad \text{(A.19)}
\end{aligned}$$

Substituting for β_T, β_1, β_- and β_+ using the formulas given after Eq. (4.16) yields, after algebraic manipulation, Eq. (4.19) of the main text.

Appendix B

In order to perform the integration of Eq. (5.31) the relations (5.32) are approximated as

$$\phi^{\rm E} = \bar{r}\phi_{\rm A} + \phi_V\,, \quad \phi_\pm^{\rm A} = (\bar{r}\pm 1)\phi_{\rm A} + \phi_V\,,$$

where $\bar{r}$ is the average value of r for the range of integration $0 < \phi_{\rm A} < 2\pi$. Denoting the coefficients of $\sin\phi_\pm^{\rm A}$ and $\sin\phi^{\rm E}$ in (5.31) as $C_\pm^{\rm A}$ and $C_\pm^{\rm E}$, and making use the above approximation, the contribution of these terms to $T_\pm'' = \int d\tau_\pm''$ is

$$\begin{aligned}
I_1^\pm &= \frac{R}{v_{\rm A}'}\int_0^{2\pi}\Big[C_\pm^{\rm A}\sin[\phi_{\rm A}(\bar{r}\pm 1)+\phi_V] + C_\pm^{\rm E}\sin[\phi_{\rm A}\bar{r}+\phi_V]\Big]d\phi_{\rm A} \\
&\equiv \frac{R}{v_{\rm A}'}\int_0^{2\pi} f_1^\pm\, d\phi_{\rm A}\,. \qquad \text{(B.1)}
\end{aligned}$$

Expanding the sine functions

$$\begin{aligned}
f_1^\pm = &\Big[C_\pm^{\rm A}\sin\phi_{\rm A}(\bar{r}\pm 1) + C_\pm^{\rm E}\sin\phi_{\rm A}\bar{r}\Big]\cos\phi_V \\
&+\Big[C_\pm^{\rm A}\cos\phi_{\rm A}(\bar{r}\pm 1) + C_\pm^{\rm E}\cos\phi_{\rm A}\bar{r}\Big]\sin\phi_V\,. \qquad \text{(B.2)}
\end{aligned}$$

Using the integrals

$$\int_0^{2\pi}\sin a\phi\, d\phi = \frac{(1-\cos 2\pi a)}{a}\,, \quad \int_0^{2\pi}\cos a\phi\, d\phi = \frac{\sin 2\pi a}{a} \qquad \text{(B.3)}$$

and (B.2) it is found that

$$I_1^{\pm} = \frac{2R}{v'_{\rm A}}\left[\frac{C_{\pm}^{\rm A}}{\bar{r}\pm 1} + \frac{C_{\pm}^{\rm E}}{\bar{r}}\right]\sin\pi\bar{r}\sin(\pi\bar{r}+\phi_V)\,. \tag{B.4}$$

Analogous calculations for the $\sin\phi_{\pm}^{\rm A}\sin\phi^{\rm E}$ (AE) and $\sin^2\phi_{\pm}^{\rm A}$ (AA) terms in (5.31) yield the respective results:

$$I_2^{\pm} = -\frac{RC_{\pm}^{\rm AE}\sin 2\pi\bar{r}\cos 2(\pi\bar{r}+\phi_V)}{2v'_{\rm A}(2\bar{r}\pm 1)}\,, \tag{B.5}$$

$$I_3^{\pm} = \frac{RC_{\pm}^{\rm AA}}{2v'_{\rm A}}\left[2\pi - \frac{\sin 2\pi\bar{r}\cos 2(\pi\bar{r}+\phi_V)}{\bar{r}\pm 1}\right]. \tag{B.6}$$

With the definitions

$$\bar{r} \equiv \frac{\beta_\Omega\bar{\gamma}_{\rm E}}{\beta'_{\rm A}} \equiv r_0\bar{\gamma}_{\rm E}\,,$$

where $\bar{\gamma}_{\rm E}$ is the average value of the time dilation factor given by Eq. (5.26) when $\phi_{\rm A}$ varies over the range 0 to 2π then

$$\bar{\gamma}_{\rm E} = 1 + \frac{\beta_V^2}{2} + \frac{\beta_\Omega^2}{2} - \frac{\beta_V\beta'_{\rm A}}{\pi}\sin\pi r_0\sin(\pi r_0+\phi_V) + {\rm O}(\beta^4)\,. \tag{B.7}$$

Combining (B.4)–(B.7) with the definitions of the coefficients $C_{\pm}^{\rm A}$, $C_{\pm}^{\rm E}$, $C_{\pm}^{\rm AE}$ and $C_{\pm}^{\rm AA}$ that can be read off from Eq. (5.31) it is found that

$$\begin{aligned} T''_{\pm} = \int d\tau''_{\pm} = \frac{2\pi R}{v'_{\rm A}}\Bigg\{1 + \beta'_{\rm A}\Bigg[\big(1-\beta_V^2\big)\left(\frac{\beta'_{\rm A}}{2}\pm\beta_\Omega\right) + \beta'_{\rm A}\left(\beta_\Omega^2 \pm \frac{\beta_\Omega\beta'_{\rm A}}{2} - \frac{\big(\beta'_{\rm A}\big)^2}{8}\right)\Bigg] \\ + \frac{\beta_V^2\beta_\Omega^2}{2} \pm \frac{\beta_V(\beta'_{\rm A})^2}{\pi(\beta_\Omega\pm\beta'_{\rm A})}\left[\frac{\beta_V^2}{2} - \frac{\beta_\Omega^2}{2} \mp \beta'_{\rm A}\beta_\Omega - \frac{\beta_V\beta'_{\rm A}}{\pi}F_1(r_0)\right]F_1(r_0) \\ + \frac{\beta_V^2\beta'_{\rm A}\big(\beta_\Omega\pm\beta'_{\rm A}\big)}{4\pi}\left[\frac{\beta_\Omega}{2\beta_\Omega\pm\beta'_{\rm A}} - \frac{1}{2}\right]F_2(r_0)\Bigg\} + {\rm O}(\beta^5)\,, \end{aligned} \tag{B.8}$$

where

$$\begin{aligned} F_1(r_0) &\equiv \sin\pi r_0\sin(\pi r_0+\phi_V)\,, \\ F_2(r_0) &\equiv \sin 2\pi r_0\sin 2(\pi r_0+\phi_V)\,. \end{aligned}$$

With $T' \equiv 2\pi R/v'_{\rm A}$ Eq. (5.33) of the main text follows directly from Eq. (B.8).

References

1. K. Schwarzschild, *Sitzungberichte Prüssiche Akademie der Wissenschaften* (1916), p. 198.
2. S. Weinberg, *Gravitation and Cosmology, Principles and Applications of the General Theory of Relativity* (John Wiley, New York, 1972), Chap. 8, Sec. 2.
3. I. I. Shapiro *et al.*, *Phys. Rev. Lett.* **26**, 1132 (1971).
4. G. Sagnac, *Comptus Rendus Acad. Sci.* **157**, 1410 (1913).

5. F. Harress, Die Geschwindigkeit des Lichtes in bewegten Korpen, Dissertation, Universität Jena (1912).
6. J. H. Field, *Fundam. J. Mod. Phys.* **10**, 1 (2017).
7. E. J. Post, *Rev. Mod. Phys.* **39**, 475 (1967).
8. R. D. Klauber, *Found. Phys. Lett.* **16**, 447 (2003).
9. F. Zernike, *Physica* **13**, 279 (1947).
10. R. Anderson, H. H. Bilger and G. E. Stedman, *Am. J. Phys.* **62**, 975 (1994).
11. G. B. Malykin, *Phys. Usp.* **40**, 317 (1997).
12. G. B. Malykin, *Phys. Usp.* **43**, 1229 (2000).
13. A. A. Michelson and H. G. Gale, *Astrophys. J.* **61**, 140 (1925).
14. N. Ashby, *Phys. Today* **55**, 41 (2002).
15. R. S. Shankland, *Am. J. Phys.* **31**, 47 (1963).
16. C.-C. Su, *Europhys. Lett.* **56**, 170 (2001).
17. C.-C. Su, *Eur. Phys. J. C* **21**, 701 (2001).
18. H. Poincaré, *The Monist* **15**, 1 (1905).
19. J. C. Hafele and R. E. Keating, *Science* **177**, 166 (1972).
20. J. C. Hafele and R. E. Keating, *Science* **177**, 168 (1972).
21. J. C. Hafele, *Am. J. Phys.* **40**, 81 (1972).
22. J. H. Field, *Fundam. J. Mod. Phys.* **6**, 1 (2013).
23. R. V. Pound and G. A. Rebka, *Phys. Rev. Lett.* **4**, 337 (1960).
24. G. B. Malykin, *Radiophys. Quantum Electron.* **59**, 290 (2015).
25. B. Paterson *et al.*, An undergraduate test of gravitational time dilation, arXiv:1710.07838.
26. R. Wang *et al.*, *Phys. Lett. A* **312**, 7 (2003).
27. R. Wang, Y. Zheng and A. Yao, *Phys. Rev. Lett.* **93**, 143901 (2004).
28. Y. Saburi, M. Yamamoto and K. Harada, *IEEE Trans. Instrum. Meas.* **25**, 473 (1976).
29. D. W. Allan, M. A. Weiss and N. Ashby, *Science* **228**, 64 (1985).
30. G. Petit and P. Wolf, *Astron. Astrophys.* **286**, 971 (1994).
31. P. Wolf and G. Petit, *Phys. Rev. A* **56**, 4405 (1997).
32. S. Weinberg, *Gravitation and Cosmology, Principles and Applications of the General Theory of Relativity* (John Wiley, New York, 1972), Chap. 8, Eq. 8.7.4.
33. A. A. Michelson and E. W. Morley, *Phil. Mag.* **24**, 449 (1887).
34. I. Newton, *The Principia*, Translated by I. B. Cohen and A. Whitman (University of California Press, Berkeley, 1999), p. 795.
35. R. J. Kennedy and E. M. Thorndike, *Phys. Rev.* **42**, 400 (1932).
36. R. J. Kennedy, *Proc. Natl. Acad. Sci.* **12**, 621 (1926).
37. K. K. Illingworth, *Phys. Rev.* **30**, 692 (1927).
38. G. Joos, *Ann. Phys.* **7**, 385 (1930).
39. D. C. Miller, *Rev. Mod. Phys.* **5**, 203 (1933).
40. R. S. Shankland *et al.*, *Rev. Mod. Phys.* **27**, 16 (1955).
41. P. Langevin, *Comptes Rendus Acad. Sci.* **173**, 831 (1921).
42. P. A. M. Dirac, *Quantum Mechanics*, 4th edn. (Oxford University Press, Oxford, 1958), Chap. 1, Sec. 3.
43. P. H. Brown and R. Q. Twiss, *Proc. R. Soc. A* **242**, 300 (1957).
44. P. H. Brown and R. Q. Twiss, *Proc. R. Soc. A* **243**, 291 (1958).
45. J. Lense and H. Thirring, *Phys. Z.* **19**, 156 (1918).
46. J.-M. Lévy-Leblond and F. Balibar, *Quantics, Rudiments of Quantum Physics* (North-Holland, Amsterdam, 1990), p. 493.

47. A. Einstein, *Ann. Phys.* **17**, 891 (1905) [English translation: W. Perrett and G. B. Jeffery, *The Principle of Relativity* (Dover, New York, 1952), p. 37; *Einstein's Miraculous Year* (Princeton University Press, Princeton, New Jersey, 1998), p. 123].
48. A. Dufour and F. Prunier, *Comptus Rendus Acad. Sci.* **204**, 1925 (1937).
49. J. H. Field, The physics of space and time III: Classification of space–time experiments and the twin paradox, arXiv:0806.3671v1.
50. J. H. Field, Primary and reciprocal space–time experiments, relativistic reciprocity relations and Einstein's train-embankment thought experiment, arXiv:0807.0158v2.
51. P. Harzer, *Astrom. Nachr.* **198**, 378 (1914).
52. P. Harzer, *Astrom. Nachr.* **199**, 10 (1914).
53. B. Pognay, *Ann. Phys.* **80**, 217 (1926).
54. B. Pognay, *Ann. Phys.* **85**, 244 (1928).
55. F. Prunier, *Comptus Rendus Acad. Sci.* **200**, 46 (1935).
56. H. von Laue, *Ann. Phys.* **23**, 989 (1907).
57. R. A. Bergh, G. Kotler and H. J. Shaw, *Electron. Lett.* **16**, 260 (1980).
58. P. Langevin, *Scientia* **10**, 31 (1911).
59. N. D. Mermin, *Am. J. Phys.* **51**, 1130 (1983).
60. N. D. Mermin, *Am. J. Phys.* **52**, 119 (1984).
61. P. Ehrenfest, *Phys. Z.* **10**, 918 (1909).
62. A. Einstein, *Relativity, the Special and the General Theory* (Princeton University Press, Princeton, 1955), p. 59 [*The Meaning of Relativity*, 5th edn., English translation: R. W. Lawson (Methuen, London, 1960), p. 82].
63. J. H. Field, *Fundam. J. Mod. Phys.* **2**, 139 (2011).
64. J. H. Field, *Fundam. J. Mod. Phys.* **4**, 1 (2012).
65. W. Nawrot, *Phys. Essays* **17**, 518 (2004).
66. G. Sagnac, *J. Phys. Radium* **4**, 177 (1914).
67. J. Anandan, *Phys. Rev. D* **24**, 338 (1981).
68. A. A. Logunov and V. Chugreev, *Sov. Phys. Usp.* **31**, 861 (1988).
69. L. D. Landau and E. M. Lifshitz, *The Classical Theory of Fields*, 4th edn. (Pergamon Press, Oxford, 1975), p. 254.
70. P. Langevin, *Comptus Rendus Acad. Sci.* **200**, 49 (1935).
71. P. Langevin, *Comptus Rendus Acad. Sci.* **205**, 304 (1937).
72. N. Ashby, *Relativity in Rotating Frames*, eds. G. Rizzi and M. L. Ruggiero (Kluwer Academic Publishers, Dordrecht, 2004), p. 15.
73. M. G. Trocheris, *Phil. Mag. Ser.* **40**, 1143 (1949).
74. D. Dieks and G. Nienhaus, *Am. J. Phys.* **58**, 650 (1990).
75. D. Dieks, *Found. Phys. Lett.* **4**, 347 (1990).
76. D. Dieks, *Eur. J. Phys.* **12**, 253 (1991).
77. A. Sommerfeld, *Optics* (Academic Press, New York, 1954).
78. P. W. Forder, *J. Phys. A: Math. Gen.* **17**, 1343 (1984).
79. W. W. Chow *et al.*, *Rev. Mod. Phys.* **57**, 61 (1985).
80. N. Ashby, *Living Rev. Rel.* **6**, 1 (2003).
81. P. Holland and H. R. Brown, *Am. J. Phys.* **67**, 204 (1999).
82. D. M. Greenberger, *Phys. Rev. Lett.* **87**, 100405 (2001).
83. H. Hernandez-Coronado Unstable particle in non-relativistic quantum mechanics?, arXiv:1106.3757v1.
84. G. B. Malykin, *Phys. Usp.* **45**, 907 (2002).
85. J. Bailey *et al.*, *Nature* **268**, 301 (1977).
86. R. P. Feynman, *Rev. Mod. Phys.* **20**, 367 (1948).

87. R. P. Feynman and A. R. Hibbs, *Quantum Mechanics and Path Integrals* (McGraw-Hill, Massachusetts, 1965).
88. J. H. Field, *Ann. Phys.* (*N.Y.*) **321**, 627 (2006).
89. J. H. Field, *Eur. J. Phys.* **34**, 1507 (2013).
90. R. P. Feynman, *Phys. Rev.* **76**, 749 (1949).
91. F. Hasselbach and M. Nicklaus, *Phys. Rev. A* **48**, 143 (1993).
92. M. Dresden and C. N. Yang, *Phys. Rev. D* **20**, 1846 (1979).
93. J. J. Sakurai, *Phys. Rev. D* **21**, 2993 (1980).
94. W. Ehrenberg and R. E. Siday, *Proc. R. Soc. B* **62**, 8 (1949).
95. Y. Aharonov and D. Bohm, *Phys. Rev.* **115**, 485 (1959).
96. J. H. Field, *Eur. J. Phys.* **33**, 63 (2011).